

Multi-Scale Molecular Dynamics Simulations

Frédéric Boussinot
frederic.boussinot@gmail.com

October 2024

Abstract

In molecular dynamics (MD), systems are molecules made up of atoms, and the aim is to determine their evolution over time. MD is based on a numerical resolution algorithm, whose role is to apply the forces generated by the various components, according to the equations of Newtonian physics. Molecular Dynamics is currently mainly used in materials science and molecular biology.

In this document, we limit ourselves to *alkanes* which are non-cyclic carbon-hydrogenated chains. In the basic “All-atom” (AA) scale, all the atoms are directly simulated. In the “United-atom” (UA) scale, one considers grains that are composed of a carbon atom with the hydrogen atoms attached to it. Grains in the “Coarse-grained” (CG) scale are composed of two consecutive UA grains. In the multi-scale approach, one tries to use as much as possible the UA and CG scales which can be more efficiently simulated than the AA scale.

In this document, we mainly put the focus on three topics.

First, we describe an MD system, implemented in the Java programming language, according to the Synchronous Reactive Programming approach in which there exists a notion of a global logical time. This system is used to simulate molecules and also to build the potentials functions at the UA and CG scales.

Second, two methods to derive UA and CG potentials from AA potentials are proposed and analysed. Basically, both methods rely on strong geometrical links with the AA scale. We use these links with AA to determine the forms and values of the UA and CG potentials. In the first method (called “inverse-Boltzmann”), one considers data produced during several AA scale molecule simulations, and one processes these data using a statistical approach. In the second method (“minimisation method”), one applies a constrained-minimisation technique to AA molecules. The most satisfactory method clearly appears to be the minimisation-based one. The UA potentials we have determined have standard forms: they only differ from AA potentials by parameter values. On the opposite, CG potentials are non-standard functions. We show how to implement them with functions defined “by cases”.

Finally, we consider “reconstructions” which are means to dynamically change molecule scales during simulations. In particular, we consider automatic reconstructions based on the proximity of molecules.

Contents

1	Introduction	5
1.1	Molecular Dynamics	5
1.2	Multi-Scale Simulations	8
1.3	Dynamic Creations and Destructions	10
1.4	Plan of the Text	10
2	Alkanes	13
2.1	Bonds	14
2.2	Valence Angles	16
2.3	Torsion Angles	16
2.4	Inter-Molecular Forces	16
3	Forces at AA Scale	21
3.1	Bonds	22
3.2	Valence Angles	23
3.3	Torsion Angles	25
3.4	Inter-Molecular Forces	28
4	Implementation	31
4.1	Reactive Programming	32
4.2	SugarCubes	33
4.3	Resolution Method	36
5	Simulations at AA Scale	39
5.1	Stability	40
5.2	Deterministic Chaos	42
6	Multi-Scale Approach	49
6.1	UA Scale	49
6.2	CG Scale	50

6.3	Complexity	53
7	Inverse-Boltzmann Method	57
7.1	UA Intra-molecular Forces	58
7.2	UA Inter-Molecular Forces	61
8	Inverse-Boltzmann for CG	65
8.1	CG Bonds	65
8.2	CG Valence Angles	66
9	Minimisation Method	69
9.1	UA Bonds	70
9.2	UA Valence Angles	71
9.3	UA Torsion Angles	71
9.4	UA Inter-molecular Forces	72
10	Minimisation for CG	77
10.1	CG Bonds	77
10.2	CG Valence Angles	78
10.3	Ponderation	80
10.4	Potential of CG Bonds	81
10.5	Potential of CG Valence Angles	82
10.6	CG Inter-molecular Forces	82
10.7	Comparison with the Inverse-Boltzmann Approach	84
11	Simulations in UA	89
12	Simulations in CG	95
12.1	Determination of the CG potential	95
12.2	CG Execution	99
13	Reconstructions	105
13.1	Inter-molecular Forces	108
13.2	Automatic Reconstructions	110
14	Conclusion	115

Chapter 1

Introduction

Numerical simulation in physics consists in modeling systems as computer programs and in running them to study the system properties. In molecular dynamics (MD) [3], systems are molecules made up of atoms, and the aim is to determine how they evolve over time. The first work on atomic-scale simulation dates back to the 50s [16], at a time when computing resources were extremely limited. The first simulated systems consisted of independent atoms (not grouped into molecules) subjected to perfectly elastic shocks (perfect gas). Then, inter-atomic (van Der Waals) forces were introduced, to obtain simulations closer to reality. Intra-molecular interactions were then taken into account, to obtain true molecular models. MD is currently mainly used in materials science and molecular biology.

1.1 Molecular Dynamics

The basis of MD is classical (Newtonian) physics, with the fundamental equation :

$$\vec{F} = m \vec{a} \tag{1.1}$$

where \vec{F} is the force experienced by a particle of mass m and \vec{a} its acceleration (the second derivative of the variation of its position, with respect to time).

The elementary components used to model molecules are as follows:

- Atoms, with 6 degrees of freedom (coordinates x, y, z and velocities sx, sy, sz).

- Bonds that link two atoms (said to be *bonded*) within a molecule; the bond that links two atoms a, b tends to keep the distance ab constant.
- Valence angles defined by two atoms a and c bonded to the same third atom b within a molecule. The valence angle tends to keep the \widehat{abc} angle at a fixed value.
- Torsion angles, also called *dihedrals*, which link four atoms a, b, c, d within a molecule; a is linked to b , b to c and c to d ; the torsion angle tends to make the two abc and bcd planes coincide.
- Van Der Waals interactions, which concern two atoms, not necessarily belonging to the same molecule; these interactions depend on the kind of atoms considered.

Molecular models can also take into account electrostatic interactions (Coulomb's law); we will not consider this aspect here.

Molecules are made up of linked atoms. An intra-molecular distance is defined to delimit the molecule atoms for which one considers that van Der Waals interactions between them are not to be treated directly, but are taken into account by the bonds and angles the atoms are involved in.

MD is based on a numerical resolution algorithm, whose role is to apply the forces generated by the various components, according to the equations of Newtonian physics. The resolution algorithm applied to a molecule has a parameter which is the Δt simulation time-step. This is of the order of the femto-second ($10^{-15}s$), for molecules at AA scale (see below).

A resolution method often used in MD systems is the *Velocity – Verlet* resolution named after its designer who proposed it in 1967 [25]. It is based on a two-stages resolution: in the first stage, velocity is calculated for a half-time-step of $\Delta t/2$ and position is calculated according to this velocity; in the second stage, the velocity is calculated for the full time-step Δt . This method has two main advantages: (1) it is very stable (simulations can be long, in a sense that will be made precise later); (2) it is energy-preserving. Energy preservation (i.e. the fact that the resolution neither adds nor removes energy during the simulation) is a fundamental criterion for physics simulations. It corresponds to a deep symmetry of classical physics (independence from the direction of time flow).

Intra-molecular forces (of bonds, valence, dihedrals) and inter-molecular forces (van Der Waals) are conservative: the work done between two points

is independent of the path followed. They can therefore be defined as derivatives of scalar fields, called *potentials*. We then have:

$$\vec{F}(\mathbf{r}) = -\vec{\nabla}U(\mathbf{r}) \quad (1.2)$$

where \mathbf{r} denotes the coordinates of the point to which the force $\vec{F}(\mathbf{r})$ applies and U is the potential from which the force is derived.

The potentials of the various components are grouped together as *force-fields*. Several force-fields exist and are used in different contexts. The OPLS force-field [11] is often used in the context of liquid simulations [3]; it is this force-field that we will consider in this document.

The definition of a force-field may require calculations on a quantum scale; we will not deal with this aspect here.

All MD systems comprise the following elements:

- Means of defining atoms and molecules.
- Implementation of the various potentials.
- Implementation of a resolution method.
- Means of defining and performing simulations.

In addition, we generally find in MD systems:

- Means of performing simulations in the context of a thermostat (temperature control) or of a barostat (pressure control).
- Means to simulate unbounded quantities of atoms (periodic conditions).

We will not consider these last two aspects here, as we are only concerned with the fundamentals of MD.

Several dozen MD systems are available, some of which have been developed in the academic world and are freely available. These include DL_POLY [1], GROMACS [21] and CHARMM [24]. These systems are written in FORTRAN or C/C++ and are interfaced with 3D visualisation tools, using translation tools between appropriate formats. The work presented in this document was carried out during the development of a MD[7] system that has been used to carry out all the simulations described in the sequel.

1.2 Multi-Scale Simulations

MD simulations at the all-atom level (*AA*) are a very powerful tool for analysing molecular systems, but they have two main limitations associated with the number of atoms that can be simulated and to the time-step of the resolution scheme used.

As far as the size of the systems that can be simulated is concerned, the main restriction lies in the size of the memory that has to be used. A few thousand atoms can reasonably be processed by a standard machine. This number can be significantly increased by using networks of distributed machines running in parallel and sharing a memory distributed across the network. In this way, clusters of distributed machines are expected to be able to simulate systems of up to a million atoms.

The time-step of the simulations is imposed by physics: it is a fraction of the period of the shortest vibration occurring in the system. For example, for hydrocarbon molecules described on the *AA* scale, the time-step depends on the vibration of the CH bond, which is 10^{-14} s ($\lambda = 2860\text{cm}^{-1}$ in the infrared spectrum). Usually, the time-step is at most one tenth of this vibration, i.e. 10^{-15} s (1 femto-second). With such a time-step, a million steps are needed to predict the dynamics of the system for just one nano-second. Thus, *AA* models are the most realistic ones at the chemical level, but the time that is simulated can rarely exceed a few nano-seconds. Many simulations, dealing with diffusion phenomena for example, require much longer time-scales. The limitation concerning the simulation time-step appears to be the main limitation, compared with that concerning the size of the system being simulated.

There are two approaches to bypass the time-step limitation, thereby increasing the simulated time. The first approach is called *Hyper-molecular dynamics* or *Accelerated-molecular dynamics* [26, 17]. It consists of a modification of the force-field, obtained by reducing the potential energy barrier between two states corresponding to two rare events, so as to increase the probability of a transition between these states.

The second approach, which is widely used and which is the one adopted in this document, consists in reducing the complexity of the molecular system by grouping certain atoms together to form “grains”. This general approach is called *coarse-grained*. The simplest reduction consists in grouping a carbon atom and the hydrogen atoms attached to it into a single grain; this is known as the “Unified Atom” model (UA).

In what follows, we will also consider grains formed by two bonded carbon atoms, together with the hydrogen atoms that are linked to them; it is to this reduction that we will refer as CG in the following.

Reducing the complexity of molecular systems allows for longer simulated times. This is due to several reasons:

- The time-step of the resolution method can be increased with respect to the *AA* scale since the shortest period of vibration is also increased (the mass of grains is greater than that of *AA* atoms).
- The number of degrees of freedom and the number of intra-molecular components (bonds and angles) is reduced compared with their number at *AA* scale. In particular, the number of inter-molecular interactions (van Der Waals forces) between grains is reduced compared to the number of interactions between atoms. This is important because the number of inter-molecular interactions can be very high and therefore costly to simulate.

With all these points taken into account, the simulated time can be increased by more than two orders of magnitude by moving from the *AA* scale to the CG scale. This increase is so significant that most MD simulations are in fact carried out on UA or CG scales.

However, the choice to use the UA or CG scale requires the force field *AA* to be transported to this scale. This transport is fairly easy from *AA* to UA [11, 12, 13, 24]. In fact, the integration of hydrogen atoms into UA grains only requires a change in the parameters of the torsion angles potentials and of van Der Waals interactions. The new parameters can be quite easily deduced analytically from those of *AA*.

For transport from *AA* to CG, the parameters are generally deduced from a statistical analysis in dense materials to reproduce certain fundamental functions of these materials (density, energy, distribution) valid on the *AA* scale. More precisely, the CG force field is constructed from an inverse-Boltzmann treatment in the references [20, 23, 22].

An important point is that this type of transfer assumes that the form of the potentials in CG is the same as in *AA*. This is a point that will be contested in the rest of the text, by proposing a different approach, justifying an analytical construction of CG and allowing *reconstructions* that are dynamic changes of scale between *AA*, UA and CG.

1.3 Dynamic Creations and Destructions

Not being able to simulate systems in which numbers of atoms and bonds may vary during simulations, is a constraint that we may wish to overcome in at least two cases:

- To simulate a chemical reaction, in which a new bond between two atoms may appear during the simulation (for example, between an oxygen atom and an iron atom, when they become too close).
- In the context of a change of scale of a molecule *during the simulation*. The change of scale can be implemented by the dynamical addition of the new version of the molecule *simultaneously* with the destruction of the old version. This is particularly important in the context of reconstructions.

It therefore seems interesting that a MD system should offer mechanisms to destroy or create simulation components dynamically, i.e. at runtime. It is a system with such a capability, based on a particular programming style called Synchronous Reactive Programming (RP), on which this document is based.

1.4 Plan of the Text

In Chap.2, alkanes, which are linear hydrocarbon molecules, are presented. Alkanes will be used throughout the document. The components of these molecules (bonds, angles) are described and their potentials defining their potential energy are presented in the form of curves (these curves correspond to the OPLS[10] force field, which is that of the AA scale in this document).

Chap.3 describes with the help of vector algebra how the intra-molecular and inter-molecular forces are applied to atoms at the AA scale.

The implementation is considered in Chap.4 starting with an introduction to reactive programming, in which programs are defined in relation to a notion of time. The Java library SugarCubes[8] is briefly described, along with the *Velocity-Verlet* time-resolution method.

AA simulations are considered in Chap.5 from the point of view of stability and determinism. The general framework of MD is deterministic chaos.

In Chap.6 we introduce the two scales of description UA and CG for which we shall seek to determine potential.

The inverse-Boltzmann method for determining a UA potential is presented in Chap.7. The case of CG is considered in Chap.8. The inverse-Boltzmann method proves to be unsatisfactory in several aspects, which justifies the consideration of an alternative “minimisation” approach. This alternative minimisation method is defined for the UA scale in Chap.9. The minimisation method is based on a geometric link between the scales UA and AA, and on minimisation of the potential energy at the AA scale. The case of CG is considered in Chap.10. The minimisation method proves to be much more satisfactory than the inverse-Boltzmann method.

UA scale simulations are considered in Chap.11. Those at the CG scale are considered in Chap.12.

The reconstructions between the three scales AA, UA, and CG are described in Chap.13.

Finally, Chap.14 concludes the document.

Chapter 2

Alkanes

Alkanes are linear chains of carbon atoms to which hydrogen atoms are attached. Alkanes are designated by formulae of the form C_nH_{2n+2} where n is the number of carbon atoms. Fig.2.1 shows an alkane molecule C_6H_{14} , composed of 6 carbon atoms and 14 hydrogen atoms.

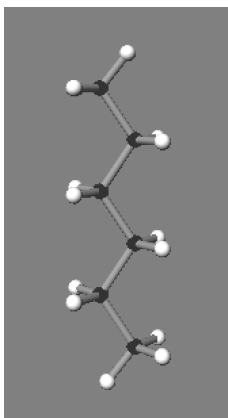


Figure 2.1: Hydro-carbon chain C_6H_{14} (6 carbon atoms, 14 hydrogen atoms).

In MD, molecules are structured into components that determine their structure and the forces that apply to their atoms. Each of these components is associated with a *potential* which is a function describing the energy of the component.

Potentials are usually grouped together in *force-fields*. The inter-molecular forces exerted between molecules are generally also included in force-fields. In

what follows, at the AA scale, we will consider only one particular force-field, called OPLS, which forms the basis of the MD system DL_POLY[1].

In OPLS, the main components of molecules are bonds connecting two atoms, valence angles connecting three atoms, and torsion angles connecting four atoms. For example, in OPLS, the molecule C_6H_{14} has 19 bonds, 36 valence angles and 45 torsion angles (also called *dihedrals*).

At both ends of alkanes there are three hydrogen atoms, while only two are linked to the other carbon atoms. To simplify, we shall often consider *fragments* of alkanes which are of the form C_nH_{2n} , i.e. all carbon atoms without exception have two hydrogen bonds.

Fig.2.2 shows the fragment C_6H_{12} .

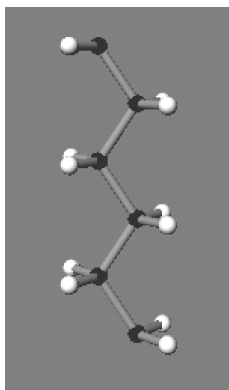


Figure 2.2: Fragment C_6H_{12} (6 carbon atoms, 12 hydrogen atoms).

The fragment C_6H_{12} has 17 bonds, 30 valence angles and 39 torsion angles.

We will now describe in more detail the main constituents of the OPLS force-field.

2.1 Bonds

A *bond* models a sharing of electrons between two atoms, generating a force between them. In OPLS, the potentials of bonds are harmonic: a *harmonic bond potential* is a scalar field \mathcal{U} defining the binding (potential) energy between two atoms at a distance r as being:

$$\mathcal{U}(r) = k(r - r_0)^2 \quad (2.1)$$

where k is the bond strength and r_0 is the equilibrium distance (distance at which no force is exerted on the two atoms).

Fig.2.3 shows the parabolic curves of the OPLS bonding potentials between two carbon atoms (CC) and between a carbon atom and a hydrogen atom (CH).

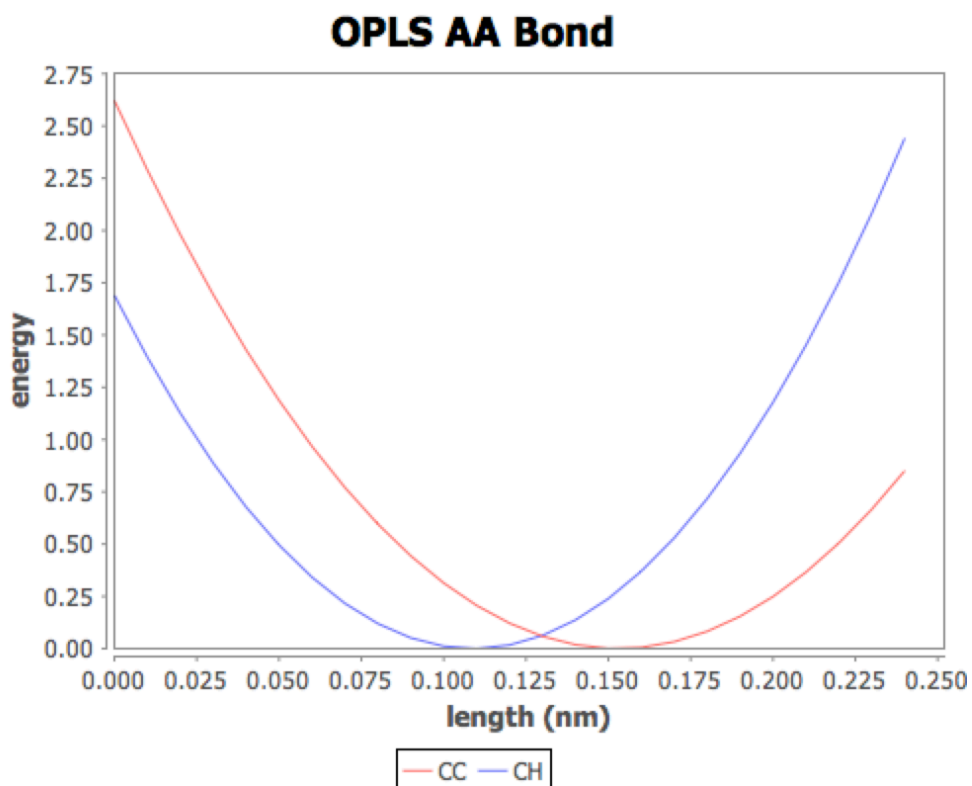


Figure 2.3: OPLS potentials (AA scale); bond between two carbon atoms: CC; bond between a carbon atom and a hydrogen atom: CH.

Distances and energies are given in the internal units of the MD system (see Chap.5 for their definitions).

2.2 Valence Angles

Valence angles tend to maintain constant the angle θ between three linked atoms. In OPLS, the valence angle potentials are harmonic: a *harmonic valence potential* is a scalar field \mathcal{U} which defines the potential energy of an angle by:

$$\mathcal{U}(\theta) = k(\theta - \theta_0)^2 \quad (2.2)$$

where k is the strength of the valence angle and θ_0 is the angle of equilibrium (the one for which no force is exerted on the three atoms by the valence angle).

Fig.2.4 shows the parabolic curves of the OPLS valence potentials between three carbon atoms (CCC), between one carbon atom and two hydrogen atoms (HCH), and between two carbon atoms and one hydrogen atom (CCH).

2.3 Torsion Angles

A torsion angle (also called *dihedral*) tends to keep constant the angle formed between two planes determined by four linked atoms. In OPLS, the potentials of the torsion angles have a “triple cosine” form, which means that the potential \mathcal{U} of a torsion angle θ is given by :

$$\mathcal{U}(\theta) = 0.5[A_1(1 + \cos(\theta)) + A_2(1 - \cos(2\theta)) + A_3(1 + \cos(3\theta))] \quad (2.3)$$

Fig.2.5 shows the curves of the torsion angle potentials between four carbons (CCCC), between two carbon atoms and two hydrogen atoms (HCCH) and between three carbon atoms and one hydrogen atom (CCCH). Note that for alkanes, in all torsion angles the two central atoms are carbon atoms. Furthermore, in OPLS no force is exerted on the four atoms when they belong to the same plane (π torsion angle).

2.4 Inter-Molecular Forces

The van Der Waals forces exerted between two atoms are extremely repulsive at short distances and weakly attractive at long distances. In OPLS, van Der Waals forces are described by *6-12 Lennard-Jones* potentials. A

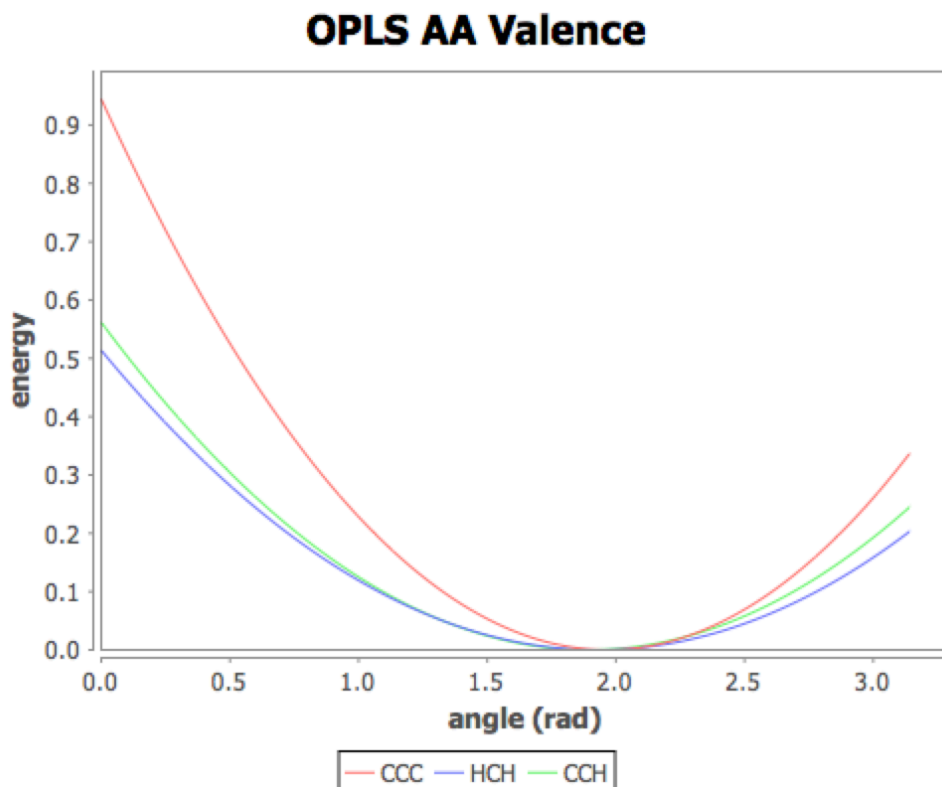


Figure 2.4: OPLS potentials of valence angles; between three carbons: CCC; between one carbon and two hydrogens: HCH; between one hydrogen and two carbons: CCH.

6-12 Lennard-Jones potential is defined by two parameters σ and ϵ ; σ is the distance at which the potential is zero and ϵ is the depth of the potential (the maximum of the attractive energy). The potential energy $\mathcal{U}(r)$ between two atoms at a distance r is defined by:

$$\mathcal{U}(r) = 4\epsilon\left[\left(\frac{\sigma}{r}\right)^{12} - \left(\frac{\sigma}{r}\right)^6\right] \quad (2.4)$$

Fig.2.6 shows the curves of the OPLS 6-12 Lennard-Jones potentials between two carbon atoms (CC), between a carbon atom and a hydrogen atom (CH), and between two hydrogen atoms (HH).

From now on, the 6-12 Lennard-Jones functions will simply be called “Lennard-Jones functions”.

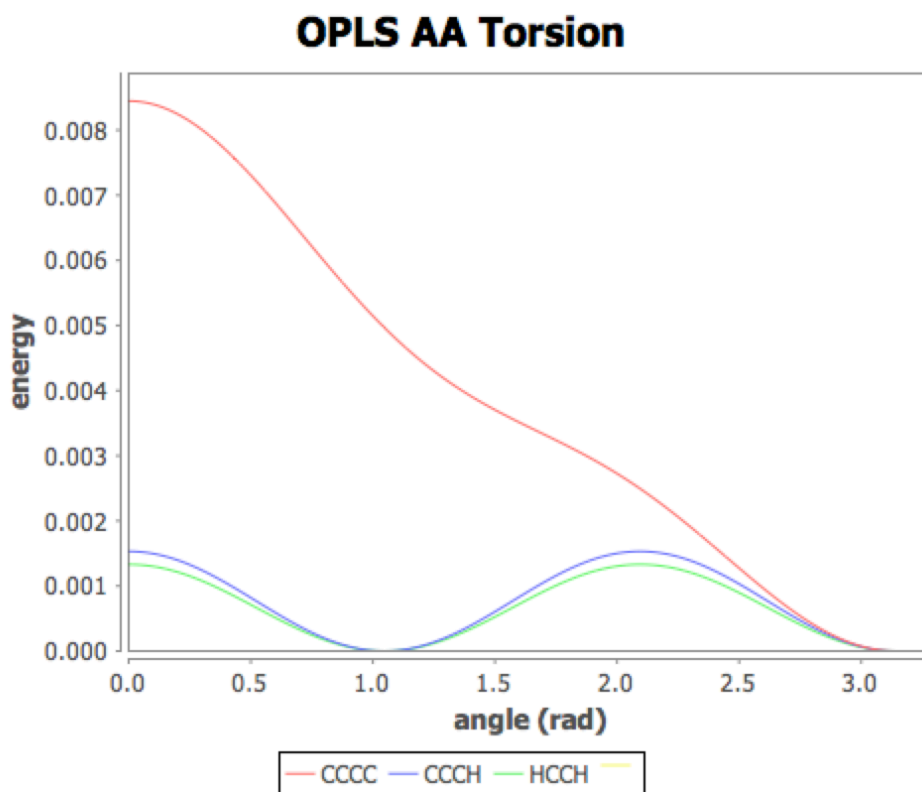


Figure 2.5: OPLS torsion angle potentials (*AA* scale); between four carbon atoms: CCCC; between three carbon atoms and one hydrogen atom: CCCH; between two carbon atoms and two hydrogen atoms: HCCH.

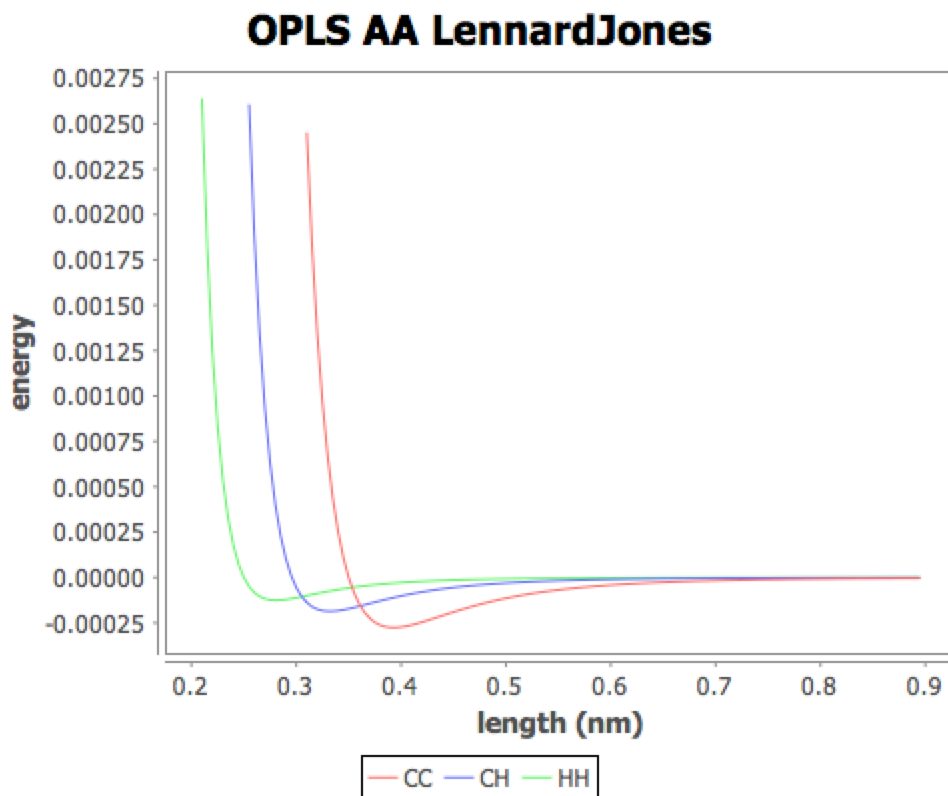


Figure 2.6: Lennard-Jones OPLS potentials (AA scale) between two carbon atoms: CC; between one carbon atom and one hydrogen atom: CH; between two hydrogen atoms: HH.

Chapter 3

Forces at AA Scale

We now describe the forces that apply at the AA scale¹.

The definition of the forces that apply to atoms must be very precise, otherwise some energy may be introduced or lost when simulating closed molecular systems.

One uses the following notations of vector algebra:

- if a and b are two atoms, we note \vec{ab} the vector with origin a and end b ; the distance between the two atoms is noted $|ab|$.
- The null vector is noted 0 .
- The length of vector \vec{u} is noted $|\vec{u}|$. One thus has: $|\vec{ab}| = |ab|$.
- Multiplication of \vec{u} by the scalar n is noted $n \cdot \vec{u}$, or more simply $n\vec{u}$.
- The vectorial product of \vec{u} and \vec{v} is noted $\vec{u} \times \vec{v}$.
- The scalar product of \vec{u} and \vec{v} is noted $\vec{u} \bullet \vec{v}$.
- We write $\vec{u} \perp \vec{v}$ when \vec{u} and \vec{v} are orthogonal ($\vec{u} \bullet \vec{v} = 0$).
- We note $norm(\vec{u})$ the normalized vector from \vec{u} (same direction, but length equal to 1) defined by $norm(\vec{u}) = (1/|\vec{u}|) \cdot \vec{u}$.
- If a , b and c are atoms, we note \widehat{abc} the angle formed by a , b and c .

¹This chapter is directly taken from [18] (also available in [19]).

3.1 Bonds

A bond models a sharing of electrons between two atoms which produces a force between them. This force is the derivative of the bond potential defined between the two atoms. Fig. 3.1 shows a (attractive) force produced between two linked atoms a and b .

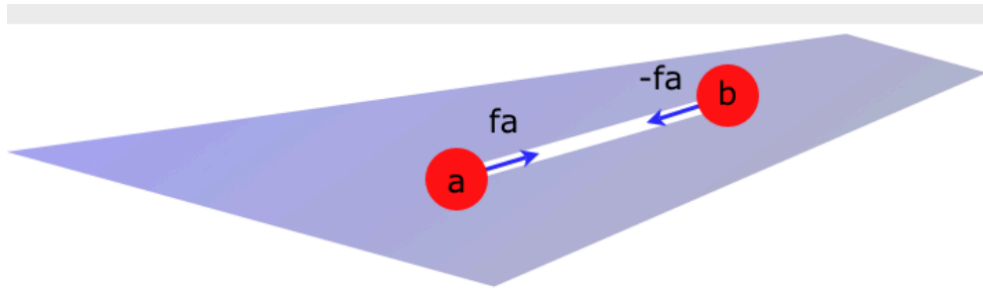


Figure 3.1: Attractive forces between two bonded atoms.

A *harmonic bond potential* is a scalar field \mathcal{U} which defines the potential energy of two atoms placed at distance r as:

$$\mathcal{U}(r) = k(r - r_0)^2 \quad (3.1)$$

where k is the strength of the bond and r_0 is the equilibrium distance (the distance at which the force between the two atoms is null). We thus have:

$$\frac{\partial \mathcal{U}(r)}{\partial r} = 2k(r - r_0) \quad (3.2)$$

The partial derivative of \mathcal{U} according to the position r_a of a is:

$$\frac{\partial \mathcal{U}(r)}{\partial r_a} = \frac{\partial \mathcal{U}(r)}{\partial r} \cdot \frac{\partial r}{\partial r_a} \quad (3.3)$$

But:

$$\frac{\partial r}{\partial r_a} = 1 \quad (3.4)$$

We thus have:

$$\frac{\partial \mathcal{U}(r)}{\partial r_a} = 2k(r - r_0) \quad (3.5)$$

Let a and b be two atoms, and $\vec{u} = \text{norm}(\vec{ba})$ be the normalization of vector \vec{ba} . The force produced on atom a is:

$$\vec{f}_a = -\frac{\partial \mathcal{U}(r)}{\partial r_a} \cdot \vec{u} = -2k(r - r_0) \cdot \vec{u} \quad (3.6)$$

and the one on b is the opposite, according to the action/reaction principle:

$$\vec{f}_b = -\vec{f}_a \quad (3.7)$$

Therefore, if $r > r_0$, the force on a is a vector whose direction is opposite to \vec{u} and tends to bring a and b closer (attractive force), while it tends to bring them apart (repulsive force) when $r < r_0$.

According to the definition of \vec{f}_a and \vec{f}_b , the sum of the forces applied to a and b is null (i.e. equilibrium of forces):

$$\vec{f}_a + \vec{f}_b = 0 \quad (3.8)$$

Note that no torque (moment of forces) is produced as the two forces are colinear.

3.2 Valence Angles

Valence angles tend to maintain at a fixed value the angle between three atoms a , b and c such that a is linked to b and b to c , as shown on Fig. 3.2.

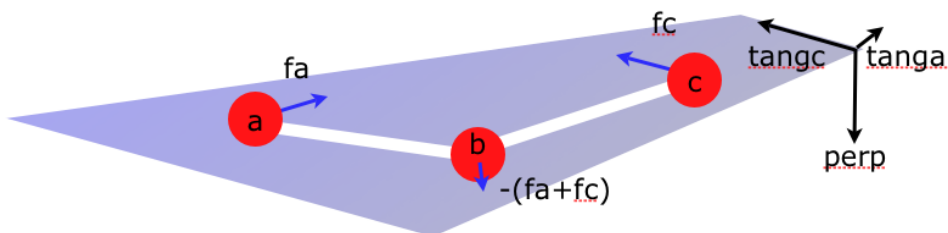


Figure 3.2: Valence Angle

The forces applied to the three atoms all belong to the plane abc defined by the points a , b , c .

The potential \mathcal{U} of a valence angle is harmonic and verifies equation Eq.2.2.

The partial derivative of \mathcal{U} according to the angle θ is thus:

$$\frac{\partial \mathcal{U}(\theta)}{\partial \theta} = 2k(\theta - \theta_0) \quad (3.9)$$

The partial derivative of \mathcal{U} according to the position r_a of a is:

$$\frac{\partial \mathcal{U}(\theta)}{\partial r_a} = \frac{\partial \mathcal{U}(\theta)}{\partial \theta} \cdot \frac{\partial \theta}{\partial r_a} \quad (3.10)$$

that is:

$$\frac{\partial \mathcal{U}(\theta)}{\partial r_a} = 2k(\theta - \theta_0) \cdot \frac{\partial \theta}{\partial r_a} \quad (3.11)$$

As a describes a circle with radius $|ab|$, centered on b , we have²:

$$\frac{\partial \theta}{\partial r_a} = \frac{1}{|ab|} \quad (3.12)$$

Let \vec{p}_a be the normalized vector in the plane abc , orthogonal to \vec{ba} :

$$\vec{p}_a = \text{norm}(\vec{ba} \times (\vec{ba} \times \vec{bc})) \quad (3.13)$$

The force applied on a is then:

$$\vec{f}_a = -\frac{\partial \mathcal{U}(\theta)}{\partial r_a} \cdot \vec{p}_a = -2k(\theta - \theta_0)/|ab| \cdot \vec{p}_a \quad (3.14)$$

In the same way, the force applied on c is:

$$\vec{f}_c = -2k(\theta - \theta_0)/|bc| \cdot \vec{p}_c \quad (3.15)$$

where \vec{p}_c is the normalized vector in plane abc , orthogonal to \vec{cb} :

$$\vec{p}_c = \text{norm}(\vec{cb} \times (\vec{ba} \times \vec{bc})) \quad (3.16)$$

The sum of the forces should be null:

$$\vec{f}_a + \vec{f}_b + \vec{f}_c = 0 \quad (3.17)$$

²The length of an arc of circle is equal to the product of the radius by the angle (in radians) corresponding to the arc of circle.

Thus, the force applied to b is:

$$\vec{f}_b = -\vec{f}_a - \vec{f}_c \quad (3.18)$$

Moreover, the two momenta exerted on b by \vec{f}_a and \vec{f}_c are opposite because :

$$\vec{ab} \times \vec{f}_a = -\vec{cb} \times \vec{f}_c \quad (3.19)$$

As a consequence, no rotation around b can result from the application of the two forces \vec{f}_a and \vec{f}_c .

3.3 Torsion Angles

A torsion angle θ defined by four atoms a, b, c, d is shown on Fig. 3.3.

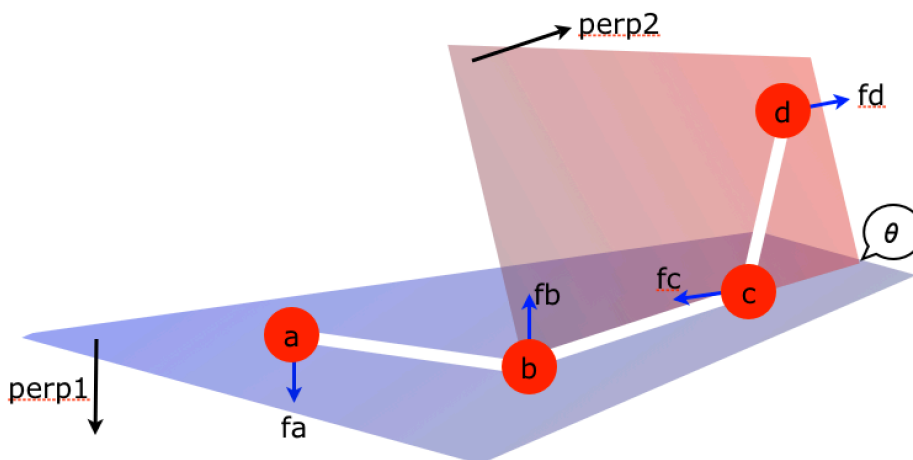


Figure 3.3: Torsion angle θ

Potentials of torsion angles have a “triple-cosine” form verifying Eq.2.3.

The partial derivative of the torsion angle potential according to the position r_a of a is:

$$\frac{\partial U(\theta)}{\partial r_a} = \frac{\partial U(\theta)}{\partial \theta} \cdot \frac{\partial \theta}{\partial r_a} \quad (3.20)$$

The partial derivative of the potential according to the angle θ is:

$$\frac{\partial U(\theta)}{\partial \theta} = 0.5(-A_1 \sin(\theta) + 2A_2 \sin(2\theta) - 3A_3 \sin(3\theta)) \quad (3.21)$$

$$= -0.5(A_1 \sin(\theta) - 2A_2 \sin(2\theta) + 3A_3 \sin(3\theta)) \quad (3.22)$$

Forces on a and d

Let us call θ_1 the angle \widehat{abc} . Atom a turns around direction bc , on a circle of radius $|ab|\sin(\theta_1)$. The partial derivative of θ according to the position of a is:

$$\frac{\partial\theta}{\partial r_a} = \frac{1}{|ab|\sin(\theta_1)} \quad (3.23)$$

We thus have:

$$\frac{\partial\mathcal{U}(\theta)}{\partial r_a} = \frac{-0.5}{|ab|\sin(\theta_1)}(A_1\sin(\theta) - 2A_2\sin(2\theta) + 3A_3\sin(3\theta)) \quad (3.24)$$

Similarly, for atom d , where θ_2 is the angle \widehat{bcd} :

$$\frac{\partial\mathcal{U}(\theta)}{\partial r_d} = \frac{-0.5}{|cd|\sin(\theta_2)}(A_1\sin(\theta) - 2A_2\sin(2\theta) + 3A_3\sin(3\theta)) \quad (3.25)$$

Let \vec{p}_1 the normalized vector orthogonal to the plane abc , and \vec{p}_2 the normalized vector orthogonal to the plane bcd (the angle between \vec{p}_1 and \vec{p}_2 is θ):

$$\vec{p}_1 = \text{norm}(\vec{ba} \times \vec{bc}) \quad (3.26)$$

$$\vec{p}_2 = \text{norm}(\vec{cd} \times \vec{cb}) \quad (3.27)$$

The force applied on a is:

$$\vec{f}_a = \frac{0.5}{|ab|\sin(\theta_1)}(A_1\sin(\theta) - 2A_2\sin(2\theta) + 3A_3\sin(3\theta)) \cdot \vec{p}_1 \quad (3.28)$$

In the same way, the force applied on d is:

$$\vec{f}_d = \frac{0.5}{|cd|\sin(\theta_2)}(A_1\sin(\theta) - 2A_2\sin(2\theta) + 3A_3\sin(3\theta)) \cdot \vec{p}_2 \quad (3.29)$$

Forces on b and c

We now have to determine the forces \vec{f}_b and \vec{f}_c to be applied on b and c . The equilibrium conditions imply two constraints: (A) the sum of the forces has to be null:

$$\vec{f}_a + \vec{f}_b + \vec{f}_c + \vec{f}_d = 0 \quad (3.30)$$

and (B) the sum of torques also has to be null³. Calling o the center of bond bc , this means:

$$\vec{o}\vec{a} \times \vec{f}_a + \vec{o}\vec{d} \times \vec{f}_d + \vec{o}\vec{b} \times \vec{f}_b + \vec{o}\vec{c} \times \vec{f}_c = 0 \quad (3.31)$$

From (3.31) it results:

$$(\vec{o}\vec{b} + \vec{b}\vec{a}) \times \vec{f}_a + (\vec{o}\vec{c} + \vec{c}\vec{d}) \times \vec{f}_d + \vec{o}\vec{b} \times \vec{f}_b + \vec{o}\vec{c} \times \vec{f}_c = 0 \quad (3.32)$$

and:

$$(-\vec{o}\vec{c} + \vec{b}\vec{a}) \times \vec{f}_a + (\vec{o}\vec{c} + \vec{c}\vec{d}) \times \vec{f}_d - \vec{o}\vec{c} \times \vec{f}_b + \vec{o}\vec{c} \times \vec{f}_c = 0 \quad (3.33)$$

which implies:

$$\vec{o}\vec{c} \times (-\vec{f}_a + \vec{f}_d - \vec{f}_b + \vec{f}_c) + \vec{b}\vec{a} \times \vec{f}_a + \vec{c}\vec{d} \times \vec{f}_d = 0 \quad (3.34)$$

From (3.30) it results:

$$-\vec{f}_a + \vec{f}_d - \vec{f}_b + \vec{f}_c = 2(\vec{f}_d + \vec{f}_c) \quad (3.35)$$

Substituting (3.35) in (3.34), one gets:

$$\vec{o}\vec{c} \times (2(\vec{f}_d + \vec{f}_c)) + \vec{b}\vec{a} \times \vec{f}_a + \vec{c}\vec{d} \times \vec{f}_d = 0 \quad (3.36)$$

thus:

$$2\vec{o}\vec{c} \times \vec{f}_d + 2\vec{o}\vec{c} \times \vec{f}_c + \vec{b}\vec{a} \times \vec{f}_a + \vec{c}\vec{d} \times \vec{f}_d = 0 \quad (3.37)$$

which implies:

$$2\vec{o}\vec{c} \times \vec{f}_c = -2\vec{o}\vec{c} \times \vec{f}_d - \vec{c}\vec{d} \times \vec{f}_d - \vec{b}\vec{a} \times \vec{f}_a \quad (3.38)$$

and finally we get the condition that the torque from \vec{f}_c should verify in order (3.31) to be true:

$$\vec{o}\vec{c} \times \vec{f}_c = -(\vec{o}\vec{c} \times \vec{f}_d + 0.5\vec{c}\vec{d} \times \vec{f}_d + 0.5\vec{b}\vec{a} \times \vec{f}_a) \quad (3.39)$$

Let us state:

$$\vec{t}_c = -(\vec{o}\vec{c} \times \vec{f}_d + 0.5\vec{c}\vec{d} \times \vec{f}_d + 0.5\vec{b}\vec{a} \times \vec{f}_a) \quad (3.40)$$

³It is not possible to simply define $\vec{f}_b = -\vec{f}_a$ and $\vec{f}_c = -\vec{f}_d$, as the sum of torques would be non-null, thus leading to an increase of potential energy.

Equation $\vec{o}\vec{c} \times \vec{x} = \vec{t}_c$ has an infinity of solutions in \vec{x} , all having the same component perpendicular to $\vec{o}\vec{c}$. We thus simply choose as solution the force perpendicular to $\vec{o}\vec{c}$ defined by:

$$\vec{f}_c = (1/|oc|^2)\vec{t}_c \times \vec{o}\vec{c} \quad (3.41)$$

Equation (3.39) is verified because:

$$\vec{o}\vec{c} \times \vec{f}_c = (1/|oc|^2)\vec{o}\vec{c} \times (\vec{t}_c \times \vec{o}\vec{c}) \quad (3.42)$$

thus⁴ :

$$\vec{o}\vec{c} \times \vec{f}_c = (1/|oc|^2)|oc|^2\vec{t}_c = \vec{t}_c \quad (3.43)$$

The value of \vec{f}_b is finally deduced from equation (3.30) stating the equilibrium of forces:

$$\vec{f}_b = -\vec{f}_a - \vec{f}_c - \vec{f}_d \quad (3.44)$$

We have thus determined four forces $\vec{f}_a, \vec{f}_b, \vec{f}_c, \vec{f}_d$ whose sum is null (3.30) and whose sum of torques is also null (3.31).

3.4 Inter-Molecular Forces

Inter-molecular potentials are Lennard-Jones potentials of the form defined by equation 2.4.

Letting $A = \sigma^{12}$ and $B = \sigma^6$, this equation becomes:

$$\mathcal{U}(r) = 4\epsilon\left(\frac{A}{r^{12}} - \frac{B}{r^6}\right) \quad (3.45)$$

The partial derivative of \mathcal{U} according to distance is thus:

$$\frac{\partial\mathcal{U}(r)}{\partial r} = 4\epsilon\left(-12\frac{A}{r^{13}} + 6\frac{B}{r^7}\right) \quad (3.46)$$

$$= 24\epsilon\left(-2\frac{A}{r^{13}} + \frac{B}{r^7}\right) \quad (3.47)$$

$$= \frac{24\epsilon}{r}\left(-2\frac{A}{r^{12}} + \frac{B}{r^6}\right) \quad (3.48)$$

$$= -\frac{24\epsilon}{r}\left(2\left(\frac{\sigma}{r}\right)^{12} - \left(\frac{\sigma}{r}\right)^6\right) \quad (3.49)$$

⁴if $u \perp v$, then $u \times (v \times u) = |u|^2 v$.

Let a and b be two atoms. The force on a is:

$$\vec{f}_a = \frac{24\epsilon}{r} \left(2\left(\frac{\sigma}{r}\right)^{12} - \left(\frac{\sigma}{r}\right)^6 \right) \cdot \vec{u} \quad (3.50)$$

where \vec{u} is the normalization of \vec{ba} .

The force on b should be the opposite of the force on a :

$$\vec{f}_b = -\vec{f}_a \quad (3.51)$$

The sum of the forces applied to a and b is thus null. As for bonds, no torque is produced because the two forces are colinear.

Resume

The forces defined in the previous sections are summed up in the following table:

Bond ab	3.6	$\vec{f}_a = -2k(r - r_0) \cdot \vec{u}$
	3.7	$\vec{f}_b = -\vec{f}_a$
Valence abc	3.14	$\vec{f}_a = -2k(\theta - \theta_0) / ab \cdot \vec{p}_a$
	3.18	$\vec{f}_b = -(\vec{f}_a + \vec{f}_c)$
	3.15	$\vec{f}_c = -2k(\theta - \theta_0) / bc \cdot \vec{p}_c$
Torsion $abcd$	3.28	$\vec{f}_a = \frac{0.5}{ ab \sin(\theta_1)} (A_1 \sin(\theta) - 2A_2 \sin(2\theta) + 3A_3 \sin(3\theta)) \cdot \vec{p}_1$
	3.44	$\vec{f}_b = -\vec{f}_a - \vec{f}_c - \vec{f}_d$
	3.41	$\vec{f}_c = (1/ oc ^2) \vec{cp} \times \vec{oc}$
	3.29	$\vec{f}_d = \frac{0.5}{ cd \sin(\theta_2)} (A_1 \sin(\theta) - 2A_2 \sin(2\theta) + 3A_3 \sin(3\theta)) \cdot \vec{p}_2$
L-J ab	3.50	$\vec{f}_a = \frac{24\epsilon}{r} \left(2\left(\frac{\sigma}{r}\right)^{12} - \left(\frac{\sigma}{r}\right)^6 \right) \cdot \vec{u}$
	3.51	$\vec{f}_b = -\vec{f}_a$

Bond In Eq. 3.6, k is the bond strength constant, r is the distance between atoms a and b , and r_0 is the equilibrium distance, for which energy is null. Vector \vec{u} is defined by $\vec{u} = \text{norm}(\vec{ba})$.

Valence In 3.14 and 3.15, k is the angle strength constant, θ is the angle \widehat{abc} , and θ_0 is the equilibrium angle, for which energy is null. In 3.14, \vec{p}_a is defined by $\vec{p}_a = \text{norm}(\vec{ba} \times (\vec{ba} \times \vec{bc}))$. In 3.15, \vec{p}_c is defined by $\vec{p}_c = \text{norm}(\vec{cb} \times (\vec{ba} \times \vec{bc}))$.

Torsion In 3.28 and 3.29, θ is the torsion angle, θ_1 is the angle \widehat{abc} , θ_2 is the angle \widehat{bcd} and A_1 , A_2 and A_3 are the parameters which define the “three-cosine” form of the torsion angle. Vector \vec{p}_1 is defined by $\vec{p}_1 = \text{norm}(\vec{ba} \times \vec{bc})$ and $\vec{p}_2 = \text{norm}(\vec{cd} \times \vec{cb})$. In 3.41, o is the middle of bc and \vec{t}_c is defined by $\vec{t}_c = -(\vec{oc} \times \vec{f}_d + 0.5\vec{cd} \times \vec{f}_d + 0.5\vec{ba} \times \vec{f}_a)$.

LJ In 3.50, σ is the distance at which the potential is null and ϵ is the depth of the potential (minimum of energy). As for bonds, one has $\vec{u} = \text{norm}(\vec{ba})$.

In each case (bond, valence, torsion, LJ interaction), the sum of the forces that are applied to atoms is always null (Eq. (3.8), (3.17), (3.30), (3.51)). Moreover, no torque is induced by application of these forces: no torque is produced by bonds and LJ interactions, as the produced forces are colinear; we have verified that no torque is produced by valence angles; for torsion angles, we have chosen the forces in such a way that the sum of the forces and the global sum of torques are always null (3.31). This means that no energy is ever added by the application of the forces during the simulation process.

It should be noted that torsion angles are the only components that bring about changes in the 3D geometry of the molecules. All the other components are producing forces that remain systematically in a same plane.

In conclusion, in this chapter we have precisely defined the forces that apply on atoms in MD simulations. The definitions are given in a purely vectorial formalism (with no use of a specific coordinate system). We have shown that the sum of the forces and the sum of the torques are always null, which means that the energy of (isolated) molecular systems is preserved while the forces are applied.

Chapter 4

Implementation

This chapter considers the question of implementing MD by describing a system implemented in the Java programming language. The library JavaFX is used for 3D visualisation¹. This system is presented in [7], the main elements of which are summarised here.

The implementation is a prototype that does not take into account a number of functions generally offered by MD systems, such as temperature control (thermostat) or pressure control (barostat), or the possibility to define molecular systems using periodic conditions (crystals).

In fact, the system we are going to consider only implements the core of MD, in other words Newtonian mechanics, and the only molecular systems that will be considered are linear chains of carbon and hydrogen atoms (alkanes) introduced in Chap.2.

The main objective is to provide an implementation of multi-scale molecular systems (cf Sec.1.2), allowing changes in the scale of description during the course of the simulation (Sec.1.3).

In IT terms, this implementation must be able to handle molecular systems that are not defined once and for all, not frozen from the start. On the contrary, the implementation must allow for *modular* definitions in which molecules can be created or removed during execution.

A central characteristics of the Newtonian physics on which MD is based is *determinism* or, what amounts to the same thing, the preservation of the energy of isolated systems over time. It is obviously imperative that the total energy of an isolated system remains the same over the course of the

¹Previous version of the system was using Java3D for visualisation.

simulation, even if changes of scale take place.

The MD system built and used here is based on a programming paradigm called “Synchronous Reactive programming” [5], which reconciles modularity and determinism. The central modularity tool in reactive programming is the *deterministic parallelism* operator, which is used through a Java library - SugarCubes [8].

The rest of this chapter describes reactive programming and the SugarCubes library that implements it in Java. We then present the resolution method used to obtain simulations that are stable over time (the stability of the implementation is discussed in Chap. 5).

4.1 Reactive Programming

Synchronous Reactive programming (RP) offers a simple programming paradigm with clear and precise semantics. The central feature of RP is that it provides primitives for expressing parallelism directly at the programming level. In RP, parallelism is a *logical* one, to be clearly distinguished from the execution parallelism linked to the operating system on which simulations are run. Logical parallelism is an extremely powerful modularity means, enabling complex systems to be broken down and coded into communicating sub-systems whose structure can evolve dynamically (dynamicity).

The logical parallelism of RP has also a fundamental characteristic: it is deterministic. Reconciling parallelism, determinism and dynamicity may seem paradoxical, but RP provides a way of resolving this paradox in a coherent computing framework.

In the reactive approach, systems are composed of parallel components sharing the same *instants* which thus define a *logical clock* shared by all the components. The components synchronise at the end of each instant and thus run at the same rate. During each instant, the components can communicate with each other using signals (called *events* in SugarCubes) which are broadcast instantaneously. These signals are analogous to radio transmissions where all the receivers listening on the same frequency immediately receive the same message. In the reactive approach, dynamicity is only taken into account at the boundaries of instants.

There exist several variants of RP, extending various general-purpose programming languages (for example, ReactiveC [5] which extends C, and ReactiveML [15] which extends the ML language). RP is also strongly related to

the synchronous programming language Esterel [4], the main difference being that dynamic program evolution is forbidden in Esterel while allowed in RP. One of the variants of RP that extends the Java language is called SugarCubes [8]. The **merge** parallelism operator in SugarCubes is completely deterministic, which means that at each time a SugarCubes program has a unique output, function of the inputs, and that the execution trace is unique.

We will now describe SugarCubes in the following section ².

4.2 SugarCubes

The two main SugarCubes classes are the **Instruction** class of reactive instructions defined with reference to instants, and the **Machine** class of reactive machines which execute the reactive instructions.

A reactive machine executes the reactive instructions for which it is responsible in a coordinated manner, allowing instructions to communicate with each other using *events* which are instantaneously broadcast. Instantaneity here means that an event generated during an instant is received during that very same instant by all instructions waiting for it.

One consequence is that the reaction to the absence of an event can only take place at the next instant. Thus, there is no case where an event is seen as present at one instant by one of the instructions executed by the reactive machine, while it is seen as absent by another instruction.

Events are automatically reset to absent by the reactive machine at the start of each new instant.

Values can be associated with events, and if this is the case, the instructions receive all of them, in the same order (the order in which they are generated during the current instant).

Reactive machines proceed by instants: execution takes place during the first instant, then during the second, then during the third, and so on indefinitely. All the instructions present in the reactive machine are executed at each instant, and the next instant only takes place when there is nothing left to execute during the current instant. In particular, execution in the current instant is continued if there remain reactive instructions blocked on generated events. In this way, we can be sure that at the end of each instant all reactive instructions have completed their execution for that instant and have reacted to all the events generated during the instant.

²We only present here the main concepts; a full description is available in [8].

New reactive instructions can only be introduced into the reactive machine between two instants. In this way, the determinism of execution during an instant is not at risk of being disrupted when new instructions are dynamically introduced in the execution machine.

Reactive instructions are always executed in parallel and deterministically by the reactive machine. This deterministic dynamic parallelism is also directly available at the coding level in the form of a reactive instruction called `merge`. Let us now describe the main reactive instructions of SugarCubes.

The main SugarCubes reactive instructions are as follows:

Next Instant. The `stop` instruction suspends execution for the current instant of the reactive instruction it appears in. Execution will resume after the `stop` instruction at the next instant.

Sequence. The instruction `seq (i1,i2)` behaves as `i1` but the execution switches immediately (i.e. without waiting for the next instant) to `i2` as soon as `i1` terminates.

Parallelism. The `merge (i1,i2)` instruction executes one instant of the `i1` instruction and one of the `i2` instruction. It ends when both `i1` and `i2` have themselves terminated. Execution always starts with `i1` then passes to `i2` when `i1` ends or is suspended (i.e. waiting for a non-generated event).

Loop. The instruction `loop (i)` executes `i` in a loop: the execution of `i` is immediately restarted by the loop as soon as it terminates. We assume that it is impossible for `i` to start and terminate during the same instant (otherwise, we would have an *instantaneous loop* which could cycle indefinitely, preventing the reactive machine from detecting the end of the current instant and therefore preventing it to start the next instant).

Java Code. The instruction `action (act)` runs the `execute` method of the Java object `act` (of type `JavaAction`) and terminates immediately. Note that `act` can be executed several time during the same instant if `action (act)` appears in a loop, provided it is not an instantaneous one.

Event Generation. The instruction `generate (event,value)` generates `event` with `value` as associated value, and then terminates immediately.

Waiting for an Event. The instruction `await (event)` terminates immediately if `event` is present (i.e. it has been previously generated during the current instant). Otherwise, the same execution will start again at the next instant.

Generated Values. The instruction `callback (event,call)` executes the `execute` method of the Java object (of type `JavaCallback`) for each value of `event` generated during the current instant. To avoid the risk of losing values, execution of the callback suspends after each value processed, and in all cases it terminates only at the next instant.

Preemption. The instruction `until (event,i)` executes `i` and terminates either because `i` terminates, or because `event` is present (i.e. has been generated during the current instant).

The sequence and parallelism instructions are naturally extended to more than two branches: for example, the instruction `seq (i1,i2,i3)` puts in sequence the three instructions `i1`, `i2`, `i3`, and has the meaning of `seq (i1,seq (i2,i3))`.

A reactive machine of class `Machine` executes its program which is a reactive instruction. The new instructions added in the machine are placed in parallel (`merge`) with the existing program. The role of the reactive machine is to execute its program, to detect the end of the current instant, i.e. when all the parallel branches of its program are either finished or suspended, and when this is the case, to move on to the next instant.

New instructions cannot be directly added during the current instant but only when it is finished, before the start of the next instant.

The execution of the program (the reactive instruction that the machine holds) for a given instant can be broken down into several successive phases, during which new events are generated, causing the instructions waiting for them to react.

For example, consider the following code, assuming that the event `e` has not been previously generated during the current instant:

```
merge (
    await e,
    generate (e,0)
)
```

Execution begins with the `await` instruction (line 2) which suspends since

`e` is absent. Execution then proceeds to the `generate` instruction (line 3) which generates `e` (with the value 0) and then terminates. The first phase of execution of the `merge` instruction is complete but the reactive machine detects that a suspended instruction remains, waiting for `e`.

A new phase then begins and the `await` instruction is executed again and terminates since `e` is now present. The instruction `merge` then also terminates because its two branches are now both terminated.

The execution of the program by a reactive machine is totally deterministic: only one trace of execution is possible. The execution of SugarCubes programs is sequential and the parallelism of SugarCubes is purely logical. The precise (formal) definition of the semantics of SugarCubes and a comparison with the standard *thread-based* approach to concurrency is available in [9].

4.3 Resolution Method

The resolution method we use is known as “*Velocity-Verlet*”. For each atom, it works in two stages: the position of the atom is determined at the end of the first stage, and its velocity is determined at the end of the second stage. The acceleration is computed (by Newton’s law) in the second stage by summing all the forces applied to the atom during this stage. At the end of the second stage, velocity and acceleration are stored in order to be used in the next stage.

We are going to describe how *Velocity-Verlet* works in more detail.

Let \mathbf{r}_t be the position of an atom at time t , \mathbf{v}_t its velocity at time t , and \mathbf{a}_t its acceleration at time t . The *Velocity-Verlet* resolution method is defined by the two following equations, where Δt is a time interval:

$$\mathbf{r}_{t+\Delta t} = \mathbf{r}_t + \mathbf{v}_t\Delta t + 0.5\mathbf{a}_t\Delta t^2 \quad (4.1)$$

$$\mathbf{v}_{t+\Delta t} = \mathbf{v}_t + 0.5(\mathbf{a}_t + \mathbf{a}_{t+\Delta t})\Delta t \quad (4.2)$$

The acceleration $\mathbf{a}_{t+\Delta t}$ of an atom is obtained by collecting the intra- and inter-molecular forces exerted on the atom at its position at time $t + \Delta t$. In order to do this, two stages are necessary: in the first stage, the atom is positioned and in the second the forces exerted on it are collected; the algorithm is as follows:

1. Calculation of the speed at half the time-step, from the speed and acceleration computed at the previous stage:

$$\mathbf{v}_{t+0.5\Delta t} = \mathbf{v}_t + 0.5\mathbf{a}_t\Delta t \quad (4.3)$$

Then, use of its result to calculate the position at the end of the complete time-step:

$$\mathbf{r}_{t+\Delta t} = \mathbf{r}_t + \mathbf{v}_{t+0.5\Delta t}\Delta t \quad (4.4)$$

2. Calculation of the acceleration at the end of the complete time-step from the forces applied to the atom, and calculation of the velocity at the end of the time-step from the forces applied to the atom. Finally, calculation of the velocity at the end of the complete time-step, using the velocity previously calculated for half the time-step:

$$\mathbf{v}_{t+\Delta t} = \mathbf{v}_{t+0.5\Delta t} + 0.5\mathbf{a}_{t+\Delta t}\Delta t \quad (4.5)$$

The instants of RP are naturally identified with the stages of the resolution method. Thus, two consecutive reactive instants are required to implement each pair of resolution stages corresponding to one time-step Δt .

It should be noted that the time-step may vary depending on the objects simulated. It is this characteristics that makes it possible to simultaneously simulate molecules at different scales of description.

Conclusion

In RP, programming is based on logical parallelism, instantaneous events and dynamic creation/destruction of instructions and events. Moreover, in the SugarCubes version of RP, programs are completely deterministic “by construction”. The MD system implemented in SugarCubes and used in this text shows that reactive programming is an interesting tool for implementing essential aspects of classical physics, particularly the following points:

- The numerical simulations are based on a discretisation of time and on a resolution method implementing an integration algorithm. The division of time into instants, which is the basis of reactive programming, naturally discretises time, and allows us to code in a very simple way the “*Velocity-Verlet*” resolution method, which is proving to be very effective in the context of MD.

- The forces of classical physics are instantaneous and are naturally implemented as instantaneously broadcast events in RP.
- Newton’s laws are deterministic. Their implementation is made much easier by using SugarCubes, whose programs are deterministic “by construction”. Newton’s laws are also reversible in time. With the help of a time-reversible resolution method (as is *Velocity-Verlet*), the intrinsic determinism of SugarCubes is also an advantage for obtaining the time reversibility property of classical physics.
- Changes in the chemical structure of the simulated systems may appear during simulations. The dynamic nature of RP, i.e. the possibility of creating/destroying objects during execution, allows these changes to be implemented in a natural, semantically clear, and deterministic way.

Logical parallelism and RP broadcast events are a powerful modularity tool that allows new parallel components to be introduced into a system without having to adapt the other components. This modularity is effective both at the coding and execution levels. In particular, *observers* can be introduced without disruption, at various stages of coding, in parallel with the program to be tested. This possibility allows programmers to adopt modular coding strategies, in line with modern approaches to programming.

Chapter 5

Simulations at AA Scale

We will now simulate molecules at the AA scale using the potentials of OPLS.

The shapes of the components of the OPLS potentials for alkanes were described in Chap.2. The forces exerted on atoms have been defined in Chap.4. In order to simulate alkanes at AA scale, we still need to give the values of the parameters of the OPLS components.

The system units are the following:

- time : pico-seconde (ps , 10^{-12} second) ;
- distances : nano-mètre (nm , 10^{-9} meter) ;
- masses : kg/mol ;
- angles : radian (rad) ;
- energies : $kg/mol.nm^2/ps^2$;
- velocities : nm/ps (also km/s).

OPLS parameter values for alkanes are given in system units, in Fig.5.1.

In Fig.5.1 one has:

- k_l is the strength of the bond l and r_l is its equilibrium distance, for $l = CC$ or $l = CH$ (Eq.2.1);
- k_a is the strength of the valence angle a and r_a is its equilibrium value, for $a = CCC$ or $a = CCH$ or $a = HCH$ (Eq.2.2) ;

$$\begin{aligned}
k_{CC} &= 112.1312 & r_{CC} &= 0.1529 \\
k_{CH} &= 142.256 & r_{CH} &= 0.109 \\
k_{CCC} &= 0.2441364 & \theta_{CCC} &= 1.9669860669976096 \\
k_{CCH} &= 0.1569 & \theta_{CCH} &= 1.8920924724829928 \\
k_{HCH} &= 0.138072 & \theta_{HCH} &= 1.9288037832146987 \\
A1_{CCCC} &= 0.00728016 & A2_{CCCC} &= -6.56888.10^{-4} \\
& & A3_{CCCC} &= 0.001167336 \\
A1_{CCCH} &= 0 & A2_{CCCH} &= 0 & A3_{CCCH} &= 0.001531344 \\
A1_{HCCH} &= 0 & A2_{HCCH} &= 0 & A3_{HCCH} &= 0.001330512 \\
\epsilon_{CC} &= 2.7614.10^{-4} & \sigma_{CC} &= 0.35 \\
\epsilon_{CH} &= 1.86188.10^{-4} & \sigma_{CH} &= 0.2958 \\
\epsilon_{HH} &= 1.2552.10^{-4} & \sigma_{HH} &= 0.25
\end{aligned}$$

Figure 5.1: Values of OPLS parameters for alkanes, given in system units.

- $A1_a$, $A2_a$ and $A3_a$ are the parameters of the torsion angles, for $a = CCCC$ or $a = CCCH$ or $a = HCCH$ (Eq.2.3);
- ϵ_p and σ_p are the parameters for pairs of atoms, for $p = CC$, $p = CH$ or $p = HH$ (Eq.2.4).

5.1 Stability

The MD system makes it possible to run very long simulations, preserving energy. To illustrate this stability, consider the simulation of a C_8H_{16} molecule which initially has been given energy by slightly lengthening its CC bonds. The simulation is carried out with a time-step of 10^{-4} ps (i.e. 0.1 femto-second). Fig.5.2 shows the molecule being simulated on the left, and the energies measured every 10^5 instants on the right. Kinetic energy is shown in blue, internal energy in green, total energy in red (inter-molecular energy, in yellow, is always zero). Stability of the total energy appears clearly.

The 4.10^7 instants correspond to a simulated time of 2 ns.

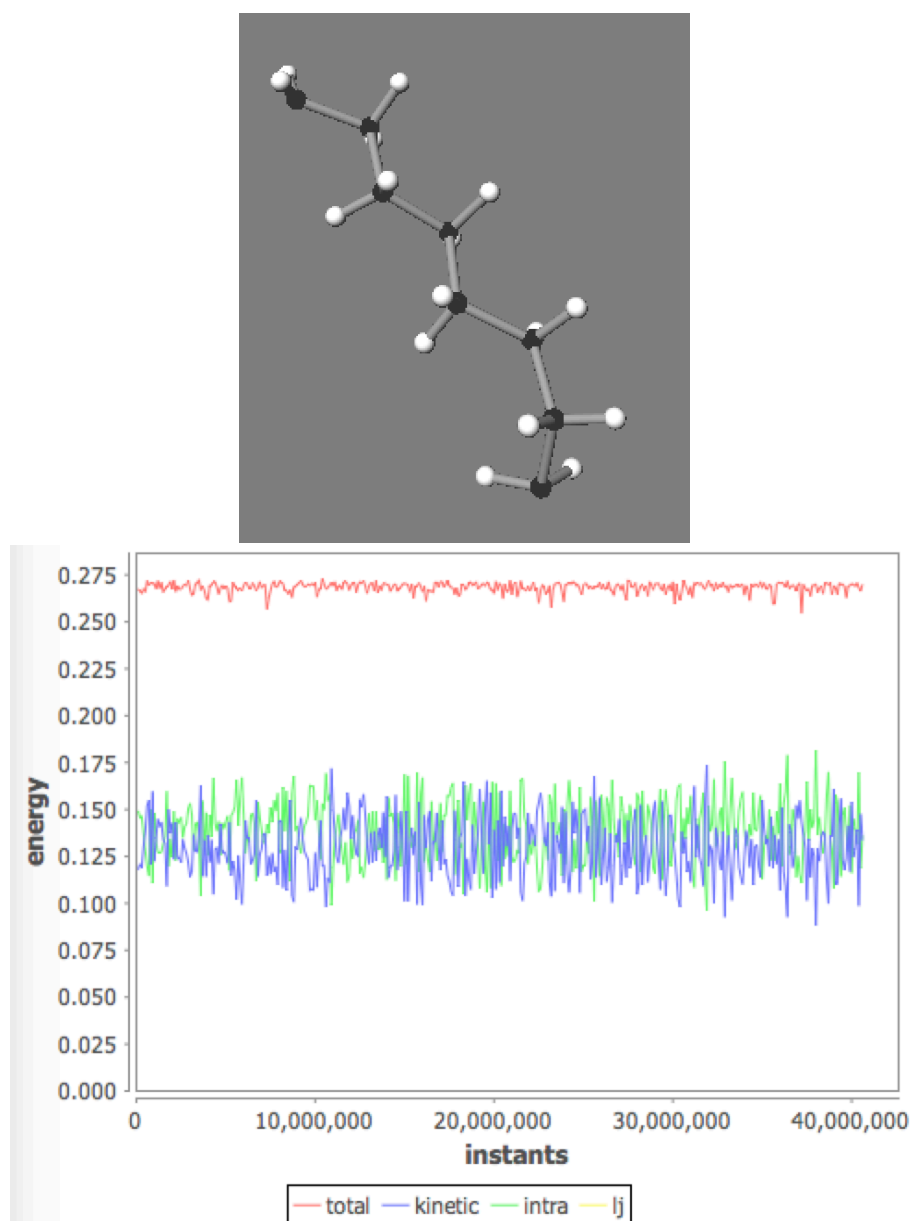


Figure 5.2: Top: molecule simulated. Bottom: energy measured every 10^5 instants.

In a second simulation, we consider two molecules placed face-to-face at

a distance of 0.9 nm. The two molecules are initially at equilibrium and the initial energy of the system is therefore the only (attractive) inter-molecular energy. Fig.5.3 shows the two molecules during simulation on the left, and the energies measured every 10^5 instants, on the right. We show in red the total energy which remains close to 0, and in yellow the inter-molecular energy which remains negative. In blue is the kinetic energy and in green the intra-molecular energy.

Let us finally consider a third simulation in which two molecules are placed face-to-face and given an initial energy, obtained by translating their first atoms upwards ($y > 0$). Fig.5.4 shows the result obtained.

5.2 Deterministic Chaos

The general context of molecular simulations is that of *deterministic chaos* (see for example [14] for an enlightening discussion about this notion). Deterministic chaos is often identified with sensitivity to initial conditions: in systems exhibiting deterministic chaos, the precision of the initial conditions is never sufficient to prevent the appearance of chaos after a certain period of time.

The physics underlying MD is classical Newtonian physics, which is perfectly deterministic and based on a set of simple laws that are reversible over time. The reversibility can be simply illustrated by choosing a negative time-step; doing so, we obtain simulations that are similar to simulations with a positive time-step. Reversibility actually corresponds to preservation of the total energy of isolated systems, over time.

In the context of MD, deterministic chaos can be demonstrated quite simply by a pair of simulations that we are going to describe now.

For both simulations, we disconnect the part of the implementation that processes van Der Waals forces. Thus, only intra-molecular forces are taken into account in the two simulations. We place ourselves in an ortho-normed reference frame where the x axis is horizontal, the y axis is vertical, and the z axis is perpendicular to the two other axes.

We first simulate two identical molecules ($C_{10}H_{22}$), initially *superimposed*, at a temperature of 1000 K. The superposition of the two molecules is possible because van Der Waals forces are not taken into account. The initial energy comes from the y translation of the first carbon of both molecules (with their linked hydrogens). The initial situation is shown on Fig.5.5.

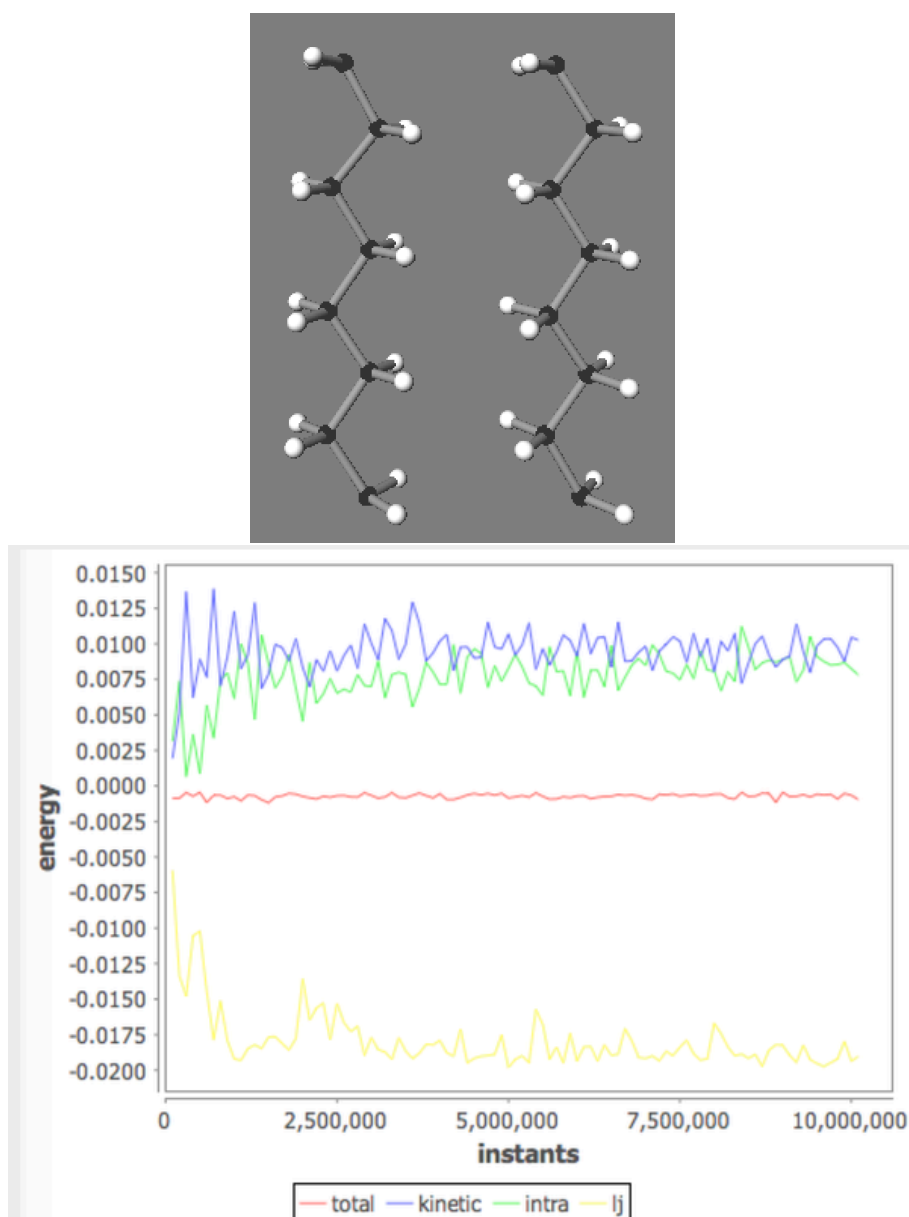


Figure 5.3: Top: two molecules initially at equilibrium, during simulation. Bottom: energy measured every 10^5 instants.

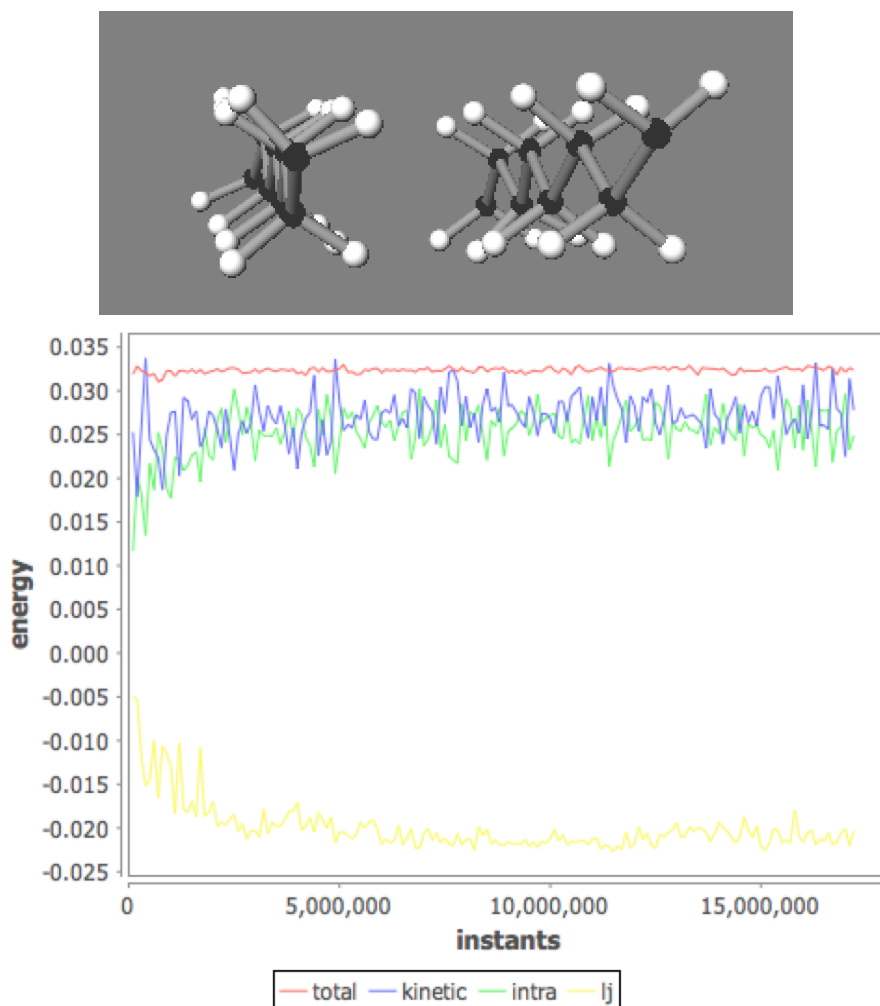


Figure 5.4: Top: two molecules, initially not at equilibrium, during simulation. Bottom: energies measured every 10^5 instants.

During the simulation, we observe that the superposition of the two molecules is maintained over time (tested up to 5 nano-seconds as shown on Fig.5.6).

The preservation of the superposition reflects the complete determinism of the execution of the two molecules.

In the second simulation, the initial conditions are slightly changed for one molecule: the y coordinate of the first carbon is translated by a very

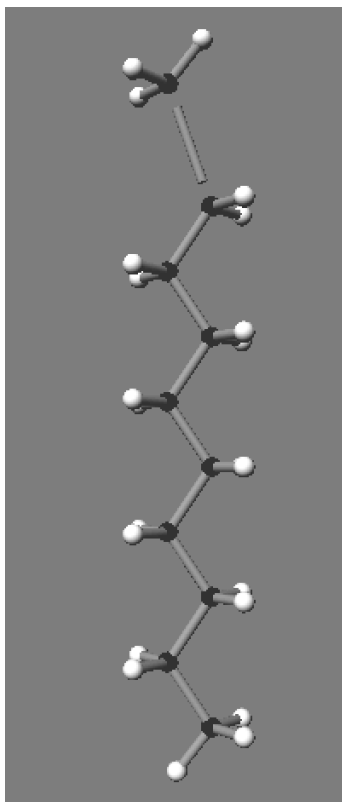


Figure 5.5: Initial situation: superposition of the two molecules. Initial energy comes from the y translation of the first carbon of both molecules (with their linked hydrogens).

small distance of 10^{-17} nm. The difference in placement is of course far too small to be observed on the screen.

However, we can observe quickly (actually, after 2.7 pico-seconds) a clear divergence in the positioning of the two molecules which are no more superimposed, as shown on Fig. 5.7.

This divergence is the manifestation of the “sensitivity to initial conditions” specific to deterministic chaos.

One important point needs to be emphasised: the total determinism of the implementation of MD is an essential asset for the development of simulation programs. In particular, a surprising result or one revealing an error *can always be reproduced*, which is not the case with implementations using

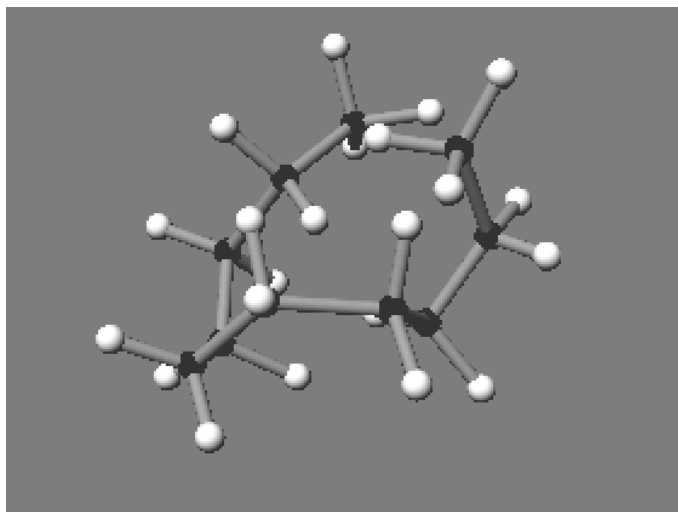


Figure 5.6: Situation after 5 *ns*: the two molecules are still superimposed.

execution threads or network communications that are non-deterministic by nature.

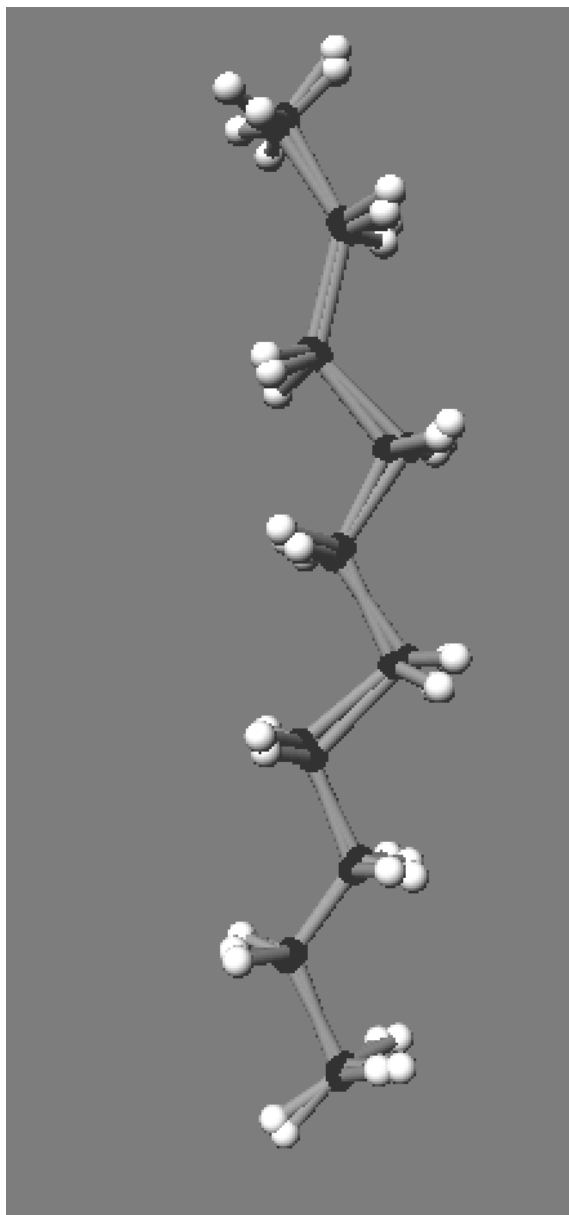


Figure 5.7: After adding to the initial y translation of only one molecule of a distance of 10^{-17} nm, one observes a divergence at 2.7 ps.

Chapter 6

Multi-Scale Approach

This chapter considers the multi-scale approach by defining two scales based on AA. The first scale is called UA and consists of ignoring hydrogen atoms: a UA grain is a carbon atom with the hydrogen atoms attached to it. The second scale, called CG, combines two UA grains into a single CG grain.

6.1 UA Scale

Molecules on the UA scale are chains of grains of two kinds: a G_2 grain contains one carbon atom and two hydrogen atoms, while a G_3 grain contains one carbon atom and three hydrogen atoms bonded to it.

As in OPLS at the AA scale, the intra-molecular components in UA are bonds, valence angles, and torsion angles.

As was done for the AA scale, we define UA fragments consisting solely of G_2 grains. In the following, for simplicity only these UA fragments will be considered. Thus, in addition to grains G_2 , we will only have to consider G_2G_2 bonds, $G_2G_2G_2$ valence angles, $G_2G_2G_2G_2$ torsion angles, and inter-molecular forces between two G_2 grains.

In the MD system, the G_2 grains are represented by cyan coloured balls, as in Fig.6.1 where the fragment considered is made up of 8 grains G_2 , 7 bonds G_2G_2 , 6 valence angles $G_2G_2G_2$ and 5 dihedrals $G_2G_2G_2G_2$.

In accordance with the interpretation of UA grains, the mass of a UA grain is the sum of the masses of the AA atoms it contains, so 0.014 for G_2 .

There is a strong geometric link between UA molecules and AA molecules: the UA molecule “equivalent” to an AA molecule is constructed by “erasing”

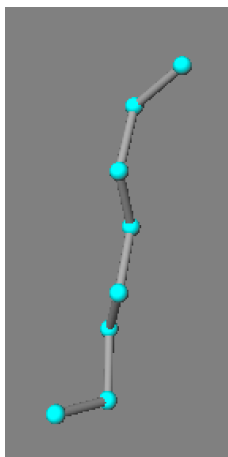


Figure 6.1: UA Fragment composed of 8 grains G_2 .

all the hydrogens, replacing the carbons by UA grains and the AA components by the corresponding UA components.

Conversely, the AA molecule equivalent to a UA molecule is constructed by replacing the UA grains with carbons, by adding hydrogens and CH bonds to these carbons, by replacing the UA components with AA components of the same type, and by introducing appropriate CH bonds, CCH and HCH valence angles, and HCCH torsion angles.

Fig.6.2 shows a molecule C_8H_{16} at equilibrium on the left, and the equivalent UA molecule on the right.

A question arises: how to define the UA potential from the AA potential? The answer will be given in Chap.11 by taking advantage of the geometrical link existing between the two scales.

6.2 CG Scale

On the CG scale, CG grains are formed by two consecutive UA grains. We thus have three types of CG grains which differ according to the number of hydrogens they contain. CG grains are denoted by CG_n where n is the number of hydrogen atoms ; n is therefore 4, 5 or 6. The CG_4 grain is shown in Fig.6.3.

The mass of a CG grain is the sum of the masses of the two carbons, plus

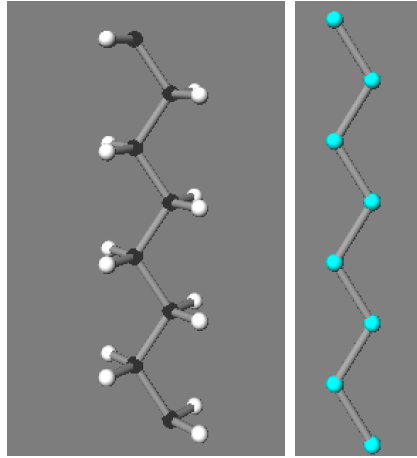


Figure 6.2: Left: AA molecule (fragment) C_8H_{16} . Right: equivalent UA molecule, containing 8 grains G_2 .

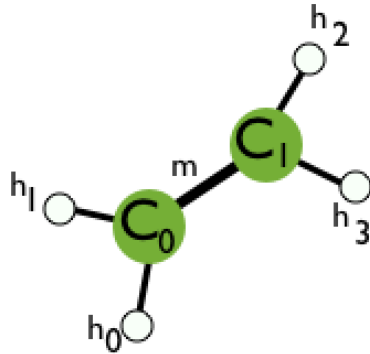


Figure 6.3: CG_4 grain composed of two carbons and four hydrogens. By definition, the centre of the CG grain is the middle m of the AA bond that joins the two carbons.

those of the hydrogens it contains. Thus, the mass of the CG_4 grain is 0.028.

In what follows, just as for the UA scale we only consider G_2 grains for the sake of simplicity, in the CG scale we will only consider CG_4 grains (i.e. made up of two carbon and four hydrogen atoms).

In the MD system, CG_4 grains are represented by yellow balls. Fig.6.4

shows a CG molecule made up of 4 CG_4 grains.

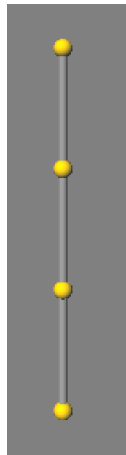


Figure 6.4: CG molecule made up of four CG_4 grains.

We establish a geometric link with the scale AA by considering that a CG grain is centred on the middle of the AA bond of the equivalent C_2H_n molecule. Thus, using the notations of Fig.6.3, the AA molecule equivalent to a grain CG_4 contains 5 bonds (h_0C_0 , h_1C_0 , C_0C_1 , h_2C_1 , h_3C_1), 6 valence angles ($h_0C_0h_1$, $h_0C_0C_1$, $h_1C_0C_1$, $h_2C_1C_0$, $h_3C_1C_0$, $h_2C_1h_3$) and 4 torsion angles ($h_0C_0C_1h_2$, $h_0C_0C_1h_3$, $h_1C_0C_1h_2$, $h_1C_0C_1h_3$).

A UA molecule at equilibrium (i.e. with zero intra-molecular energy) has for CG equivalent a molecule whose CG_4 grains are all aligned. The CG molecule in Fig.6.4 is thus the CG equivalent of the AA and UA molecules in Fig.6.2.

At equilibrium, in CG, the valence angles are flat (their value is π).

Let us now consider the case of torsion angles at the scale CG. A CG torsion angle that is not at equilibrium must contain at least one non-flat CG valence angle (indeed otherwise, if the two CG valence angles were flat, the CG torsion angle would be at equilibrium).

Therefore, in CG, it is possible to consider that the energy of a torsion angle is actually *distributed between the two CG valence angles* it contains. This choice simplifies the determination of CG potentials: the CG torsion angles have no longer to be considered.

We have therefore chosen to define only CG bonds and CG valence angles as components of CG molecules, without considering torsion angles on this

scale. Thus, the CG molecule of Fig.6.4 has only three bonds and two valence angles as components.

It should be noted that the “absorption” of torsion angles by the valence angles associated with them is possible on the CG scale, but not on the AA scale nor on the UA scale. In fact, in AA and UA a torsion angle can have energy while the two associated valence angles are at equilibrium, which is impossible on the CG scale.

As with UA, the basic question is how to define the CG potentials from the AA ones, taking advantage of the geometric link between the two scales. This question will be considered in Chap.12.

6.3 Complexity

In the transition from an AA molecule to an equivalent UA or CG molecule, the number of atoms and intra-molecular components (bonds, valence angles, torsion angles) decreases significantly. As a result, UA or CG simulations have a lower complexity, making it possible to simulate longer molecules, with higher simulated time / real-time ratios.

The difference in complexity is even more obvious in the case of inter-molecular forces which grow with the square of the number of atoms or grains.

Fig.6.5 compares the complexities at the three scales.

The x-axis shows the size n of the molecules (n carbon atoms for AA, n grains G_2 for UA, and $n/2$ grains CG_4 for CG). In the top image of Fig.6.5, we have on the ordinate the number of intra-molecular components (bonds, valence angles, and torsion angles) to be simulated at each instant.

In the bottom image of Fig.6.5, we have the number of pairs of atoms or grains that need to be analysed to determine the inter-molecular forces between two molecules of size n .

To illustrate the real-time gain obtained with the UA and CG scales, we consider a situation where two molecules are placed face-to-face and launched at opposite speeds, one against the other. Each molecule will bounce against the other and then move apart.

The initial configurations at the three scales are shown in Fig.6.6.

All three coordinate axes are present in the three images. At each scale, the molecule on the left is slightly shifted upwards in y (by 0.3 nm). The time step is 10^{-4} ps for all three simulations. The initial distance between

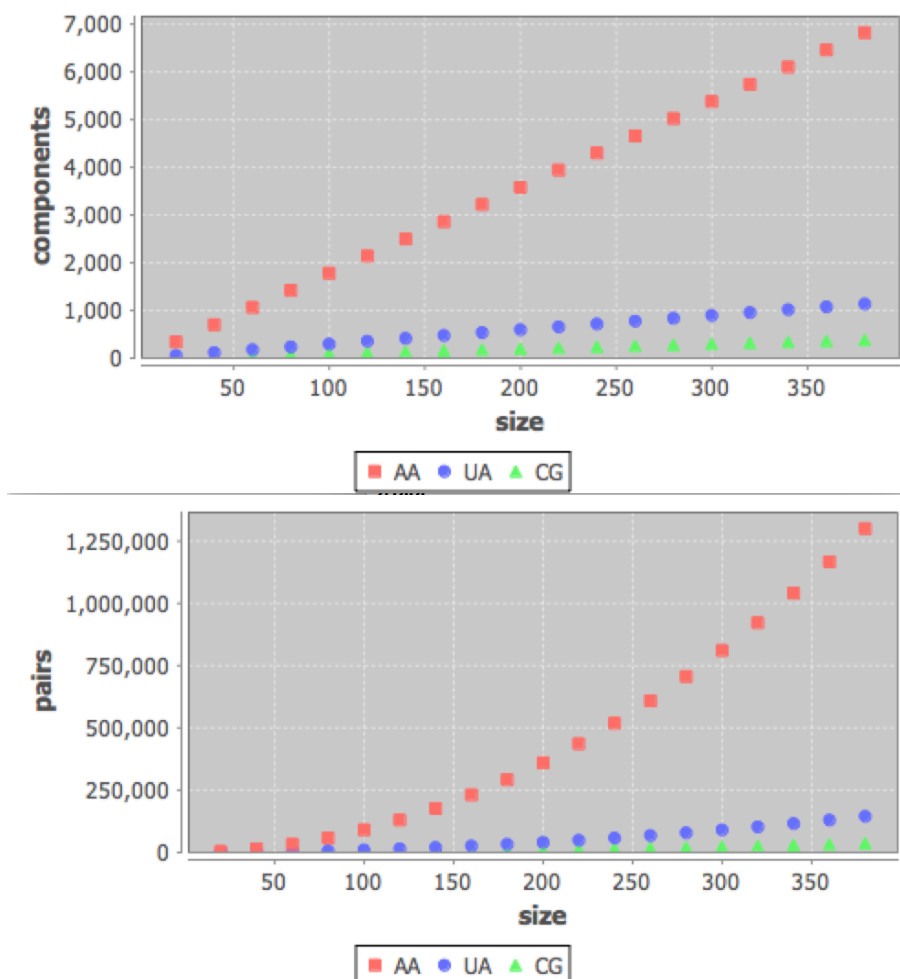


Figure 6.5: Comparison of complexity of simulations at the three scales. Top: intra-molecular forces; Bottom: inter-molecular forces.

each molecule and the centre of coordinates is $\Delta = 2 \text{ nm}$ and the absolute value of the initial velocity is 1 nm/ps .

In each simulation, we measure the real-time (in milli-seconds) until the distance, after bouncing, between the molecules and the center is greater than $\Delta + 0.5 \text{ nm}$.

Results are as follows: for AA, 13.108 ms ; for UA, 2.004 ms ; for CG, 1.144 ms . One observes thus a factor 11 between AA and CG.

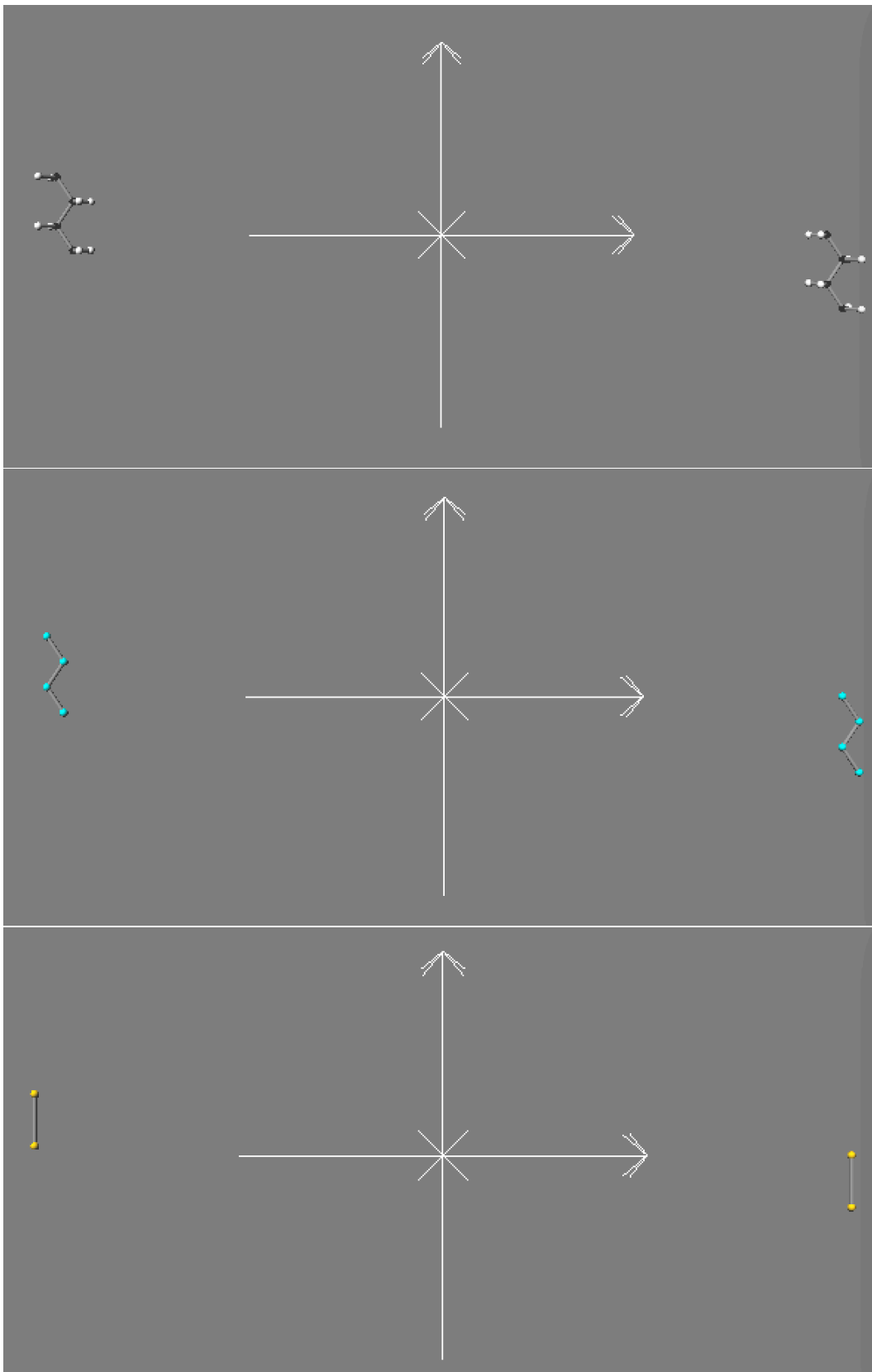


Figure 6.6: Initial configurations of simulations at the three scales.

Chapter 7

Inverse-Boltzmann Method

In this chapter we describe a method, called *inverse-Boltzmann*, to determine the UA potentials from the ones at the AA scale. The determination of the CG potentials using the same method is considered in Chap.8.

The inverse-Boltzmann method is based on a statistical processing of data obtained during simulations. In this approach, one determines the potential energy of an oscillator from the probability density of the oscillator presence in a given state.

To implement the method, we divide the space of variation into N classes of equal size. Each class C_i has an associated counter P_i which is incremented at each simulation step if the oscillator value (for example, in the case of a bond, its length) belongs to the class C_i . More precisely, the formula defining the potential energy U_i associated with the class C_i is:

$$U_i = -k_B \times T \times \ln(P_i/P_0) \quad (7.1)$$

where k_B is the Boltzmann constant, T is the temperature of simulation, P_0 is the value of the counter of the class containing the maximum number of elements (the “most populated” class), and P_i is the value of the counter of class C_i .

Let us now consider the case of an isolated harmonic oscillator. We find that the maximum density of presence corresponds to the maximum kinetic energy. Since the oscillator is an isolated system, the state of maximal kinetic energy is also the state of minimal potential energy because in an isolated system the sum of the kinetic and potential energies is constant.

In the inverse-Boltzmann method, we generalise the previous case of an harmonic oscillator to the various components of molecules.

One uses the same simulation for all molecule components. Three sets of data will therefore be produced, one for bond lengths, one for valence angles, and one for torsion angles.

Two points should be immediately stressed:

1. The obtained energies depend on the temperature T , which thus becomes a crucial simulation parameter.
2. The inverse-Boltzmann approach only delivers relative energies: one needs to state the value of one of the classes (for example, the class with the maximal number of elements) in order to be able to determine the energies of the other classes.

This approach raises two fundamental questions. First, the components (for example, the bonds) are not isolated: they continuously exchange energy with the others oscillators present in the molecule. To what extent do these exchanges disturb the method ?

Second, is the relationship between potential energy and probability density of presence valid for all cases of oscillators ?

In the remainder of this chapter, we describe the application of the inverse-Boltzmann method to the UA scale.

7.1 UA Intra-molecular Forces

The treatment of bonds, valence angles and torsion angles is carried out using the same molecular dynamics simulation of the molecule C_6H_{12} at the temperature of 218.152 K .

The simulation begins with 2×10^7 stabilisation steps without filling in the classes. Then, classes are filled at the end of each of the following 10^8 steps. The probabilities of presence in each class are finally calculated at the end of the simulation.

UA Bonds

The UA bonds are processed by segmenting the domain of values into 200 evenly distributed classes. Fig.7.1 shows the obtained curve.

In the case of UA bonds, the inverse-Boltzmann method gives a good result which can be made more accurate by increasing the number of classes or the simulation time.

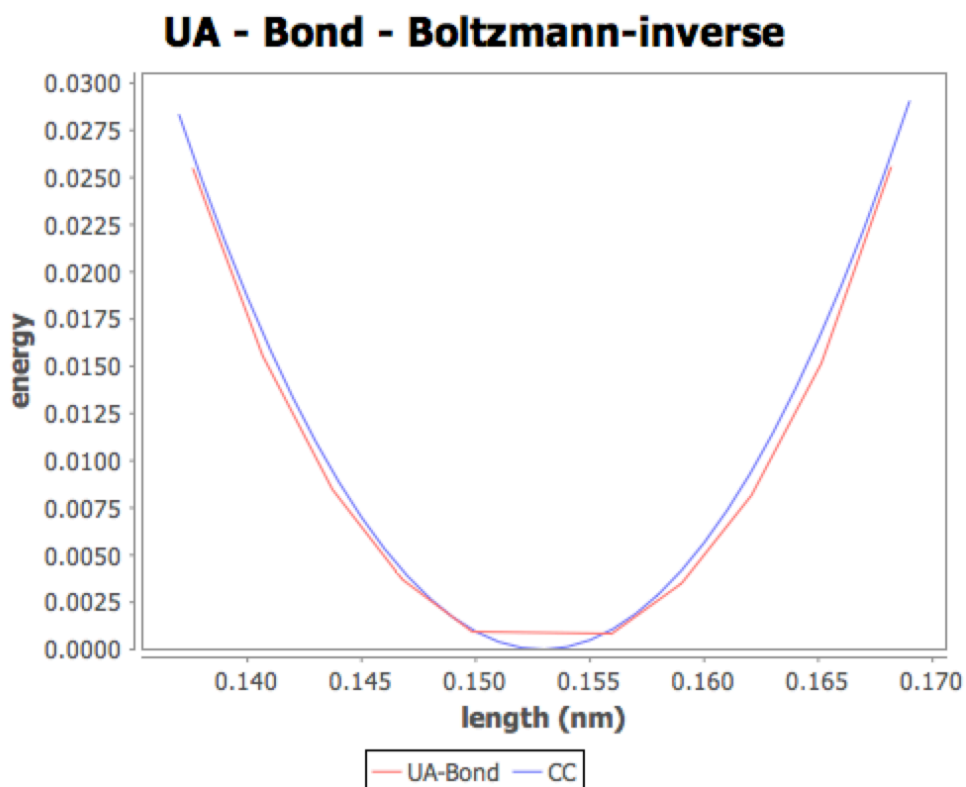


Figure 7.1: UA bond potential obtained by inverse-Boltzmann method from the molecule C_6H_{12} at the temperature of 218.152 K compared with the AA potential of the bond CC.

We can therefore consider that the energy exchanges of UA bonds with the other components (bonds, valence or torsion angles) do not disturb the approach which associates a harmonic potential to the UA bond, very close to that of the CC bond potential at the AA scale.

UA Valence Angles

For GGG valence angles, the range of variation is segmented into 180 classes. Fig.7.2 shows the obtained curve.

The result differs slightly from the CCC potential. This discrepancy will be explained later by the effect of the CCH valence angles, which are strongly correlated to the valence angle considered.

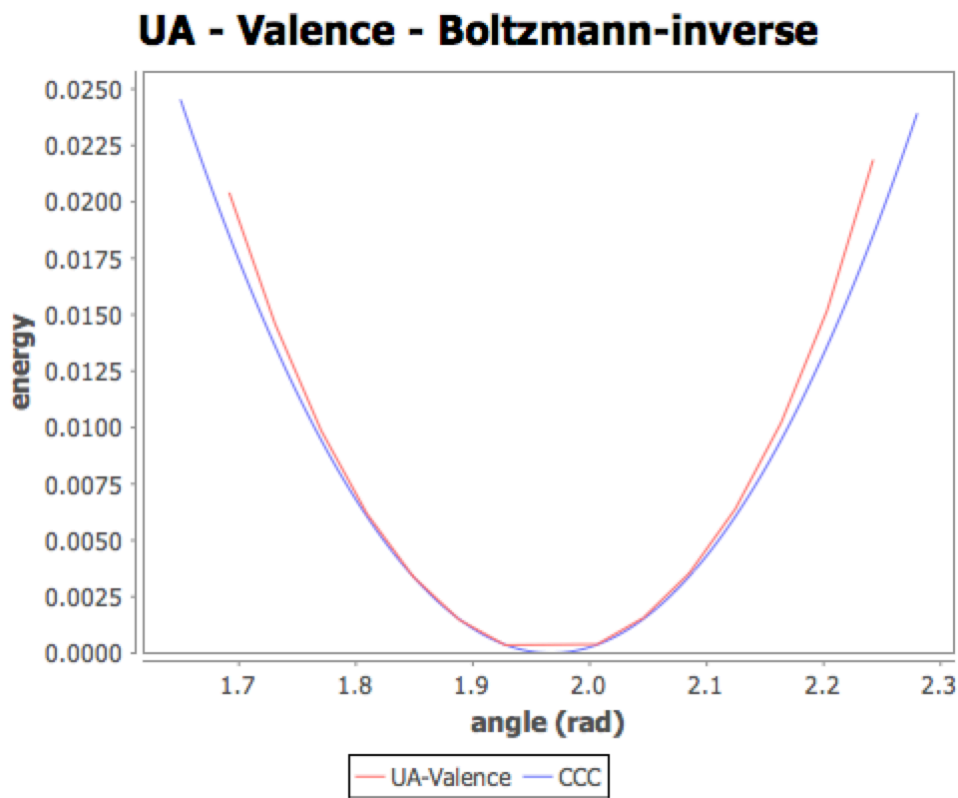


Figure 7.2: UA valence potential obtained by inverse-Boltzmann from the molecule C_6H_{12} at the temperature of 218.152 K, compared with the AA potential of the CCC valence angle.

The exchange of energy between the UA valence angle and the other molecule components have little effect: the method gives UA valence angles a harmonic potential very close to that of the AA CCC valence angle potential.

UA Torsion Angles

For UA torsion angles, we segment the range of variation into 180 classes. The UA torsion angle potential is in good correspondence with the sum of the AA potentials of all the torsion angles sharing the same central bond.

Fig.7.3 shows a bond CC (in red).

On Fig.7.3, one sees that there are nine torsion angles sharing the same

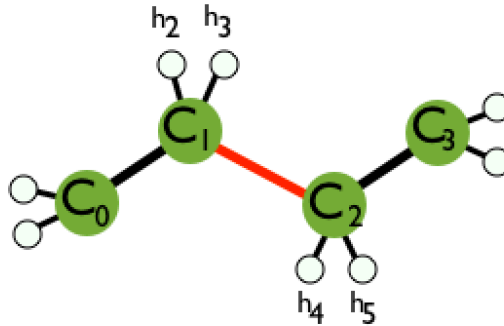


Figure 7.3: Torsion angles sharing the same central bond (in red).

central bond C_1C_2 :

- the angle CCCC $C_0C_1C_2C_3$;
- the four angles HCCH: $h_2C_1C_2h_4$, $h_3C_1C_2h_4$, $h_2C_1C_2h_5$, $h_3C_1C_2h_5$;
- the four angles HCCC: $h_2C_1C_2C_3$, $h_3C_1C_2C_3$, $C_0C_1C_2h_4$, $C_0C_1C_2h_5$.

Fig.7.4 shows the potential of the UA torsion angle obtained by inverse-Boltzmann and compares it with the sum of the potentials of the nine torsion angles sharing the same central bond. One observes that the two curves are in good correspondance.

Thus, the energy exchanges of the torsion angle UA with the other components of the molecule have little effect. The torsion angle UA potential is in accordance with the sum of the AA potentials of the torsion angles associated.

7.2 UA Inter-Molecular Forces

The data obtained with the inverse-Boltzmann method from the simulation of two UA grains is given in Fig.7.5.

It can be seen that the right-hand side of the inverse-Boltzmann curve is not asymptotic to a parallel to the $y = 0$ axis but, on the contrary, tends to increase with positive values of y . This is not consistent with the dynamics:

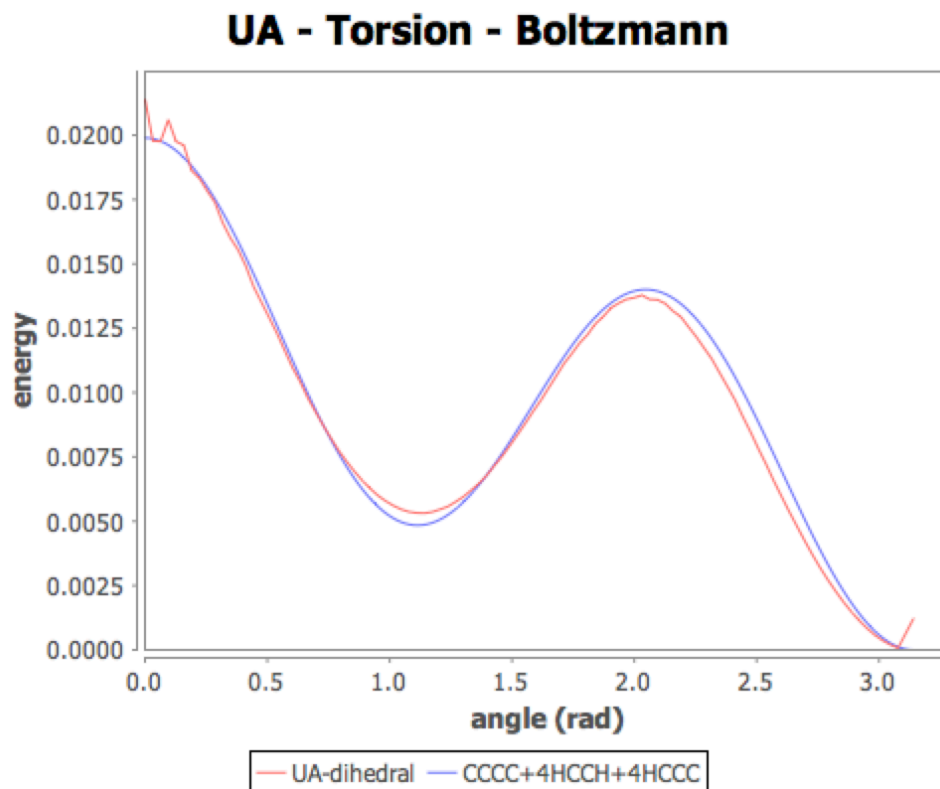


Figure 7.4: UA torsion angle potential obtained by inverse-Boltzmann from the molecule C_6H_{12} at a temperature of 218.152 K.

one indeed expects that the potential becomes weaker and weaker as the grains move further apart.

The curve obtained with the inverse-Boltzmann method is thus clearly not that of an inter-molecular potential.

Let us try to explain what happens by considering rare events. Actually, we have two disjoint sets of rare events: events corresponding to the strongly repulsive domain, when the grains are very close, on the one hand; on the other hand, events corresponding to the weakly attractive domain, when the grains are very far apart.

Thus, in the first case the potential must be very high, while in the second case it must be very low. However, the inverse-Boltzmann method only takes into account the relative rarities of events and therefore tends to

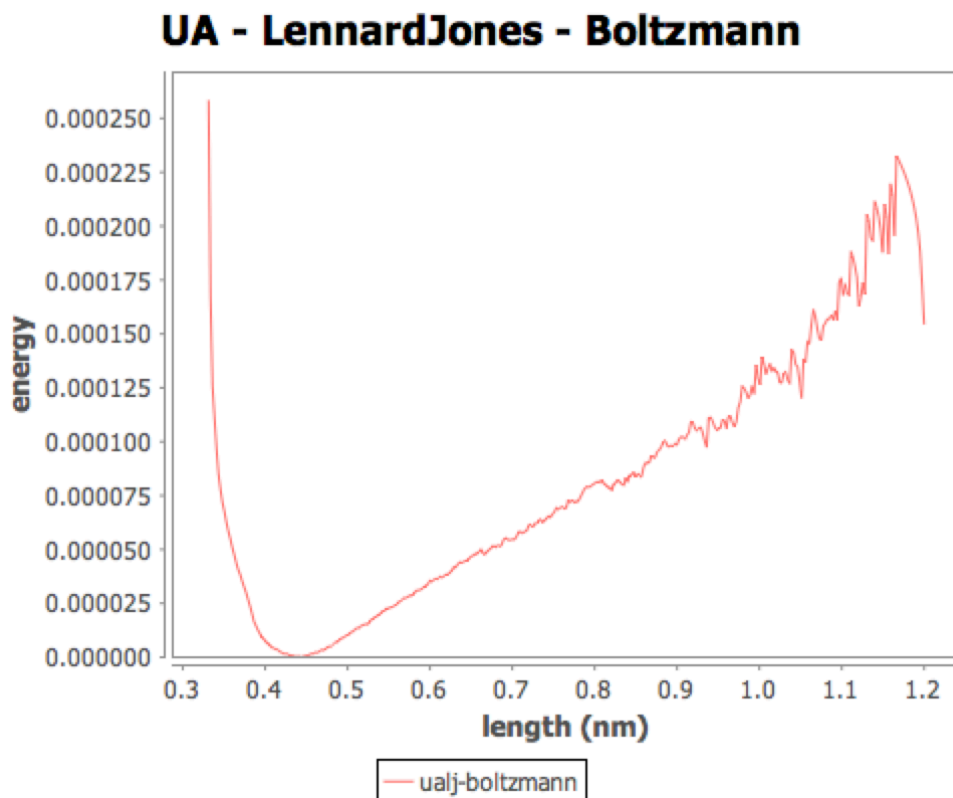


Figure 7.5: UA inter-molecular potential obtained by the inverse-Boltzmann method from two molecules C_1H_2 .

identify these events giving them the same energy, which clearly contradicts the dynamics.

The inverse-Boltzmann method for determining the inter-molecular potential UA therefore stumbles on a major obstacle. Looking ahead, we see that the preceding reasoning also applies to the determination of the CG inter-molecular potential. Actually, the inverse-Boltzmann method seems unsuitable for the determination of inter-molecular potentials in general.

Chapter 8

Inverse-Boltzmann for CG

We apply now the inverse-Boltzmann method to the CG scale.

The inverse-Boltzmann method being unsuitable for the treatment of inter-molecular forces (cf. Chap.7), we will only consider the intra-molecular CG components. The treatments of CG bonds and valence angles are based on the same molecular dynamics simulation of the C_6H_{12} molecule, as in Chap.7.

The simulation starts with 2×10^7 stabilisation steps, without filling-in the classes. Then, classes are filled-in at the end of each of 10^8 steps. Finally, the probabilities of presence in each class are calculated at the end of the simulation.

8.1 CG Bonds

CG bonds are processed by segmenting the range of variation of the values into 200 evenly distributed classes. Fig.8.1 shows the obtained curve for a temperature of 218.152 K. The curve obtained depends on the simulation temperature, as shown in Fig.8.2 where three different temperatures are considered. At the temperature of 111 K, the domain covered does not contain the inflection point: the central torsion angle is never triggered. At the temperature of 218 K, one observes the torsion of the central angle.

At a temperature of 322 K we can see that that the potential is lower at the inflection point. At higher temperatures the inflection becomes less and less marked.

Here, we are faced with a difficulty: what temperature should we choose

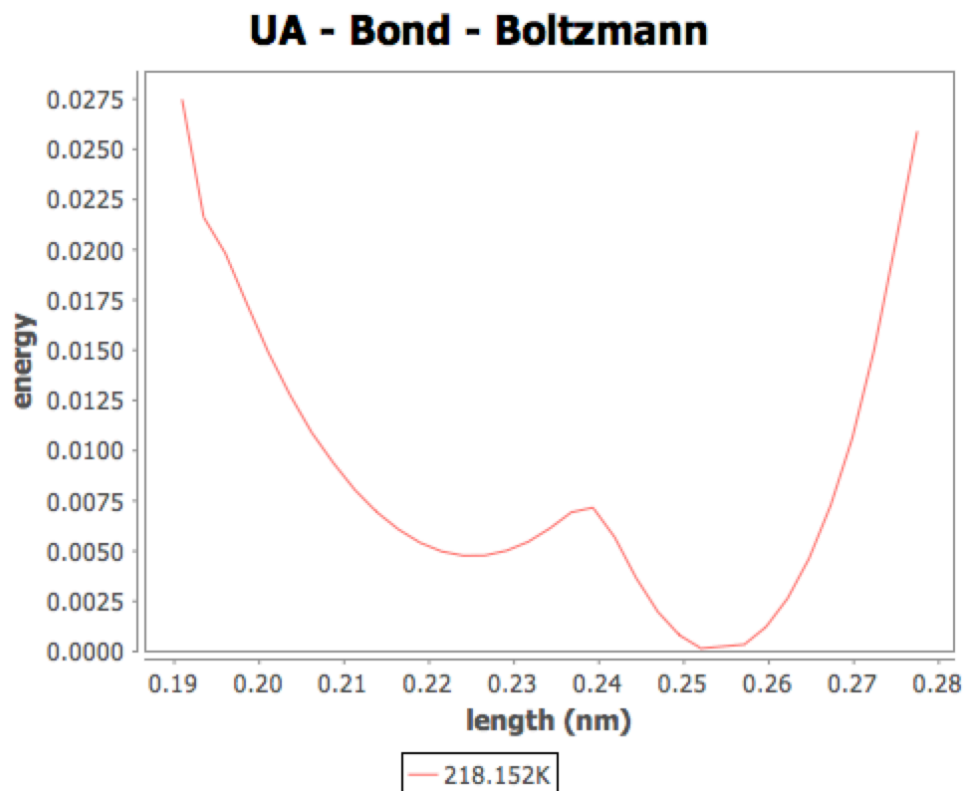


Figure 8.1: CG bond potential obtained by the inverse-Boltzmann method from the molecule C_6H_{12} at the temperature of 218.152 K.

to determine the CG bond potential ? The inverse-Boltzmann method does not provide any answer to this question.

8.2 CG Valence Angles

For CG valence angles, the range of variation is segmented into 180 classes. Fig.8.3 shows the curve obtained. The right-hand side of the curve (angle greater than 3 radians) is clearly wrong. In fact, the potential energy is minimal when the CG grains are aligned, which corresponds to a CG valence angle equal to π and this is not what the curve shows. This anomaly occurs independently of the temperature.

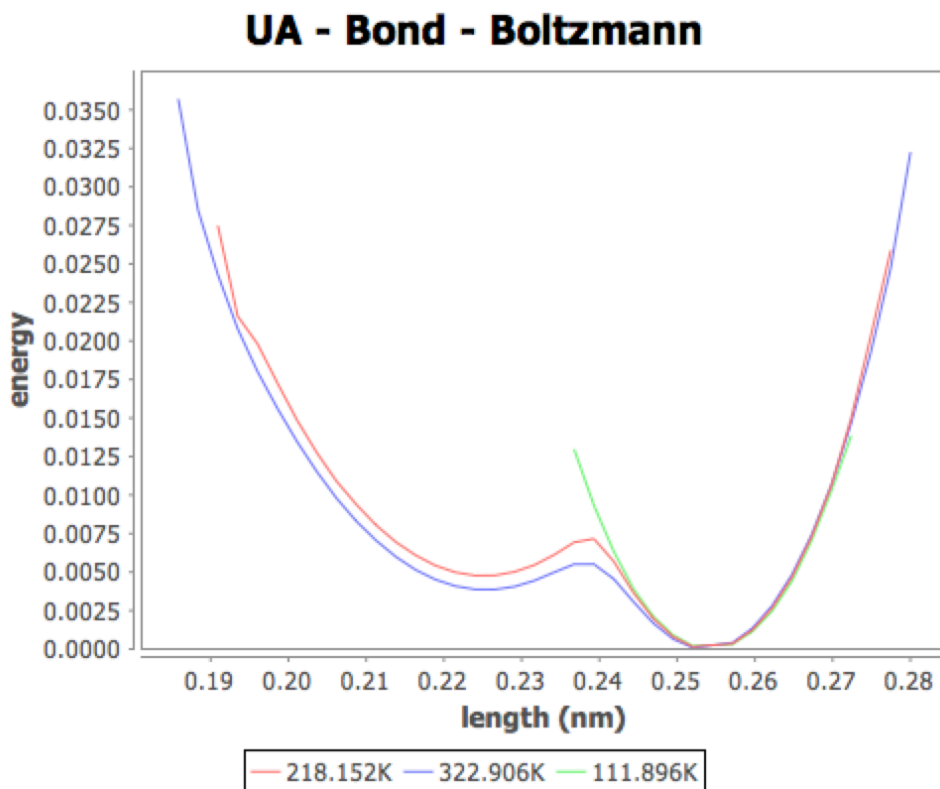


Figure 8.2: CG bond potential determined at three different temperatures.

In addition, the curve of the CG valence angle varies according to the temperature: in the same way as for CG bonds, it is not clear which temperature to choose for determining the CG valence potential.

Conclusion

Several conclusions can be drawn concerning the inverse-Boltzmann method:

- Correct handling of rare events requires large numbers of events, and thus simulations that take very long execution times.
- When the number of events is not sufficient to process correctly a range of values, the potential energy may be underestimated.

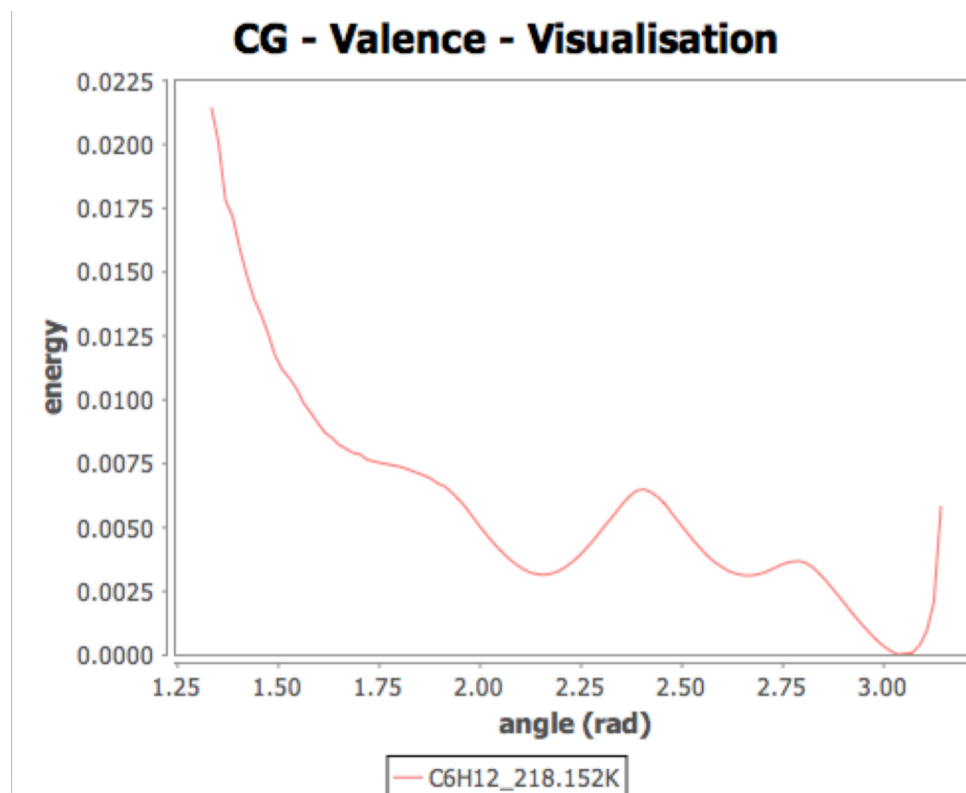


Figure 8.3: CG valence angle potential obtained by inverse-Boltzmann from the molecule C_6H_{12} at the temperature of 218.152 K.

- The curves obtained may depend on the temperature, which raises the question of the choice of temperature to consider.
- In addition, the simulation temperature limits the range of values analysed and therefore the range of definition of the potential function.
- Finally, the method gives wrong answers in the case of inter-molecular potentials.

We will now consider another means of determining potentials: the minimisation method.

Chapter 9

Minimisation Method

In this chapter, we propose a method for determining the potentials of molecular components based on a *constrained minimisation* technique. This method is fundamentally based on the existence of geometric links with the basic scale AA .

To determine the potential of a molecular component (for example, the UA valence angle), we choose a molecule in which this component appears and set the value v of the component. We then calculate the global potential p of the underlying molecule (geometrical aspect) at the scale AA , after performing a minimisation process which preserves the value v of the component (constrained aspect). The potential of the component is by definition p for the component value v . By varying v , we determine the potential we are looking for.

For example, for the UA valence angle, we fix the angle between three UA grains, i.e. between three carbon atoms, and we minimise all the AA components of the molecule except this angle.

Thus, the carbon atoms of the three grains of the UA angle remain immobile, while the other atoms, either carbons or hydrogens, move to minimise the energy of the overall molecule.

The bonds and angles involving the hydrogen atoms are thus placed in equilibrium positions where their energy is minimal. The same applies to carbon atoms, with the exception of those forming the UA valence angle. The final energy of the AA molecule after complete minimisation is that associated with the UA valence angle.

In the remainder of this chapter, we apply the minimisation method to the UA scale. Recall that a UA grain is formed by a carbon atom and the

hydrogen atoms bonded to it. The centre of a UA grain coincides with the carbon atom. The minimisation applied to CG is described in Chap.10.

9.1 UA Bonds

To deal with the UA potential of the G_2G_2 bond, we consider the equivalent molecule (in fact, a fragment) C_2H_4 and the minimisations are carried out by keeping constant the distance between the two carbons of the molecule.

The match with the OPLS potential AA is perfect and is illustrated in Fig.9.1.

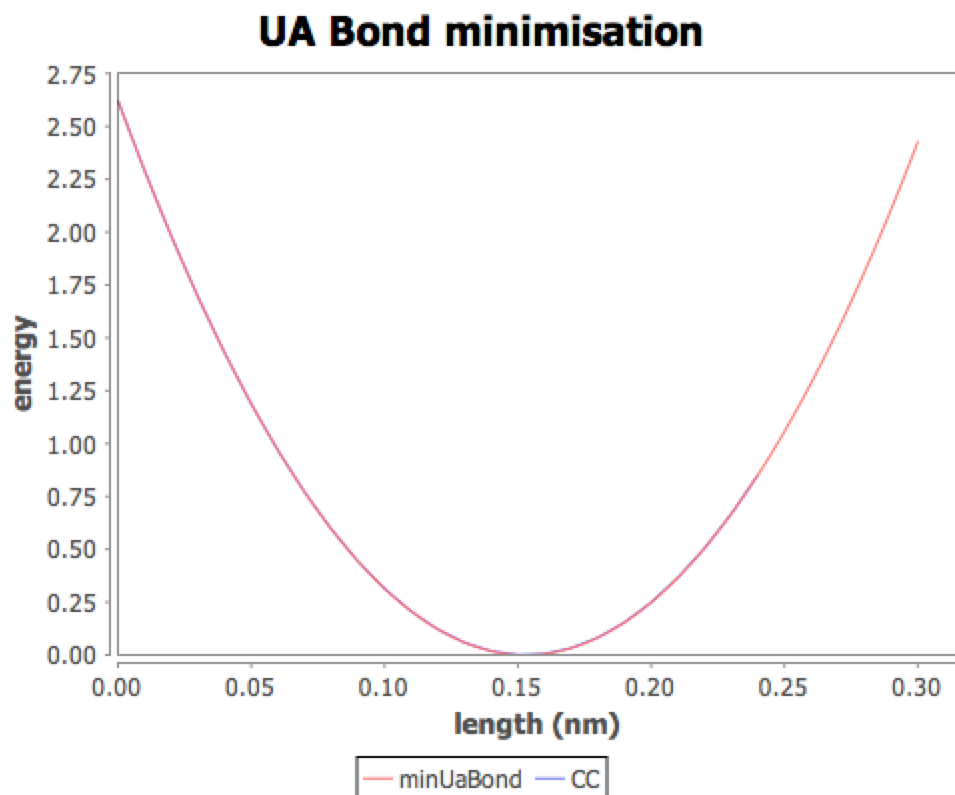


Figure 9.1: Potential of the bond G_2G_2 obtained by minimisation, compared with the OPLS potential CC .

This result reflects the independence that exists between the CC bond

and the valence angles HCH and HCC in the molecule C_2H_4 : the HCH and HCC angles can be at their equilibrium values independently of the bond value.

9.2 UA Valence Angles

For the UA valence potential $G_2G_2G_2$, we consider the fragment C_3H_6 and the minimisations are carried out keeping the valence angle CCC constant (remark: the results are exactly the same with the full molecule C_3H_8).

The minimisation result is shown in Fig.9.2. It can be seen that the curve produced by the minimisation method does not exactly coincide with the CCC potential, in particular in the part corresponding to the extension of the valence angle.

The potential UA for the valence angle $G_2G_2G_2$ therefore differs from the AA potential of the valence angle CCC.

By removing the potential energy of the eight valence angles CCH one exactly recovers the CCC potential, as shown in Fig.9.3.

The difference with the valence potential CCC lies in the partial correlation (actually, only in extension of the valence angle) between the angle CCC and the angles CCH.

The potential $G_2G_2G_2$ is in fact the sum of two functions, the first f_{inf} defined for angles smaller than the angle of equilibrium, the second f_{sup} defined for bigger angles. The f_{inf} function coincides on its definition space with the harmonic function CCC, while f_{sup} multiplies CCC by a factor of 1.142.

The two functions f_{sup} and f_{inf} can be both approximated by a single harmonic function which is the harmonic function CCC multiplied by a factor of 1.1. We will use this approximation in the following; the UA valence potential $G_2G_2G_2$ will be considered as being a harmonic potential equal to the valence potential AAA multiplied by the factor 1.1.

9.3 UA Torsion Angles

To deal with the torsion potential $G_2G_2G_2G_2$, we start from the fragment C_4H_8 and carry out the minimisations keeping the torsion angle CCCC constant (results are exactly the same with the molecule C_4H_{10}).

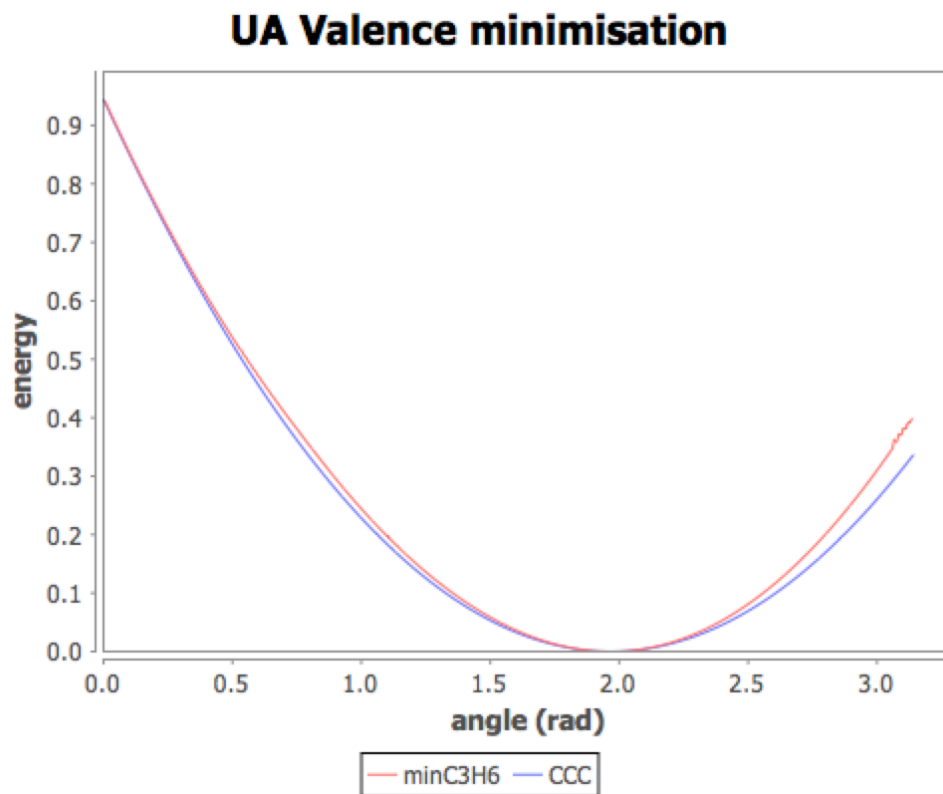


Figure 9.2: Potential of the valence angle $G_2G_2G_2$ obtained by minimisation, compared with the OPLS potential CCC.

The CCCC torsion angle is in fact totally correlated with the HCCH and HCCC torsion angles centred on the middle of the central CC bond. Four HCCH torsion angles and four HCCC torsion angles are thus involved. Fig.9.4 shows the potential obtained by minimisation compared to the sum CCCC+4HCCH+4HCCC. It can be seen that the two curves exactly correspond to each other.

9.4 UA Inter-molecular Forces

To determine the Lennard-Jones potential between two UA grains, we use two C_1H_2 molecules placed face-to-face. The curve obtained by varying the

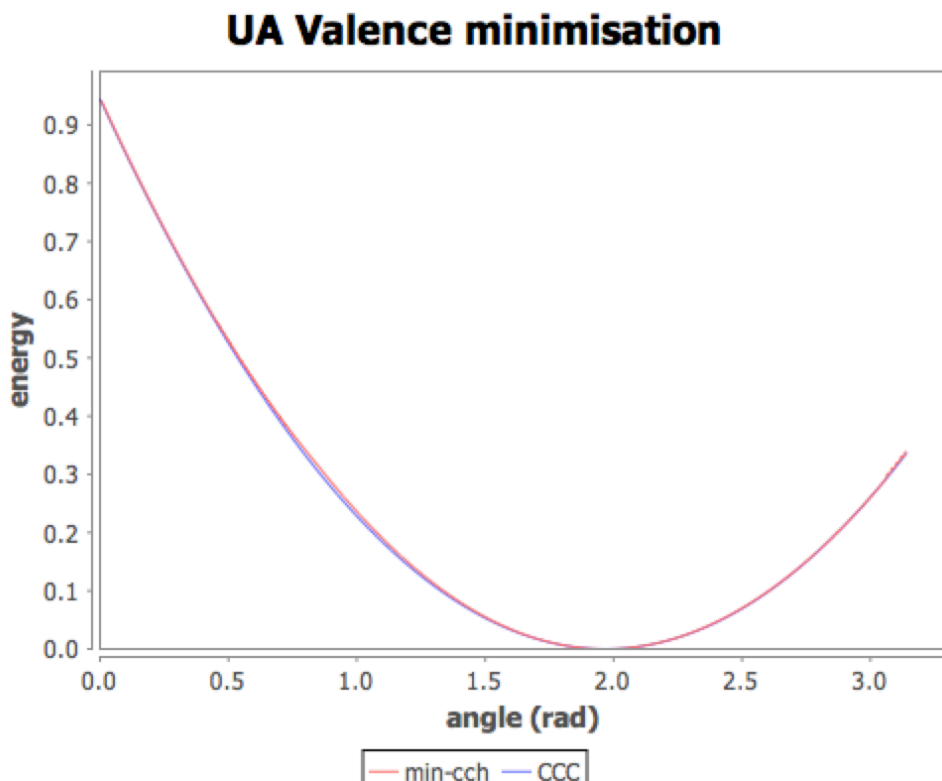


Figure 9.3: Potential of the valence angle $G_2G_2G_2$ obtained by minimisation, removing the components of the valence angles CCH, compared with the OPLS potential CCC.

distance between the two molecules is shown on Fig.9.5.

We obtain a Lennard-Jones potential which takes into account the presence of hydrogens, as can be seen on Fig.9.6.

In Fig.9.6, the parameters of the Lennard-Jones potential are $\epsilon = 5.5 \times \epsilon_{CC}$ and $\sigma = 0.917 \times \sigma_{CC}$.

Conclusion

The fragment C_2H_4 is used to calculate the UA bond and we obtain exactly the same potential as that of the AA CC bond (Fig.9.1). In other words, the bond potentials AA and UA coincide and are both harmonic.

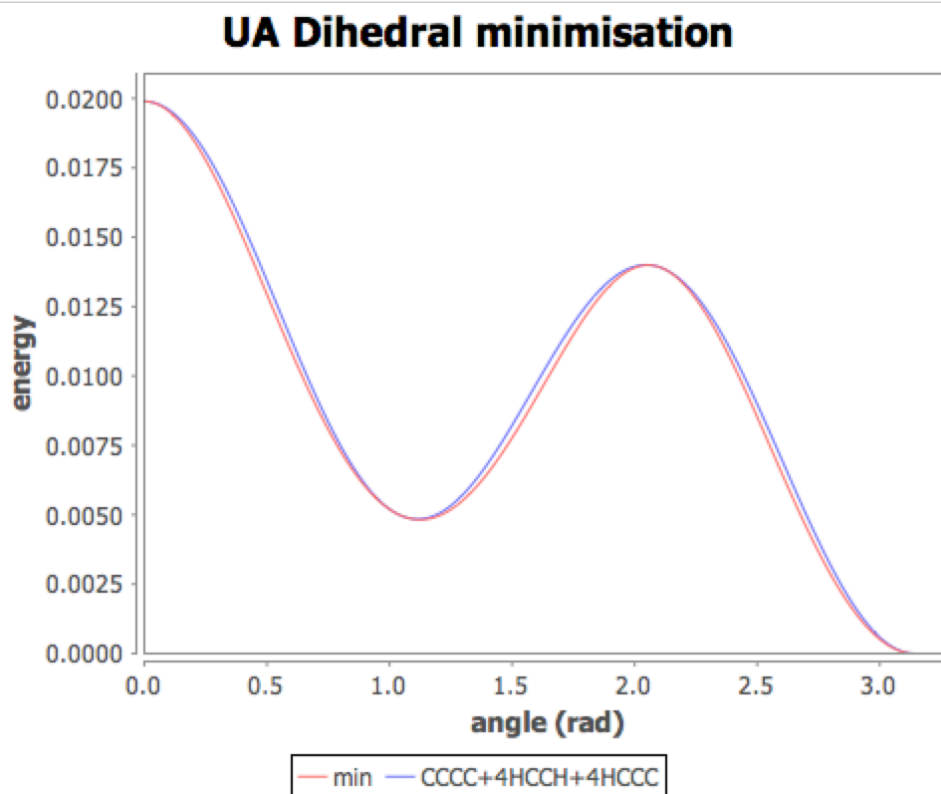


Figure 9.4: Potential of the torsion angle $G_2G_2G_2G_2$ obtained by minimisation, compared with the sum of OPLS potentials $CCCC+4HCCH+4HCCC$.

The fragment C_3H_6 is used to determine the UA valence angle potential. (Fig.9.2). The UA valence potential is different (and non-harmonic) but nevertheless very close to the AA valence potential.

From the fragment C_4H_8 we obtain the curve in Fig.9.4 as the potential of the UA torsion angle. The UA potential of a torsion angle θ is therefore the sum of the CCCC potentials of the θ angle, plus four times the HCCH potential of θ , plus four times the HCCC potential of θ .

Finally, Fig.9.5 shows the potential UA between two G_2 grains. This potential has three main characteristics: it has the form of a Lennard-Jones potential; it coincides with the inter-molecular potential AA when the grains are very close or sufficiently far apart; its central part is clearly more “excavated” than the inter-molecular potential AA.

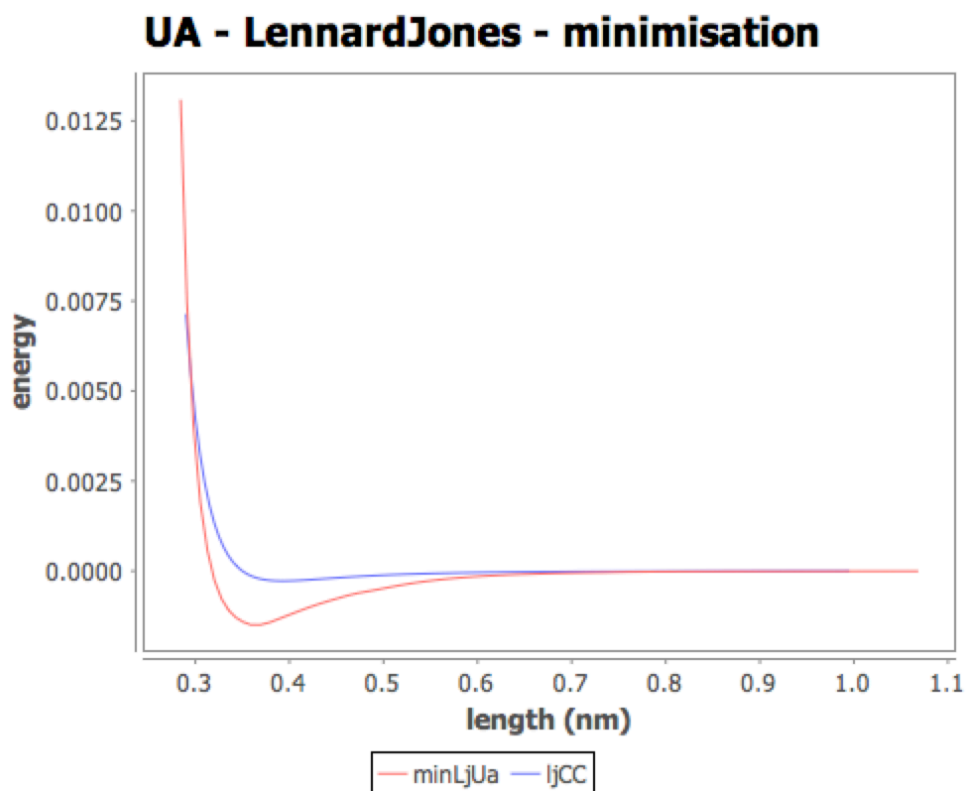


Figure 9.5: Inter-molecular potential between two UA grains obtained by minimisation, compared with the OPLS Lennard-Jones potential between two carbon atoms.

Preservation of the Lennard-Jones shape indicates that the UA inter-molecular potential behaves globally like the inter-molecular potential AA, i.e. the presence of hydrogen atoms does not change the shape of the interactions between UA grains.

The “excavated” aspect is linked to the hydrogen atoms which, at a short distance, contribute significantly to the attractive forces between grains.

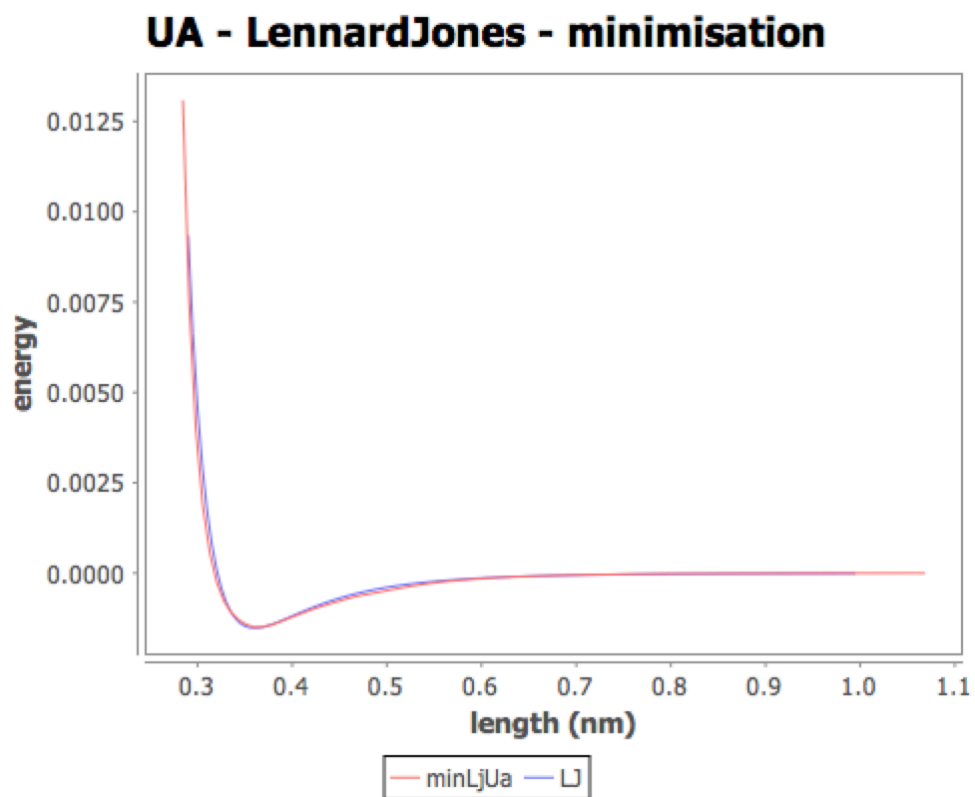


Figure 9.6: Inter-molecular potential between two UA grains obtained by minimisation, compared with a Lennard-Jones curve.

Chapter 10

Minimisation for CG

As we have seen in Sec.6.2, the determination of the CG potential by minimisation should be broken down into three aspects only: binding potential, valence potential and inter-molecular potential; no torsion potential should be considered at the CG level.

10.1 CG Bonds

To determine the potential of CG bonds, one uses the fragment C_4H_8 of Fig.10.1.

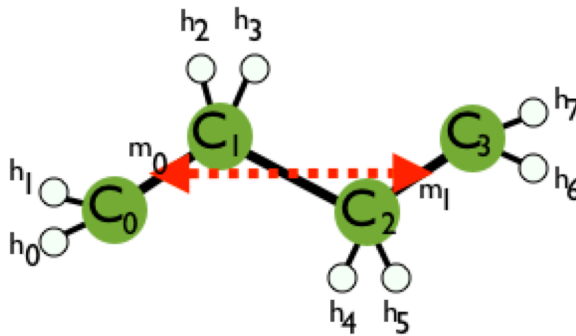


Figure 10.1: Molecule C_4H_8 . The CG bond is in red.

This molecule is considered to be made up of two grains: the first com-

prises the two carbons C_0 and C_1 and the hydrogens attached to them, and the second comprises the two carbons C_2 and C_3 and their attached hydrogens. The first grain is centred on the middle m_0 of the AA bond between C_0 and C_1 . The second grain is centred on the middle m_1 of the AA bond between C_2 and C_3 . The CG bond links the two middles m_0 and m_1 .

The CG bond potential is calculated by minimising the energy of the molecule while keeping constant the length l between m_0 and m_1 (constrained minimisation).

We begin by defining the energy eg_0 of the G_0 grain centred on m_0 as the sum of the energies of the internal components of the grain:

- bonds (5): $h_0C_0, h_1C_0, C_0C_1, C_1h_2, C_1h_3$;
- valence angles (6): $h_0C_0C_1, h_0C_0h_1, h_1C_0C_1, h_2C_1C_0, h_2C_1h_3, h_3C_1C_0$;
- torsion angles (4): $h_0C_0C_1h_2, h_0C_0C_1h_3, h_1C_0C_1h_2, h_1C_0C_1h_3$.

We define in the same way the energy eg_1 of the grain G_1 centered on m_1 .

The binding energy el between the two grains is the sum of the energies of the components connecting the two grains:

- bond (1): C_1C_2 ;
- valence angles (6): $C_0C_1C_2, h_2C_1C_2, h_3C_1C_2, C_1C_2C_3, C_1C_2, h_4, C_1C_2h_5$;
- torsion angles (13): $h_0C_0C_1C_2, h_1C_0C_1C_2, C_0C_1C_2C_3, C_0C_1C_2h_4, C_0C_1C_2h_5, h_2C_1C_2h_4, h_2C_1C_2h_5, h_2C_1C_2C_3, h_3C_1C_2h_4, h_3C_1C_2h_5, h_3C_1C_2C_3, C_1C_2C_3h_6, C_1C_2C_3h_7$.

The (potential) energy ep of the molecule C_4H_8 is the sum of the energies of its 50 AA components (bonds, valence angles and torsion angles). This energy must be equal to the sum of eg_0 , eg_1 and el :

$$ep = eg_0 + eg_1 + el \quad (10.1)$$

10.2 CG Valence Angles

To determine the CG valence potential, we use the molecule (fragment) C_6H_{12} made up of three grains (Fig.10.2). The first grain comprises the

carbons C_0 and C_1 , the second grain the carbons C_2 and C_3 , and the third grain the carbons C_4 and C_5 .

The first grain is centered on the middle m_0 of the AA bond C_0C_1 ; the second grain on the middle m_1 of the AA bond C_2C_3 ; and the third grain in the middle m_2 of the AA bond C_4C_5 .

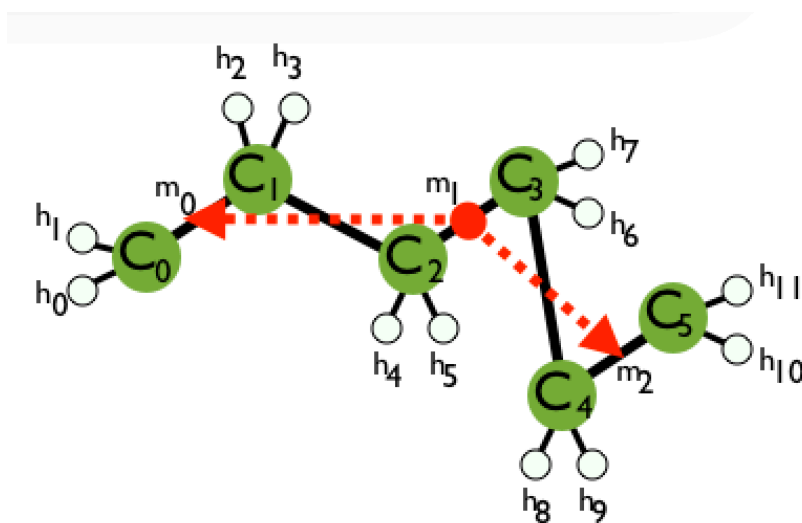


Figure 10.2: Molecule C_6H_{12} . The CG valence angle is the angle formed by the two red arrows.

The CG valence potential is calculated by minimising the energy of the molecule while keeping constant the angle formed by the three centers m_0 , m_1 , and m_2 (so this is also a case of constrained minimisation).

We define the angle energy ea of the three grains as that of the central torsion angle $C_1C_2C_3C_4$.

The potential energy ep of the molecule C_6H_{12} is the sum of the energies of its 86 AA components (bonds, valence angles, and torsion angles).

The potential energy must be equal to the sum of the energies of the grains eg_0 , eg_1 , eg_2 , plus the two binding energies el_1 and el_2 , plus the angle energy ea :

$$ep = eg_0 + eg_1 + eg_2 + el_1 + el_2 + ea \quad (10.2)$$

10.3 Ponderation

The potential energy of a CG molecule is the sum of the energies of the grains, plus the energies of the CG bonds and those of the CG valence angles making up the molecule. This sum must be equal to the potential energy of the AA molecule. To obtain this result, it is necessary to *weight* the energies of the grains, in order to avoid to count these energies several times. The weighting factor P chosen is $1/5$:

$$P = 1/5 \quad (10.3)$$

To justify the value of P , let us consider the CG molecule in Fig.10.3, more precisely the grain G_2 in it. This grain participates in the two bonds G_1G_2 and G_2G_3 , and also in the three valence angles $G_1G_2G_3$, $G_0G_1G_2$ and $G_2G_3G_4$.

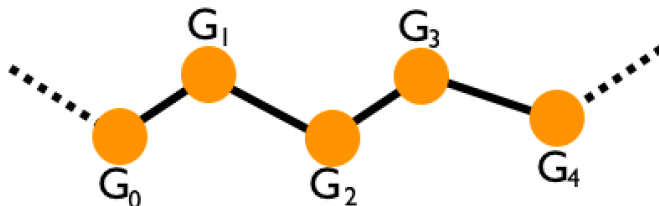


Figure 10.3: CG fragment.

These are the only five CG components in which G_2 appears. The same applies to each of the CG grains, with the exception of those near the two ends of the molecule, which should be treated differently, i.e. with different weightings.

For the sake of simplicity, in the following we will only consider grains far away from extremities (i.e. grains similar to the grain G_2 in Fig.10.3) and the only weighting to be used will be $P = 1/5$ ¹.

When calculating the CG potentials, the minimisations are performed with perturbations steps ranging from 10^{-3} nm to 10^{-9} nm.

¹For a complete treatment of alkanes, it would be necessary to distinguish three types of grains: E grains at the extremities; F grains connected directly to extremities; and the others grains, of type G . We would have then to define the ponderations of the bonds EF , FG , GG , and those of the valence potentials EFG , GGF , and GGG .

10.4 Potential of CG Bonds

The potential of a CG bond is the sum of the weighted energies of the two grains, plus the energy of the link between them:

$$eb = P \times eg_1 + P \times eg_2 + el \quad (10.4)$$

For the potential of CG bonds we obtain the curve shown in Fig.10.4.

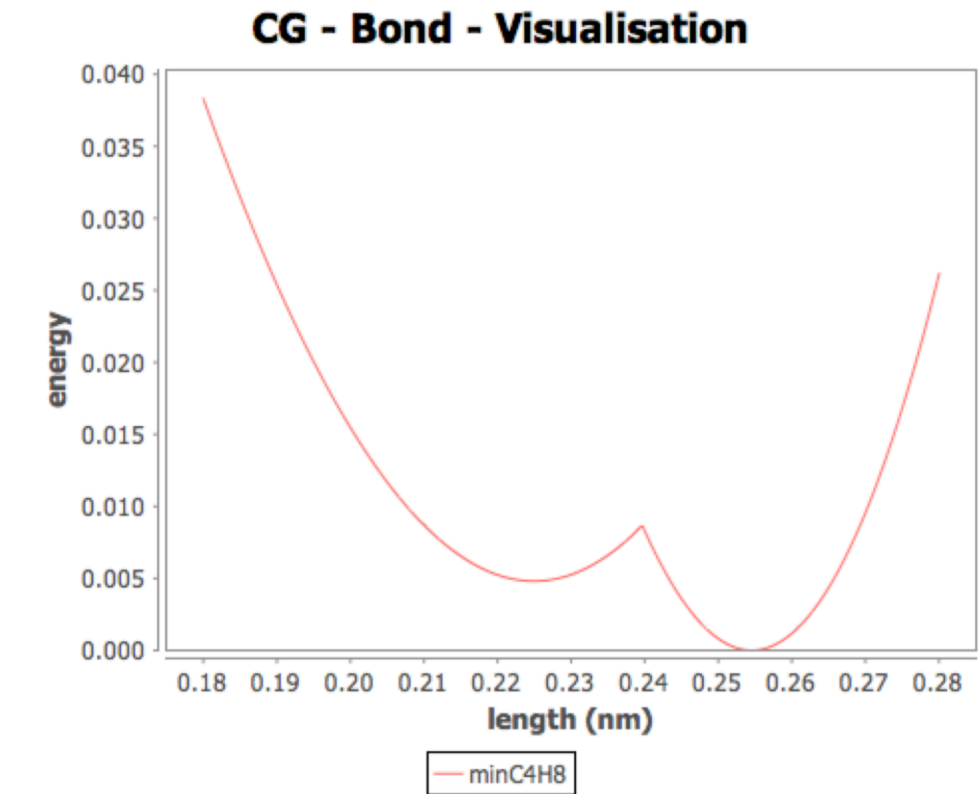


Figure 10.4: Potential of a CG bond between two C_2H_4 grains. The potential is obtained by minimisation of the C_4H_8 fragment.

The curve obtained does not depend on the size of the molecule. It shows an inflection point at around 0.24 nm. This inflection comes from the triggering of the central torsion angle $C_0C_1C_2C_3$.

To calculate the potential of the CG bond, the size of the CG bond is decremented up to 0.18 nm, then increased up to 0.28 nm, in steps of 10^{-4} nm.

10.5 Potential of CG Valence Angles

The CG valence angle potential is the sum of the weighted energies of the three grains making up the valence angle, plus the energy of the angle:

$$ev = P \times eg_1 + P \times eg_2 + P \times eg_3 + ea \quad (10.5)$$

The CG valence potential corresponds to the curve of Fig.10.5.

As with the binding potential, the curve obtained does not depend on the size of the molecule. The curve obtained shows three inflection points. The two inflection points on the left correspond to the triggers of the two torsion angles $C_0C_1C_2C_3$ and $C_2C_3C_4C_5$. The right-hand inflection point corresponds to the triggering of the central torsion angle $C_1C_2C_3C_4$.

In the implementation, the CG valence angle is decremented from π radians to 0.9 radians, then increased up to π , in steps of 0.017 radians (262 measurements).

10.6 CG Inter-molecular Forces

To determine the force exerted between two CG grains, we consider two C_2H_4 molecules at a fixed distance d . The potential is calculated by minimising the energy of the two grains, while keeping constant the distance d (conditioned minimisation).

The ep energy is the value of the potential between the two grains obtained after minimisation maintaining the distance d . By varying the parameter d , one obtains the CG van Der Waals potential curve shown in Fig.10.6.

The ep energy is the sum of the thirty-six energies of the Lennard-Jones potentials associated with the pairs of atoms between the two grains (the AA Lennard-Jones potentials are represented in Fig.2.6).

The potential obtained by minimisation in Fig.10.6 does not have the form of a Lennard-Jones potential, defined by the equation Eq.2.4. In Fig.10.7 the obtained potential is compared with a Lennard-Jones potential ($\epsilon = 12.5 \times \epsilon_{CC}$, $\sigma = 0.9 \times \sigma_{CC}$): it can be seen that the potential obtained differs

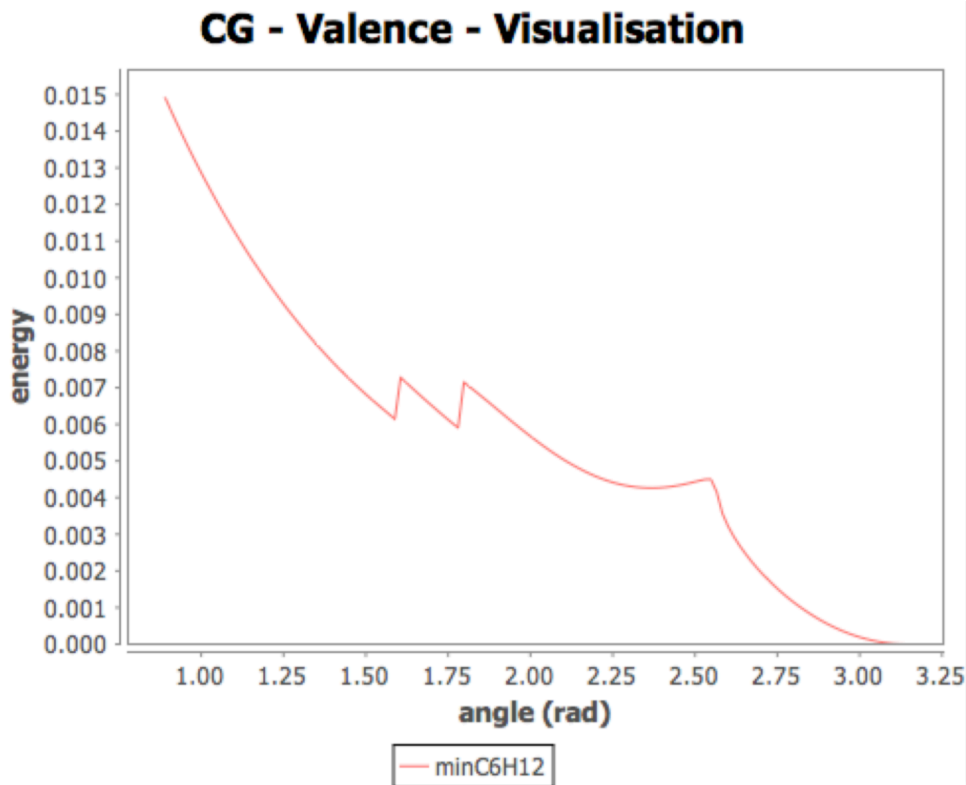


Figure 10.5: Valence potential CG between three grains C_2H_4 . The potential is obtained by minimisation of the molecule C_6H_{12} . The minimum energy value is zero and corresponds to a valence angle of value π .

over a significant range (between 0.4 nm and 0.7 nm) with the Lennard-Jones potential.

The inter-molecular potential CG is linear in the domain where it does not coincide with a Lennard-Jones potential. In this domain, minimisation has the effect of reorganising the AA components in the two CG grains in such a way as to minimise their energies. Within each grain, the energy exchanges between these components induce a linear evolution of the overall grain energy.

Outside the linear zone, the CG inter-molecular potential behaves like a standard Lennard-Jones potential, which means the absence of reorganisation of the CG grains in the zones of close proximity of the two grains or of long

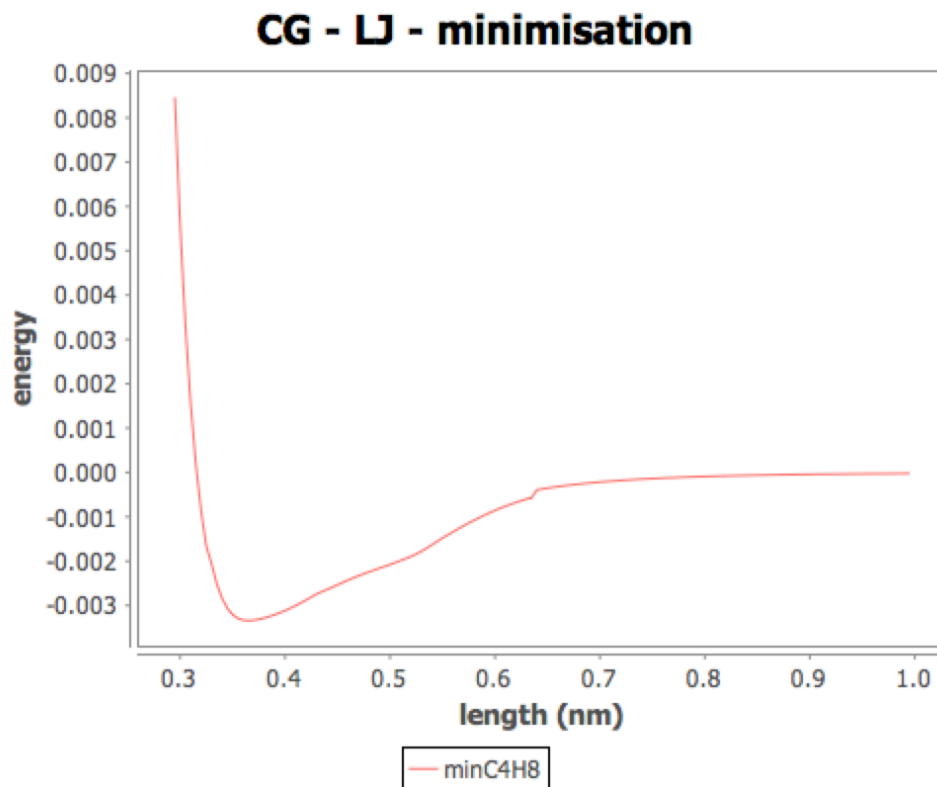


Figure 10.6: Inter-molecular potential between two CG grains obtained with the minimisation method.

distance between them.

10.7 Comparison with the Inverse-Boltzmann Approach

To compare the inverse-Boltzmann and the minimisation approaches in the calculation of the CG bond potential, we superimpose in Fig.10.8 the curves in Fig.10.4 and Fig.8.1.

There is good agreement between the curves, except for the inflection point, at around 0.24 nm . This point corresponds to the triggering of the central dihedral, a rare event to which, therefore, is associated a potential

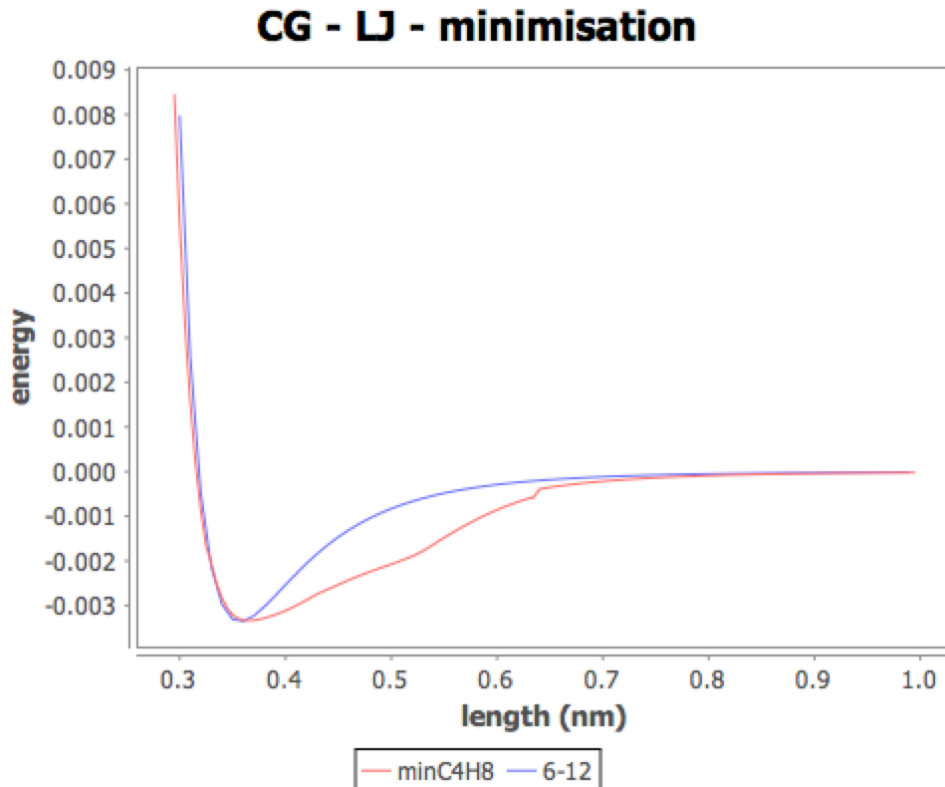


Figure 10.7: Potential of van Der Waals force between two CG grains obtained with the minimisation method, compared with a Lennard-Jones curve.

energy lower than it should be (this can be seen as an intrinsic weakness of the inverse-Boltzmann approach).

To compare the inverse-Boltzmann and minimisation approaches in case of the CG valence potential, we superimpose in Fig.10.9 the curves of Fig.10.5 and Fig.8.3.

The inverse-Boltzmann curve is systematically higher than the minimisation curve for angles less than 1.9 radians. This is due to the temperature being too low for the angular exploration below 1.9 to be really significant.

We can consider that the part of the inverse-Boltzmann curve situated below the minimisation curve results from a lack of precision due to a too small set of events.

To increase the number of events taken into account, longer molecules

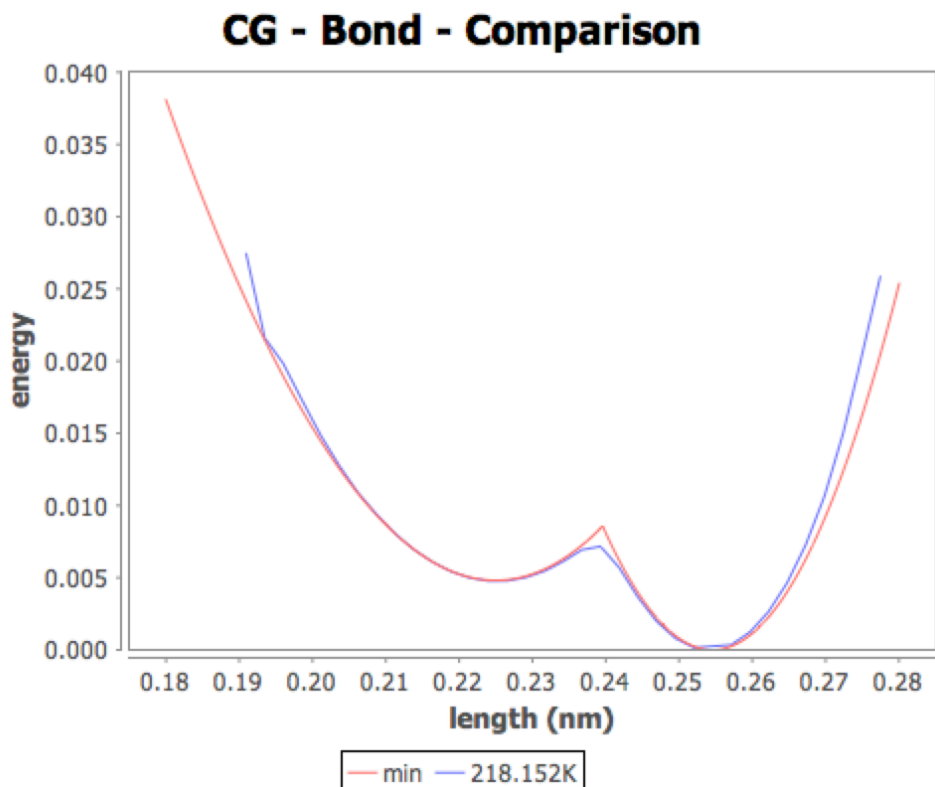


Figure 10.8: CG bond potential obtained with the inverse-Boltzmann method from molecule C_6H_{12} at temperature of 218.152 K compared with the potential obtained with the minimisation method.

can be used, for example the $C_{30}H_{60}$ molecule at the temperature of 206 K. The result is shown in Fig.10.10 where it can be seen that the part of the inverse-Boltzmann curve situated under the minimisation curve is greatly reduced.

With a sufficiently large number of events, we conjecture that the inverse-Boltzmann curve will always be above the curve obtained by minimisation. This could be seen as a (indeed partial) validation of the minimality of the curve obtained by minimisation, which is lower to all those obtained from actual simulations.

10.7. COMPARISON WITH THE INVERSE-BOLTZMANN APPROACH87

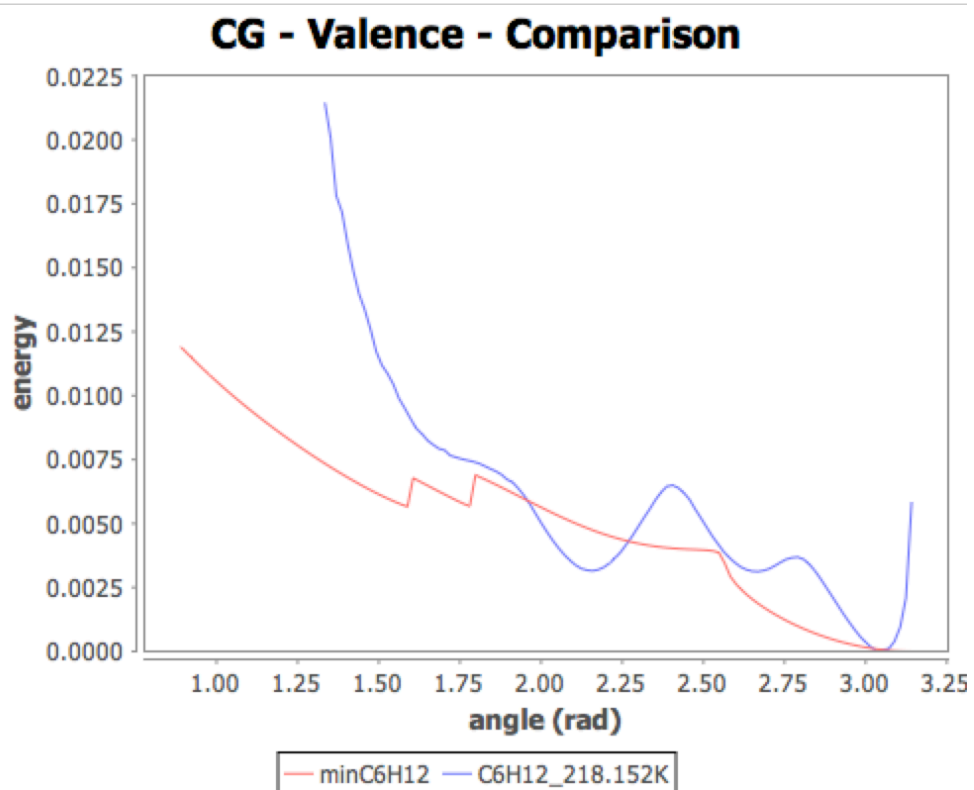


Figure 10.9: CG valence potential obtained with inverse-Boltzmann from molecule C_6H_{12} at temperature of 218.152 K (in blue) compared with the potential obtained with minimisation (in red).

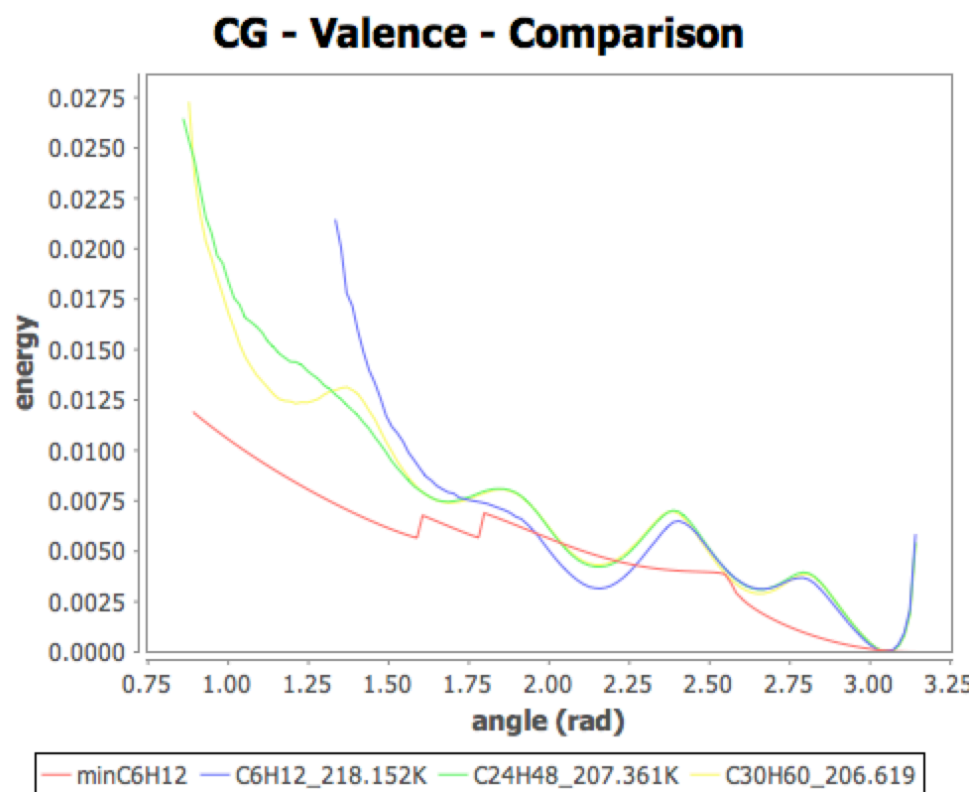


Figure 10.10: CG valence potential obtained with inverse-Boltzmann from the molecule C_6H_{12} at temperature of 218.152 K (in blue) compared with the one obtained with the molecule $C_{30}H_{60}$ at the temperature of 206.619 K (in green).

Chapter 11

Simulations in UA

Using the minimisation method, we have determined the potentials of the components of UA molecules formed from G_2 grains, which makes it possible to simulate molecules at this scale. The UA potentials obtained from the AA potentials are summarised in Fig.11.1.

$$\begin{aligned}k_{G_2G_2} &= k_{CC} & r_{G_2G_2} &= r_{CC} \\k_{G_2G_2G_2} &= 1.1 \times k_{CCC} & \theta_{G_2G_2G_2} &= \theta_{CCC} \\A1_{G_2G_2G_2G_2} &= A1_{CCCC} & A2_{G_2G_2G_2G_2} &= A2_{CCCC} \\A3_{G_2G_2G_2G_2} &= A3_{CCCC} + 4 \times A3_{CCCH} + 4 \times A3_{HCCH} \\ \epsilon_{G_2G_2} &= 5.5 \times \epsilon_{CC} & \sigma_{G_2G_2} &= 0.917 \times \sigma_{CC}\end{aligned}$$

Figure 11.1: UA parameter values associated with grains G_2 , expressed in internal units (AA OPLS parameters are given in Fig.5.1).

The potential of the valence angle $G_2G_2G_2$ is approximated by a harmonic potential whose strength is that of CCC multiplied by 1.1, as we saw in 9.2. The torsion angle potential was determined in 9.3 and the inter-molecular potential in 9.4.

In the MD system, the G_2 grains (i.e. made up of one carbon atom and two hydrogen atoms) appear as cyan-coloured balls. Fig.11.2 shows a UA molecule composed of 8 G_2 grains at equilibrium (its energy is zero).

Simulations of UA molecules are very stable, as can be seen in Fig.11.3.

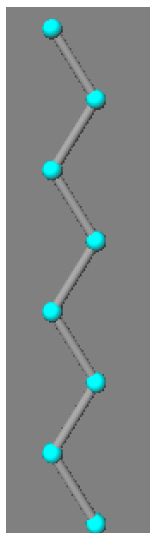


Figure 11.2: UA molecule at equilibrium made up of 8 grains G_2 .

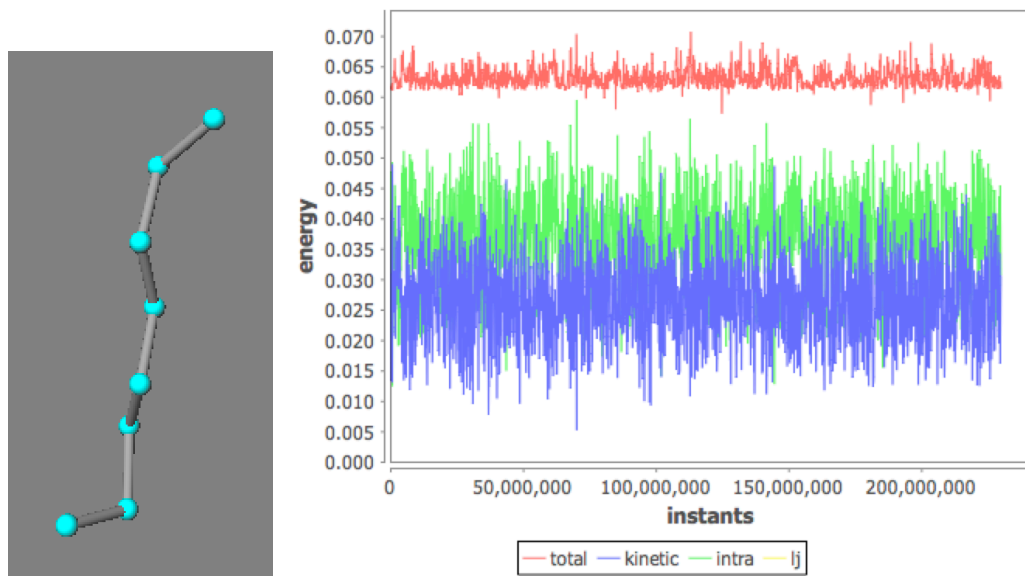


Figure 11.3: Simulation of one UA molecule made up of 8 grains G_2 .

On the left, a molecule with eight grains G_2 is shown during simulation. Initially the molecule is given an initial energy obtained by shifting the grains towards the positive y (vertical axis).

On the right, one can see the evolution of energies over time. The red curve represents the total energy of the molecule, which remains stable, as we can see.

Fig.11.4 describes the simulation of two UA molecules with 8 grains, placed face-to-face at a distance of 1.8 nm . Initially the two molecules are at equilibrium. The energy of inter-molecular forces is shown in yellow, the kinetic energy in blue, the intra-molecular energy in green, and the sum of the energies in red.

UA scale simulations are more efficient than AA scale ones: the number of degrees of freedom to be simulated is smaller and the time-step can be increased. We will show this increased efficiency on an example.

We first simulate an AA C_8H_{16} molecule during 10^7 instants with a time step of 0.1 femto-second. The real-time of simulation¹ is 1053 seconds. This corresponds to a simulated time of 0.5 nano-second. The energies are shown on the left-hand side of Fig.11.5.

We now simulate the corresponding UA molecule, made up of 8 grains G_2 with a time-step of 0.5 femto-second. The simulation lasts 175 seconds which corresponds to a simulated time of 2.5 nano-seconds. Energies are shown on the right-hand side of Fig.11.5.

Compared with the previous AA simulation, the real-time of simulation is therefore reduced by a factor 6, while the simulated time is increased by a factor 5. The advantage of UA over AA is therefore real.

¹with a MacBook Pro, i7 processor at 2.6GHz, with 16GB of memory

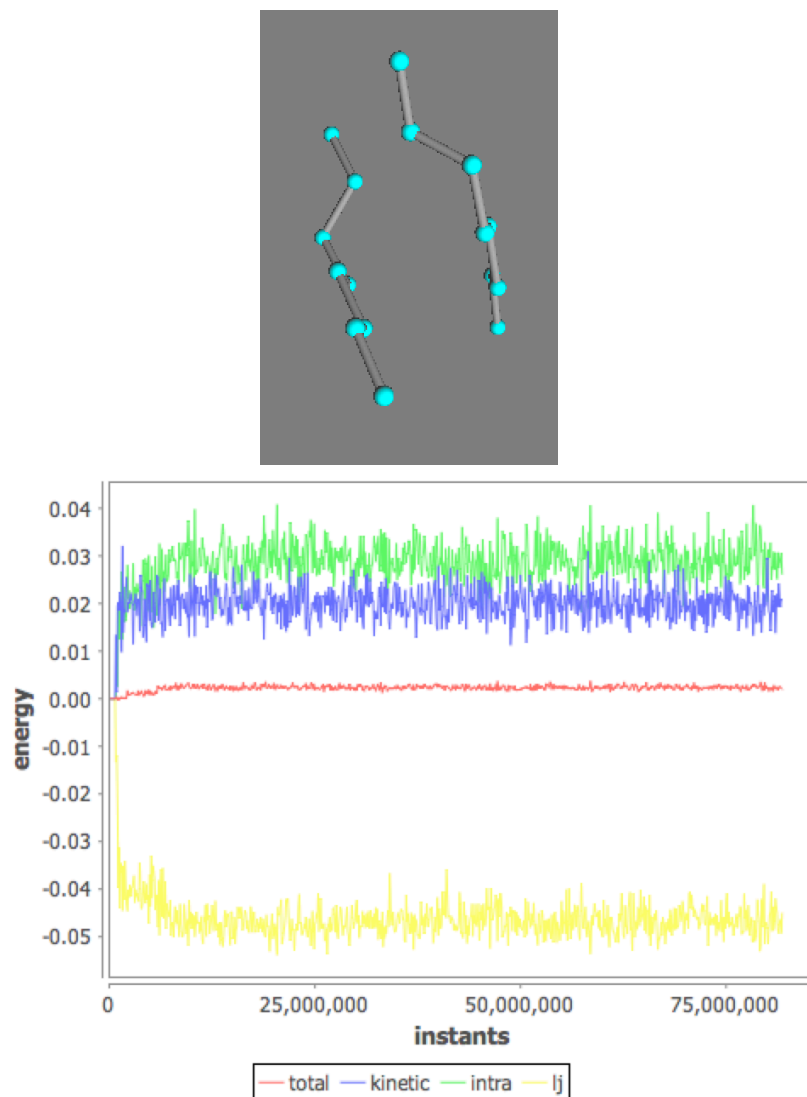


Figure 11.4: Simulation of two UA molecules made up of 8 grains G_2 .



Figure 11.5: Energies during 10 millions of instants. Top, molecule AA C_8H_{16} . Bottom, molecule UA made up of 8 grains.

Chapter 12

Simulations in CG

Unlike the AA and UA potentials previously described, CG potentials do not have standard forms as harmonic, “three-cosine”, or Lennard-Jones functions. We must therefore first precisely define what are these non-standard forms of CG potentials.

12.1 Determination of the CG potential

Bonds

The CG bond potential appears to be made up of two harmonic functions, applied on either side of a split value ($split = 0.241 \text{ nm}$). One first defines a functional that produces harmonic functions as:

$$harm : k, r, d \rightarrow k \times (r - d)^2$$

where k is the strength, r is the equilibrium value and d is a value parameter (a length in nm in the case of bonds, and an angle in radians in the case of valence angles).

The CG bond potential can now be defined using the functional $harm$ as the following function $cgBond$:

$$\begin{aligned} &split = 0.241 \\ &h_1 : d \rightarrow harm(16.5, 0.225, d) \\ &h_2 : d \rightarrow harm(38.5, 0.255, d) \\ &cgBond : d \rightarrow \mathbf{if} \ d < \mathit{split} \ \mathbf{then} \ h_1(d) + 0.0049 \ \mathbf{else} \ h_2(d) \end{aligned}$$

On left of 0.241 (that is, for values less than 0.241 nm), the function h_1 defined by $k = 16.5$ and $r = 0.225$ applies. Moreover, a constant shift of 0.0049 in y is added to the result.

For values greater than 0.241 nm , the harmonic function h_2 with parameters $k = 38.5$ and $r = 0.255$ applies.

Fig.12.1 compares the CG potential obtained by minimisation of the C_4H_8 molecule (in red) and the previous *cgBond* function, constructed “by cases” using the two harmonic functions h_1 and h_2 (in blue).

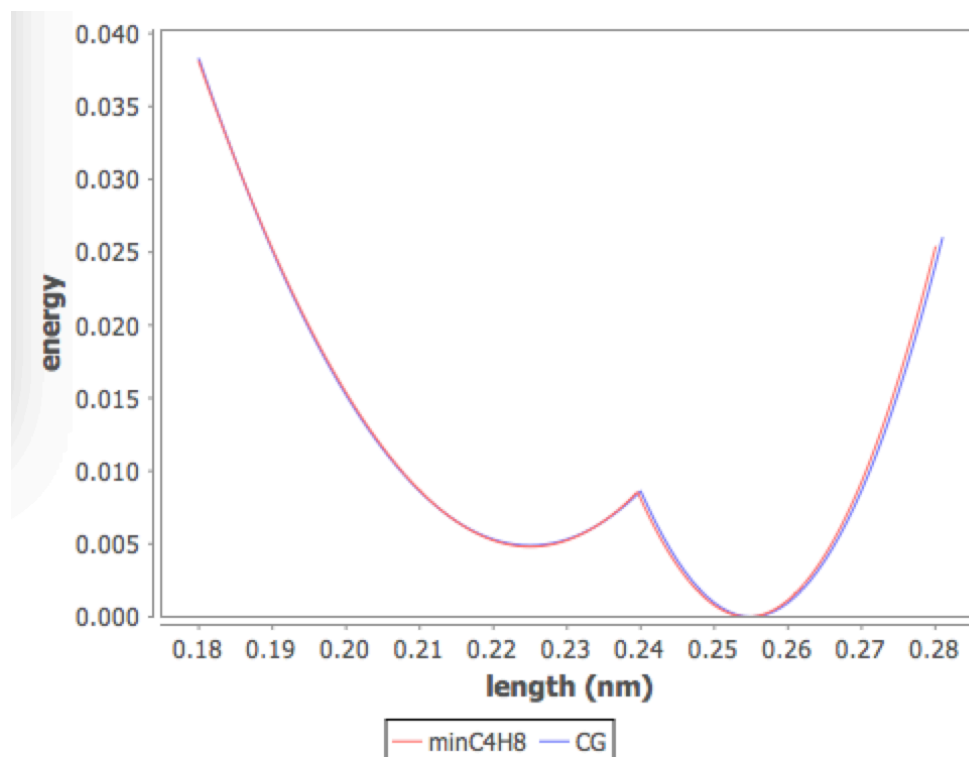


Figure 12.1: The CG potential (in blue) is built “by case” with the aid of two harmonic functions.

One observes the exact match of the two curves, the one obtained by minimisation, and the other built “by cases” with the aid of two auxiliary harmonic functions.

Valence Angles

Building up the CG valence potential needs four functions h_0, h_1, h_2, h_3 defined using the functional *harm* as follows:

$$\begin{aligned} split_0 &= 2.56 & h_0 &: a \rightarrow harm(0.0095, \pi, a) \\ split_1 &= 1.79 & h_1 &: a \rightarrow harm(0.0055, split_0, a) + 0.004 \\ split_2 &= 1.6 & h_2 &: a \rightarrow harm(0.041, split_1, a) + 0.0056 \\ & & h_3 &: a \rightarrow harm(0.0059, 2.0, a) + 0.0047 \end{aligned}$$

The *cgValence* function is then defined “by cases” as:

$$\begin{aligned} cgValence : a \rightarrow & \quad \mathbf{if} \ a > split_0 \ \mathbf{then} \ h_0(a) \\ & \quad \mathbf{else if} \ a > split_1 \ \mathbf{then} \ h_1(a) \\ & \quad \mathbf{else if} \ a > split_2 \ \mathbf{then} \ h_2(a) \\ & \quad \mathbf{else} \ h_3(a) \end{aligned}$$

The *cgValence* function is represented by the blue curve in Fig.12.2, the red curve being the result obtained by minimisation.

As for CG bonds, one gets an exact match of the two curves, the one obtained by minimisation, and the other built “by cases” with the aid of four auxiliary harmonic functions.

Inter-molecular Forces

The inter-molecular (van Der Waals) forces are often represented by Lennard-Jones functions that can be produced using the functional *lj6_12* defined by:

$$lj6_12 : \epsilon, \sigma, r \rightarrow 4\epsilon \times ((\sigma/r)^{12} - (\sigma/r)^6)$$

To build the CG inter-molecular potential, we start by defining a particular Lennard-Jones function *lj* as follows:

$$\begin{aligned} \epsilon &= 0.00336 \\ \sigma &= 0.318 \\ lj : d &\rightarrow lj6_12(\epsilon, \sigma, d) \end{aligned}$$

The function *lj* is represented by the green curve in Fig.12.3.

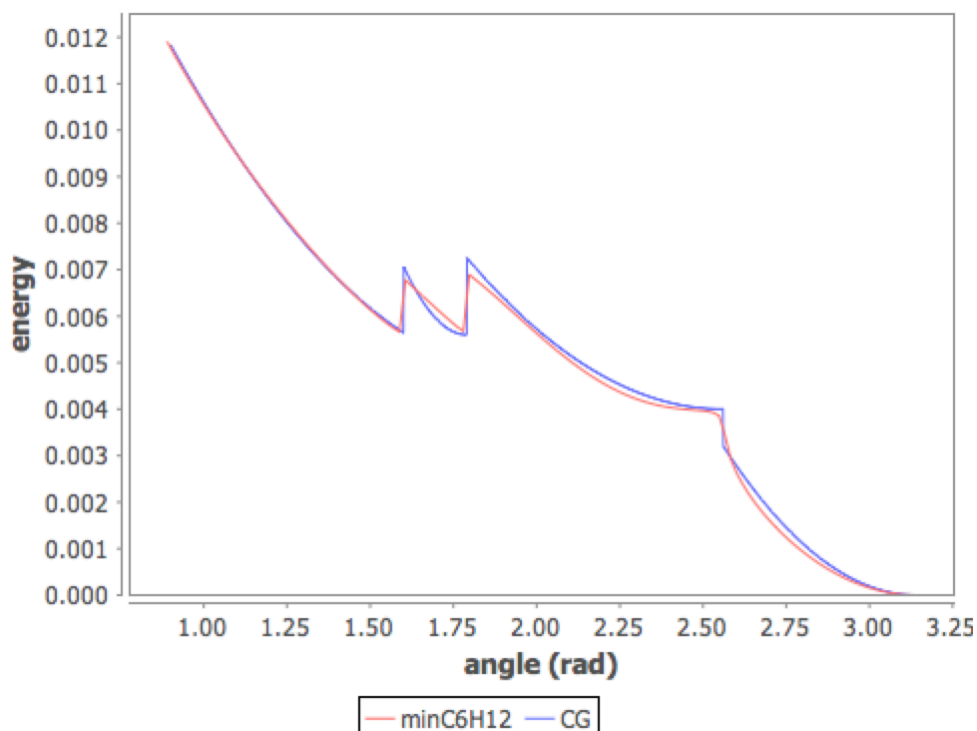


Figure 12.2: The CG valence potential (in blue) is built “by cases” with the aid of four harmonic functions.

To completely determine the CG Lennard-Jones potential, one needs to define two points: the point $p_1 = (0.365, -\epsilon)$ whose coordinate in y is minimal and the point $p_2 = (0.68, -0.00195)$.

Between these two points, the potential is globally a straight line, corresponding to the affine function joining the two points.

The definition of the CG inter-molecular potential $cgLj$ is then:

$$cgLj : d \rightarrow$$

$$\text{if } d < 0.365 \text{ or } d > 0.68 \text{ then } lj(d) \text{ else } line(d)$$

where the function $line$ is the affine function linking the two points p_1 et p_2 .

The CG potential is represented by the blue curve in Fig.12.3. The red curve is the CG potential obtained with the minimisation method.

Here again, we observe the good matching between the curve obtained with the minimisation method and the previous curve built “by cases”.

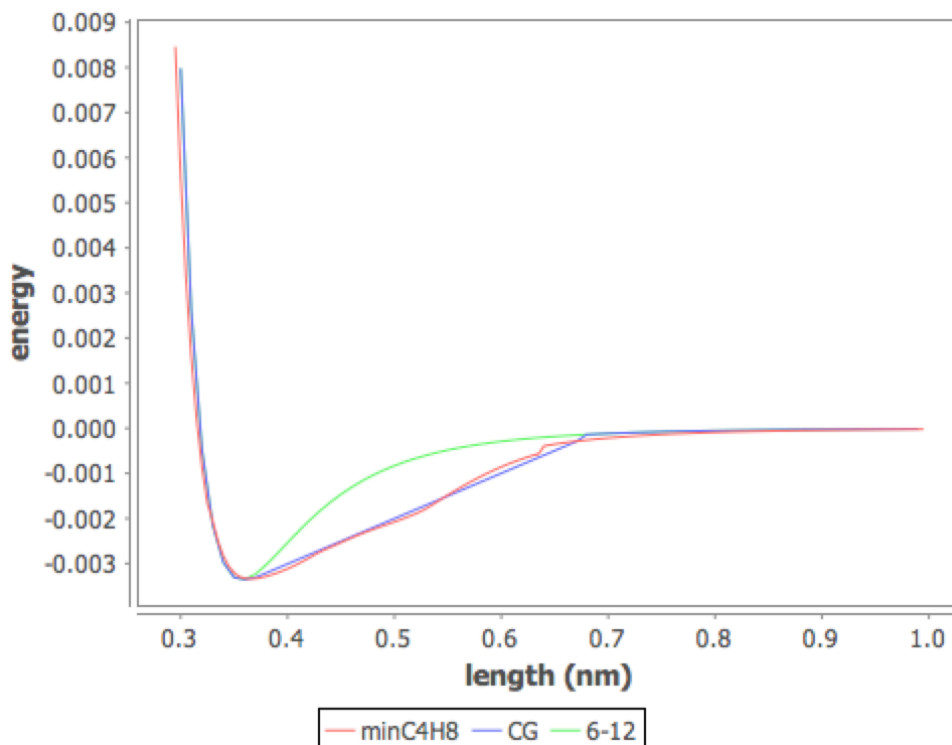


Figure 12.3: The inter-molecular potential CG (in blue) is defined with the aid of a Lennard-Jones function (in green) and an affine function. In red, the potential obtained by minimisation.

12.2 CG Execution

To illustrate the CG execution, we first consider an isolated CG molecule made up of six CG_4 grains. The x coordinates are represented horizontally, the y coordinates vertically, and those in z are represented in height.

Some energy is initially supplied to the molecule at equilibrium by shifting its first grain in the direction of increasing y . Thus, the first CG bond is stretched and it is the energy due to this stretching that is initially supplied to the molecule.

The right-hand side of Fig.12.4 shows the evolution of the various energy components over time. Measurements are taken every 10^5 instants. The kinetic energy is in blue, the intra-molecular energy is in green and the total

energy in red (the inter-molecular energy is always zero).

The molecule is shown during execution on the left of the figure and we can see that it remains linear. This is consistent with the fact that the forces here are solely due to the initial bond stretching.

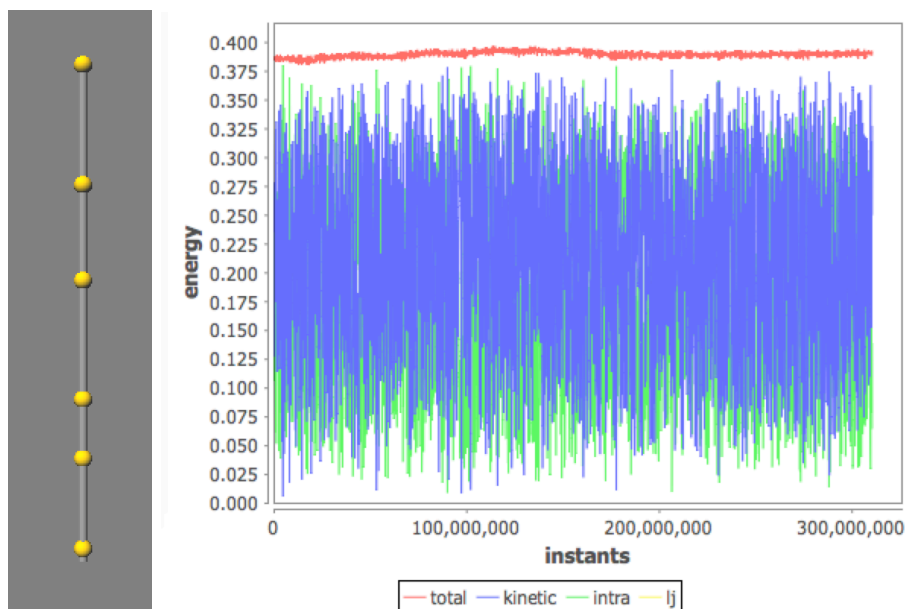


Figure 12.4: Simulation of a CG molecule made up of 6 grains CG_4 . Initially, only the first bond has some energy. On the left, the molecule after 3×10^8 instants.

We now change the initial conditions by rotating the first grain around the second, while remaining in the same plane. The initial energy is then only that of the first valence angle, formed by the first three grains.

The execution results are shown in Fig.12.5 where we can see that the molecule is no longer linear but always remains in the same plane: in fact, all the forces exerted during execution are co-planar forces.

Finally, we introduce a twist into the molecule, shifting the first grain in the x coordinate and the last one in the z coordinate. These two shifts mean that the molecule is no longer planar. The simulation is shown in Fig.12.6.

We will now consider the case of inter-molecular forces. We consider a simulation where two identical molecules in equilibrium are placed face-to-face. The two molecules are linear and co-planar. Each molecule is made up of six grains.

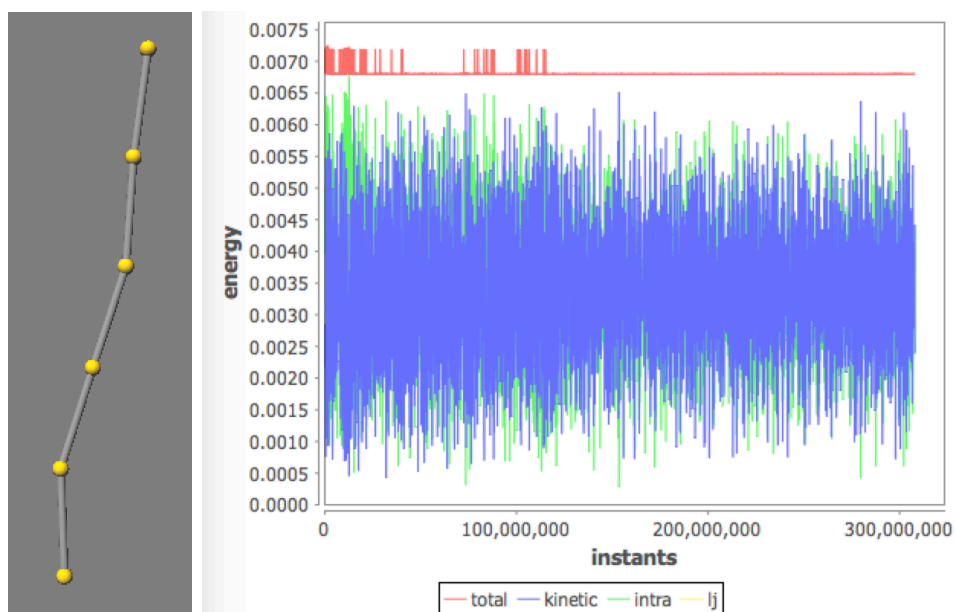


Figure 12.5: Simulation of a CG molecule made up of 6 grains CG_4 . Initially, only the first valence angle contains some energy. On top image, the molecule after 3×10^8 instants.

The right-hand side of Fig.12.7 shows the various energies: in blue, the kinetic energy; in green, the intra-molecular energy; in yellow, the inter-molecular energy, and in red the total energy. The simulation lasts 10^8 instants, corresponding to 25 ns (the time-step is 10^{-4} ps).

The two molecules, initially co-planar, remain so during the execution, as shown on the left of the figure. The van Der Waals forces remain in the same plane as the molecules.

This is not the case when the molecules are not co-planar. To illustrate this, we repeat the previous simulation but after having rotated one of the two molecules around the x axis, by an angle of one degree. This means that the two molecules are no longer initially co-planar. After a short time, the molecules begin to describe 3D trajectories.

CG molecules that are longer than those shown in the previous images may show foldings that can be very accentuated. This is the case, for example, for the molecule made up of 40 grains in Fig.12.9.

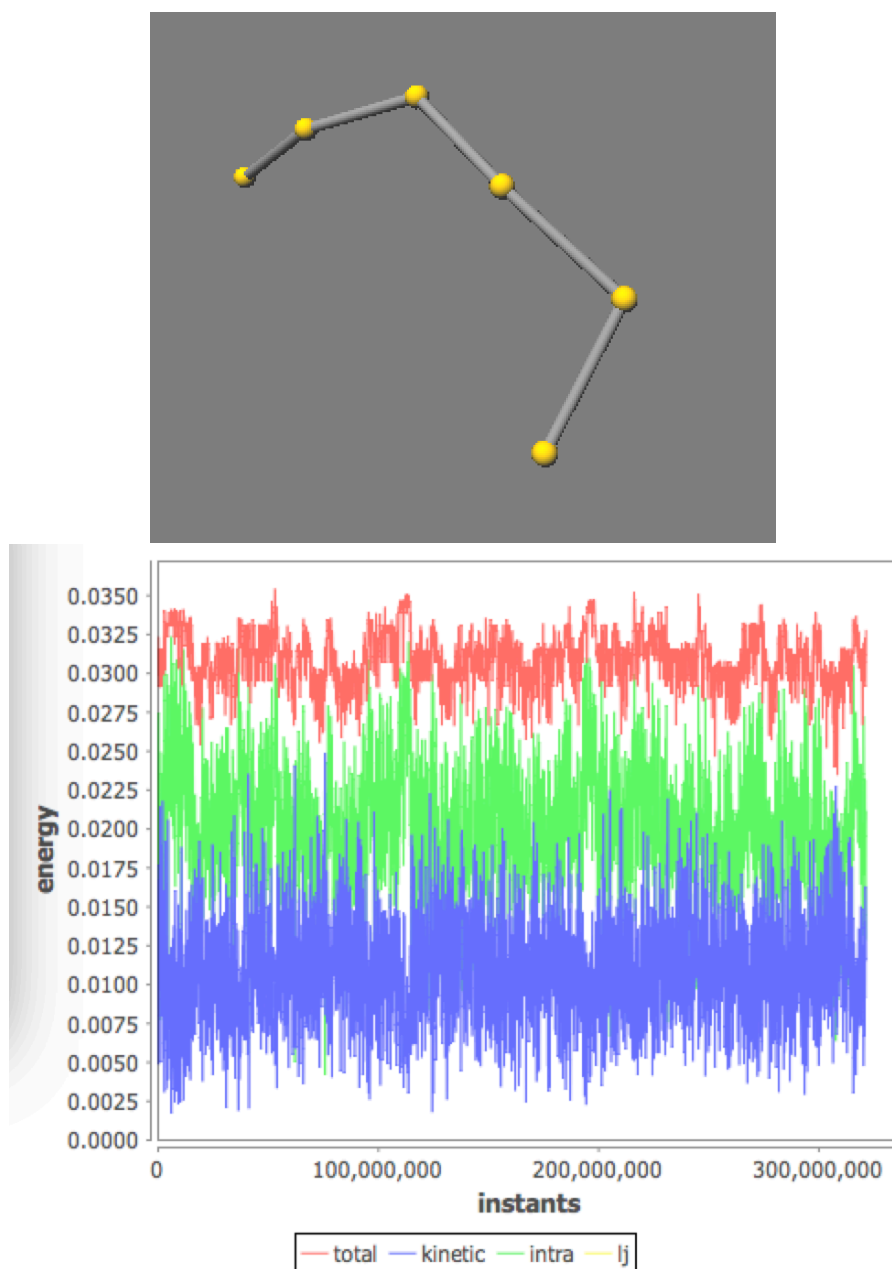


Figure 12.6: Simulation of a CG molecule made up of 6 grains CG_4 . Initially, the first grain is shifted in x and the last in z . The molecule is no longer planar. On top image, the molecule after 3×10^8 instants.

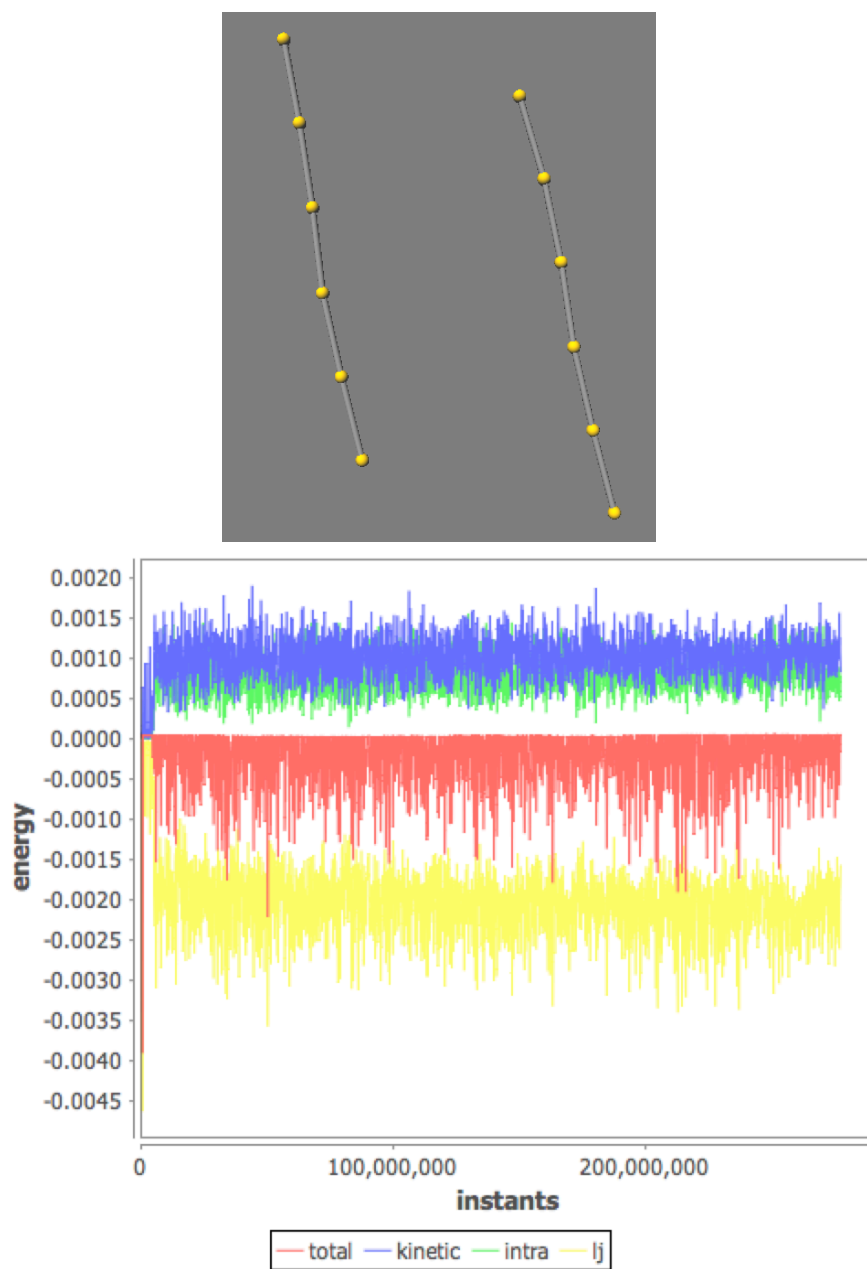


Figure 12.7: Top: simulation of two molecules CG made up of 6 grains CG_4 and initially co-planar. Bottom: variation of the energies.

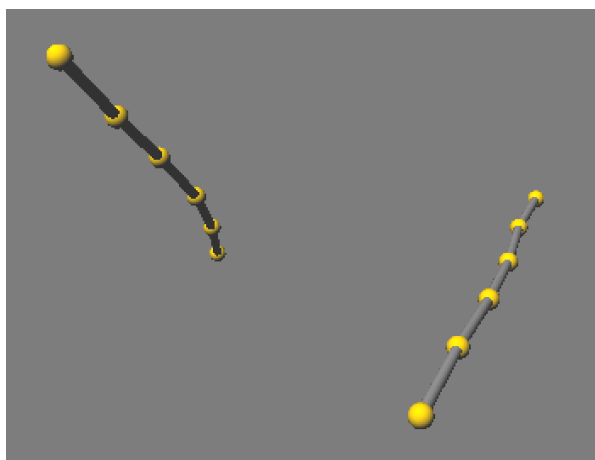


Figure 12.8: Simulation of two CG molecules made up of 6 grains CG_4 , initially not co-planar, after 20^6 instants.

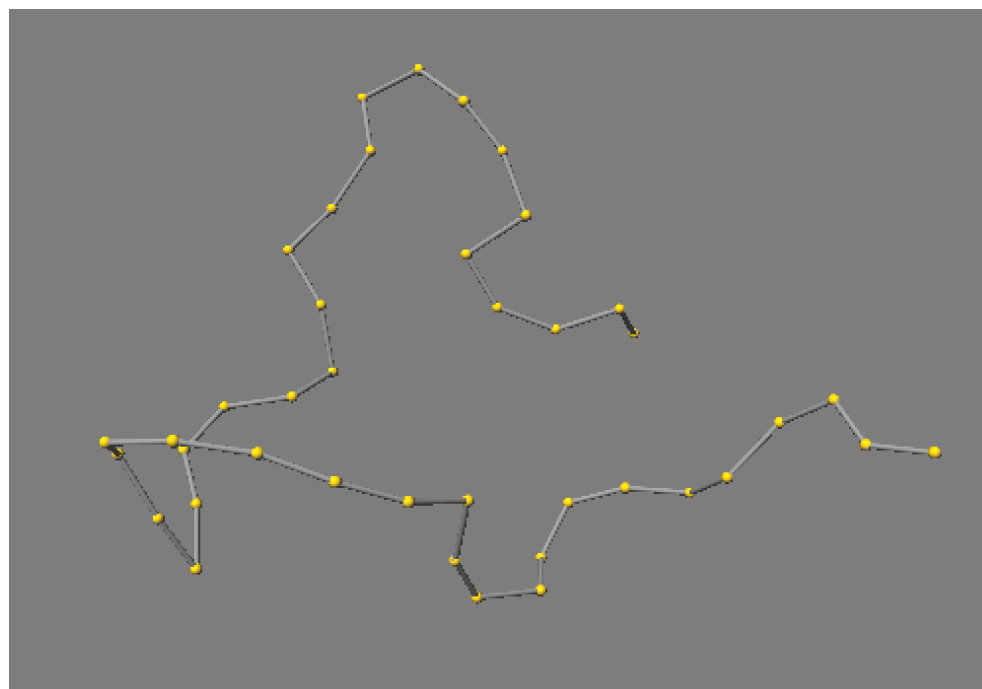


Figure 12.9: CG molecule made up of 40 grains CG_4 , initially not co-planar, during simulation.

Chapter 13

Reconstructions

Molecule reconstructions make it possible to change *during the same simulation* the scale at which molecules are simulated. Typically, when a molecule is isolated, we prefer to simulate it at the UA or CG scale, much more efficient than the AA scale. However, when the molecules come close to one another, it may become necessary to go back to the AA scale, to take into account the interactions between them.

To manage reconstructions, several issues need to be addressed. The first is that, during a reconstruction, the reconstructed molecule must “immediately” replace the initial molecule. This means that during the simulation, the two molecules are not allowed to coexist (their interactions would be meaningless). In the reactive approach, this replacement, i.e. the destruction of the initial molecule and the introduction of the reconstructed molecule, is naturally carried out between instants.

A second question concerns the very possibility of reconstruction. It is difficult to implement reconstruction mechanisms that never cause any pathological increase in the energy of the reconstructed molecule. Reconstruction mechanisms need to be evaluated with this aspect in mind.

A third issue is that of interactions between molecules at different scales. In this respect, we can introduce automatic reconstruction mechanisms into the simulation, triggered by the proximity of the molecules, in order to bring the interacting molecules to the same scale.

Reconstructions between AA and UA

The AA→UA reconstruction consists of constructing a UA scale molecule from an AA scale molecule. In fact, it amounts to “erasing” the hydrogen atoms of the AA scale, by “absorbing” them into the grains of the UA scale according to the equation:



The mass is preserved, since the sum of one carbon with two hydrogens is 0.014 in internal units (the mass of C is 0.012 and that of H is 0.001), which is also the mass of the grain G_2 . The grain G_2 is positioned exactly on the atom C , which has the effect of eliminating the potential energies of the two CH bonds and that of the HCH angle, which disappear in the reconstruction.

The sum of the potentials of the AA molecule is then always greater than the sum of the UA potentials of the reconstructed molecule, resulting in a systematic loss of potential energy during the AA→UA reconstruction.

The reverse reconstruction UA→AA consists of constructing a molecule AA from a UA one. It involves replacing a G_2 grain by a carbon atom with two hydrogen atoms linked to it, according to the equation:



As in the equation (13.1), masses are consistent. We place the carbons exactly on the G_2 grains and then try to place the hydrogen atoms. Ideally, these should be placed in such a way that the added energy (issued from CH bonds, HCH angles and HCC angles) is minimal. To achieve this, a minimisation phase of the AA molecule preserving the positions of the carbons should be launched before resuming the simulation.

Such a global minimisation phase is clearly very cumbersome, which is why we have chosen not to implement it, preferring instead to adopt a pragmatic but unsafe technique.

In this technique, each carbon is grafted with a pair of CH bonds in equilibrium with the two hydrogens forming a HCH angle also in equilibrium (see Fig.13.1). Thus the added CH bonds and HCH valence angle do not introduce any additional energy.

For the valence angles HCC and the torsion angles HCCH and HCCC, we proceed in the same way as when creating a molecule at equilibrium, by alternating the pairs of hydrogens in parallel planes (see Fig.13.2).

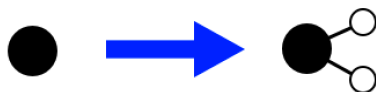


Figure 13.1: Introduction of hydrogen atoms, of bonds HC, and of the valence angle HCH.

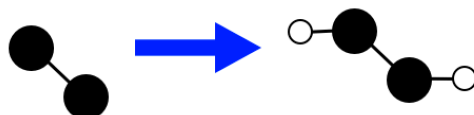


Figure 13.2: Introduction of valence angles HCC and of torsion angles HCCH and HCCC.

Thus, contrary to what happens with the AA→UA reconstruction, additional energy can appear, corresponding to the energies of the HCC, HCCH and HCCC angles introduced. This extra energy can even lead to an explosion in the simulation, particularly when, due to a torsion of the molecule, hydrogen atoms are too close together.

Reconstructions between UA and CG

The UA→CG reconstruction consists of constructing a CG scale molecule from a UA scale one. In fact, it amounts to combining two UA grains into a single CG grain according to the equation:



The mass of a grain CG_4 is 0.028. The CG_4 grain is positioned in the middle of the bond between the two G_2 grains and a CG bond is introduced between two consecutive CG_4 grains.

The inverse reconstruction CG→UA consists of constructing a UA scale molecule from a CG scale one. Each CG grain corresponds to two UA grains:



The two UA grains are placed on either side of the CG grain, so that the CG grain is in the middle of the two UA grains. A UA bond is introduced

between the two closest UA grains. We adopt a similar technique to that used for the UA→AA reconstruction, in the placement of the UA grains, with the same risk of incorrectly positioning the UA grains by introducing additional energy, which could cause the simulation to “over-explode”.

Reconstructions between AA and CG

The reconstructions between AA and CG can be considered as a sequence of two reconstructions, one between AA and UA and the other between UA and CG. The AA→CG reconstruction links two reconstructions which systematically lower the energy, and therefore does not pose a problem of energy explosion. However, this is not the case for the reverse CG→AA reconstruction, where an explosion can occur both when the UA grains are introduced and when the hydrogen atoms are introduced, during the UA→AA reconstruction.

Manual Reconstructions

Fig.13.3 shows a simulation in which the user, by clicking in the control panel, can change the scale of the molecule being simulated (a $C_{10}H_{20}$ molecule, initially supplied with some potential energy). The change from the AA molecule to the UA molecule occurred in response to the click in the →ua part of the panel. The change from the UA molecule to the CG molecule occurred in response to the click in →cg. Clicks produce SugarCubes events which are instantly broadcast to all parts of the program.

13.1 Inter-molecular Forces

The treatment of inter-molecular forces is tricky during reconstructions for two reasons: the first is that the introduction of hydrogens during UA→AA or CG→AA reconstructions can lead to explosions, as they come too close together. A similar issue occurs with UA grains in CG→UA reconstructions. The second reason is that the equilibrium distances between molecules are not the same at the various scales, which means that the repulsive inter-molecular forces can increase sharply when molecules that are too close are reconstructed. We will now consider this case.

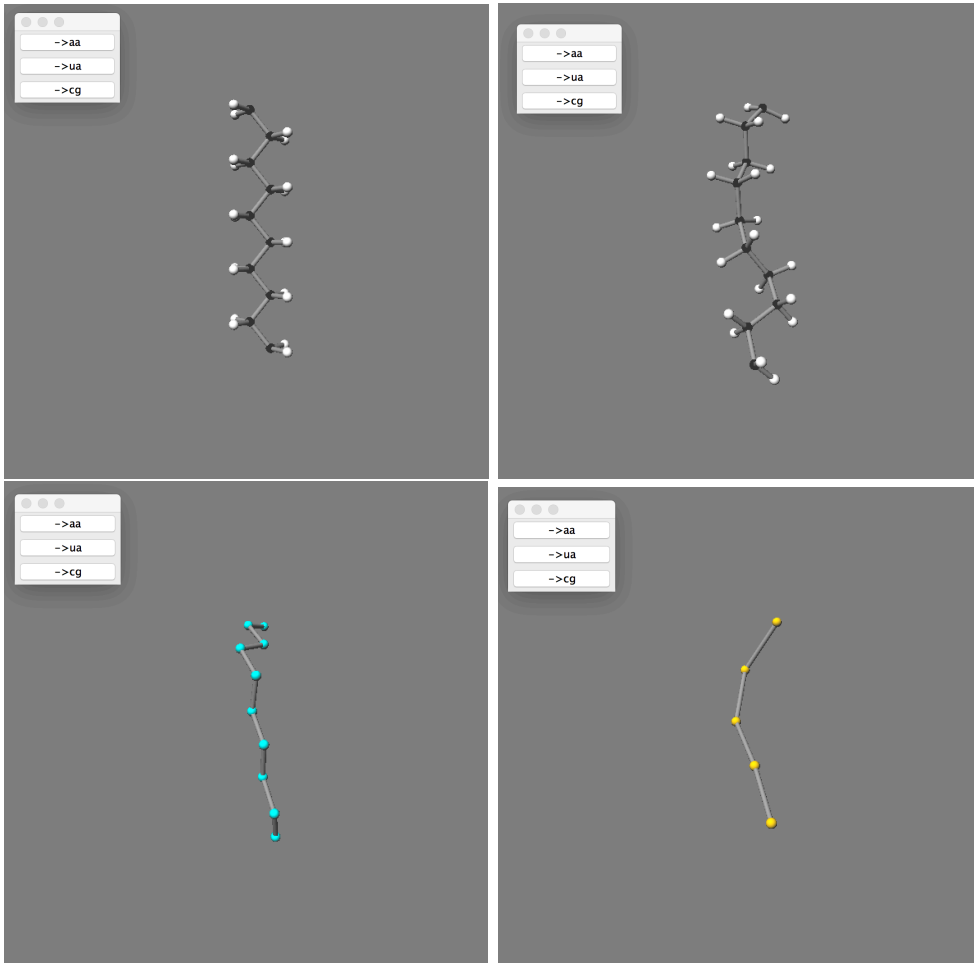


Figure 13.3: Top/left: initial AA molecule. Top/right: AA molecule after several instants. Bottom/left: after reconstruction of the AA molecule into UA. Bottom/right: after reconstruction of the UA molecule into CG.

The equilibrium distance between two atoms (or grains) governed by a Lennard-Jones potential is:

$$rn = 2^{1/6}\sigma \quad (13.5)$$

where σ is the distance at which the potential is zero. In fact, the force cancels out in equation 3.50 when $2(\frac{\sigma}{r})^{12} - (\frac{\sigma}{r})^6 = 0$ which means, assuming $X = (\frac{\sigma}{r})^6$, that $2X^2 - X = 0$. Hence $X(2X - 1) = 0$, whose only valid

solution is $X = 1/2$, i.e. $r = 2^{1/6}\sigma$.

At the equilibrium distance, the repulsive and attractive forces between the two atoms or grains balance out and the potential has the minimum value $-\epsilon$. Here are the values of rn for the inter-atomic potentials associated with alkanes:

$$rnCC = 0.39286171690828053$$

$$rnCH = 0.33202427388991257$$

$$rnHH = 0.28061551207734325$$

$$rnUA = 0.36025419440489326$$

$$rnCG = 0.35694293136238064$$

The value of $rnCG$ is obtained from that of the Lennard-Jones curve in Fig.12.3 whose minimum coincides with that of the CG inter-molecular potential.

The distances at which the repulsive and attractive forces balance out are not the same, which can be problematic in certain cases, for example when two AA molecules are placed face-to-face, as in Fig.13.4 at a distance of 0.436 nm, the distance at which the overall repulsive and attractive forces cancel each other out.

The AA→CG reconstruction destroys the balance of forces and results in a repulsive force that pushes the two CG molecules apart at high speed, which certainly does not correspond to reality.

13.2 Automatic Reconstructions

We now introduce a mechanism for automatic reconstructions triggered according to the proximity of molecules. For simplicity, we will only consider CG→UA and UA→AA reconstructions, as other types of reconstruction can be treated in a similar way.

The triggering mechanism is implemented as a loop executed at each instant that measures distances to other molecules and generates a reconstruction event when a molecule is detected at a distance below a specified threshold. This mechanism is added to the molecules that can be automatically reconstructed.

The detection thresholds are chosen empirically to avoid energy explosions as far as possible:

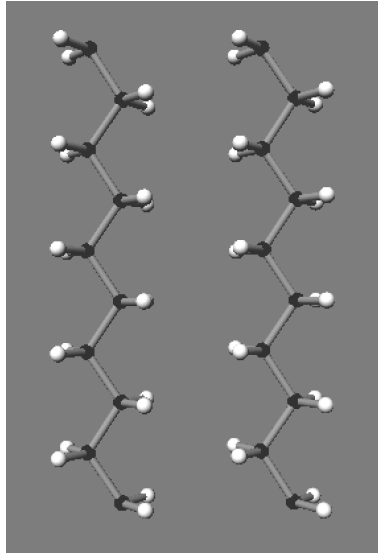


Figure 13.4: Two molecules $C_{10}H_{20}$ at a distance of 0.436 nm . The two molecules are at equilibrium: the sum of attractive forces is equal to the sum of repulsive forces.

$$\begin{aligned} \text{detectUA} &= 0.39 \\ \text{detectCG} &= 0.71 \end{aligned}$$

A UA molecule which detects that the nearest carbon atom of an AA molecule is at a distance less than detectUA automatically reconfigures itself into an A molecule. A CG molecule which detects that the nearest carbon atom of an AA molecule is at a distance less than detectCG reconfigures itself as an AA molecule. Similarly, when the CG molecule detects that the nearest grain of a UA molecule is at a distance less than detectCG , it reconfigures into a UA molecule.

It should be noted that the reconstructions can only concern a subset of the simulated molecules, which means that it is necessary to define the inter-molecular potentials between atoms and grains at different scales. To do this, we choose the highest scale (these being ordered by $AA < UA < CG$), which results in the following table:

	AA	UA	CG
AA	AA	UA	CG
UA	UA	UA	CG
CG	CG	CG	CG

Fig.13.5 and Fig.13.6 show a simulation of four CG molecules, each composed of two grains.

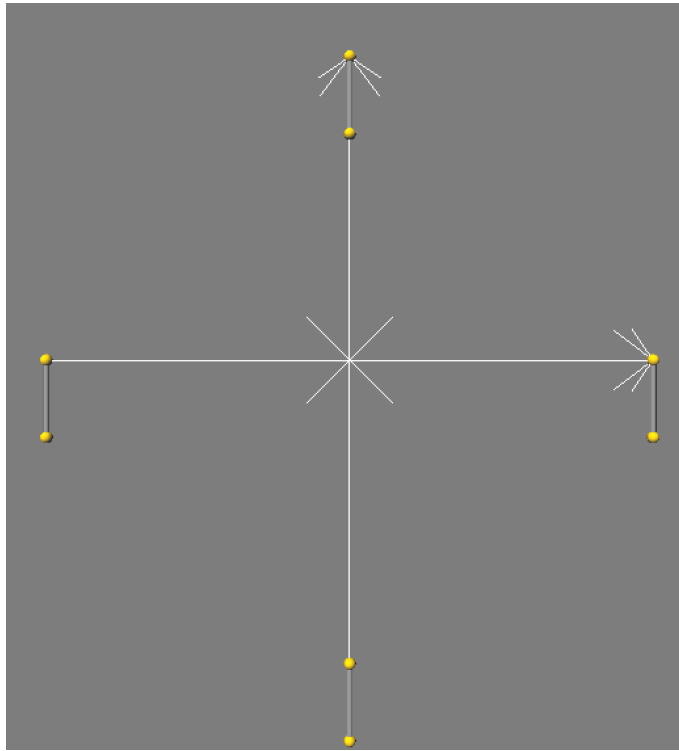


Figure 13.5: Initial configuration: four CG molecules placed at the four vertices of a square.

The initial situation is that of Fig.13.5 where four CG molecules are present. The four molecules reconfigure to UA (left/top image of Fig.13.6). Quite quickly, the UA molecules are detected and reconfigure themselves into AA molecules (right/top image).

The last two images (bottom) show the evolution of the four AA molecules. The last image (bottom/right) shows that the molecules are moving definitively away from the centre of the figure, grouped together in pairs.

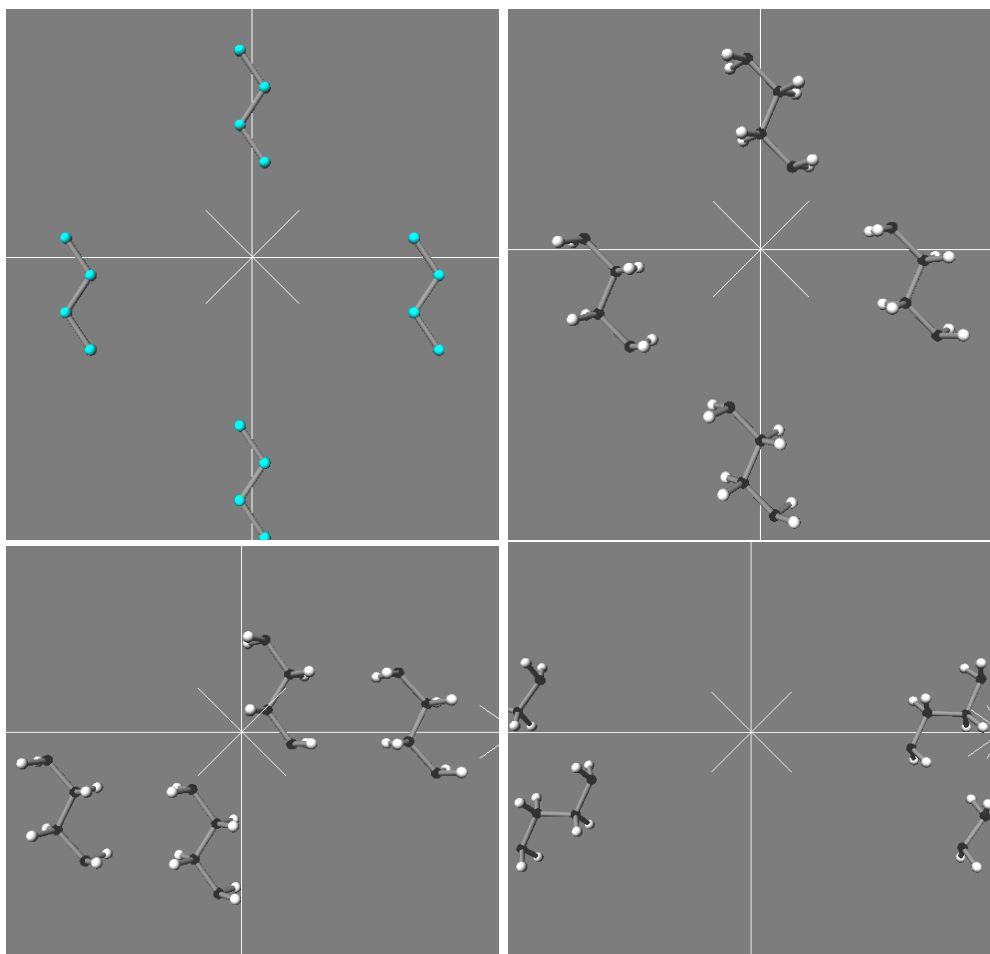


Figure 13.6: Scenario of the sequence of reconstructions of molecules initially placed as in Fig.13.5.

Conclusion

As far as reconstruction is concerned, we have adopted a pragmatic approach in which effectiveness is given priority over safety (i.e. non-exploding simulations).

More precisely, the reconstructions presented are not reliable in the sense that they can fail by introducing too much energy into the reconstructed molecule. This is the case when grains of the same molecule are very close,

leading to grains or atoms being placed in positions that are too close. A reconstruction can also fail when grains of different molecules are too close, which forces the grains or atoms introduced by the reconstruction to produce inter-molecular forces that are too strong.

On the contrary, the reconstructions presented are effective in the sense that, when they are successful, the energy of the initial molecule and that of the reconstructed molecule generally differ very little. This is particularly the case for molecules with low intra-molecular energy, since in this case the process of reconstruction is very close to the process of molecule creation at equilibrium.

The reconstructions described are therefore not suitable for molecules with high intra-molecular energy or, concerning inter-molecular forces, for molecules that are too close together.

It therefore seems reasonable to reserve the reconstructions for cases where the energy of the molecules is not too large and when the molecules are sufficiently far apart.

The alternative to the approach presented, to make reconstructions safe, would be to introduce a phase of minimisation of the reconstructed molecule, a process that can take up a lot of simulation time.

Automatic reconstructions $AA \rightarrow UA$ and $UA \rightarrow CG$ could be envisaged, when the distances are sufficiently large, which would be additional means of speeding up simulations. This type of reconstruction has not been implemented in the current system, but it could be done without too much difficulties.

Chapter 14

Conclusion

The reactive approach provides a good framework for programming MD systems. It has a clear and precise formal semantics (Chap.4). It makes it possible to deal with aspects related to temporal resolution, modularity of programming, determinism, and dynamicity (non-fixed structure of systems, which can evolve dynamically during simulations).

The question of determining potentials on the UA and CG scales for alkane molecules was raised. The aim was to “derive” the UA and CG potentials from the AA potentials.

The determination of coarse-grain potentials based on an inverse-Boltzmann statistical physics method, using data obtained from simulations, comes up against a number of problems, in particular the temperature dependency of the results and the incorrect treatment of inter-molecular forces.

The determination of potentials by the minimisation method differs radically from that of the inverse-Boltzmann method. The minimisation is not based on simulation data, like inverse-Boltzmann, but on energy minimisations at the AA scale (although the minimisations are performed with the same MD system, strictly speaking it is more a question of *molecular mechanics* than a question of MD).

A fundamental point is that minimisations are made possible at the UA and CG scales because strong geometric links with the AA scale have been established.

The stability of the MD system used relies on a complete explanation of the forces acting on the atoms (Chap.3) as well as on the use of an extremely stable resolution method (*Velocity – Verlet*).

UA Potential

The UA potentials determined by the minimisation method have several characteristics:

- They have the same form as the corresponding *AA* potentials: the bond and valence UA potentials are harmonic; the torsion potential is a “triple-cosine” potential; the inter-molecular potential is a Lennard-Jones potential.
- The UA bond potential is identical to the *AA* bond potential.
- The UA valence potential is very close to the *AA* valence potential. It can be seen as taking into account the valence angle CCC of the carbons, as well as the associated CCH angles.
- The UA torsion potential is the sum of the CCCC potential with the HCCH potentials sharing the same central CC bond.
- The UA inter-atomic potential is a Lennard-Jones potential more “excavated” than the *AA* inter-atomic potential as it takes into account the inter-molecular forces between the hydrogen atoms.

Thus, to resume, the UA potential is obtained from the *AA* one by a simple change of parameter values.

CG Potential

Determining the CG potential is considerably more difficult than determining the UA potential (although there is no torsion angle potential in CG). The minimisation method gives potentials which do not have the standard form of the *AA* or UA potentials and which are represented in the three figures Fig.10.4, Fig.10.5, and Fig.10.6. In a way, the work presented here can be seen as summarised in these three curves.

Reconstructions

Reconstruction mechanisms (i.e. molecule scale changes during the course of simulations) have been defined and implemented. In particular, we have considered automatic reconstructions based on the proximity of molecules. The

reconstructions defined are not safe in the sense that they do not systematically preserve energy. They should therefore be reserved for molecules with low intra-molecular energy, being sufficiently far apart so as not to induce too large inter-molecular energies during reconstruction.

Outlook

Several possible extensions to the work presented here seem interesting, among which the three following ones.

The first area of work concerns “true parallelism”, using a new version of SugarCubes (SugarCubesv5 [2]) in which the use of graphical cards (GPU) to perform calculations in real parallelism becomes possible. The use of multi-processor machines would also be of great interest.

The second area of work would be to implement a safe reconstruction technique, based on the minimisation of reconstructed molecules (see Chap.13).

The third area of work would involve extending the class of molecules taken into account, by not limiting ourselves to alkanes. Carbon chains, similar to alkanes, but in which one end contains oxygen atoms (“soap” molecule) could naturally be taken into account by mechanisms very similar to those used for reconstructions (some experiments have been carried out on this point).

Context

This text was written by Frédéric Boussinot. It describes some of the work carried out by Bernard Monasse and Frédéric Boussinot when they were both researchers at the CEMEF laboratory of École des Mines de Paris. This text is the English version of [6].

The SugarCubes are the outcome of Jean-Ferdy Susini's thesis work at Inria Sophia Antipolis, in the Mimosa team.

Thanks to Pierre Montmitonnet for his numerous comments, corrections and suggestions concerning the French version of the document.

Bibliography

- [1] DL_POLY. https://www.scd.stfc.ac.uk/Pages/DL_POLY.aspx.
- [2] SugarCubesv5. <http://cedric.cnam.fr/index.php/labo/membre/view?id=160>.
- [3] M. P. Allen and D. J. Tildesley. *Computer Simulation of Liquids*. Oxford, 1987.
- [4] G. Berry and G. Gonthier. The Esterel Synchronous Programming Language: Design, Semantics, Implementation. *Science of Computer Programming*, 19(2):87–152, 1992.
- [5] F. Boussinot. Reactive C: An Extension of C to Program Reactive Systems. *Software Practice and Experience*, 21(4):401–428, april 1991.
- [6] F. Boussinot. Simulations multi-échelles en Dynamique Moléculaire, 2023. hal-04267212.
- [7] F. Boussinot, B. Monasse, and J-F. Susini. Reactive programming of simulations in physics. *International Journal of Modern Physics C (IJMPC)*, 26(12):1–16, 2015.
- [8] F. Boussinot and J-F. Susini. The SugarCubes Tool Box - A Reactive Java Framework. *Software Practice and Experience*, 28(14):1531–1550, december 1998.
- [9] F. Boussinot and J-F. Susini. Java Threads and SugarCubes. *Software Practice and Experience*, 30(14):545–566, 2000.
- [10] W. Damm, A. Frontera, J. Rirado-Rives, and W. L. Jorgensen. OPLS All-Atom Force Field for Carbohydrates. *Journal of Computational Chemistry*, 18(16):1955–1970, 1997.

- [11] W. Damm, A. Frontera, J. Tirado-Rives, and W.L. Jorgensen. OPLS All-atom Force Field for Carbohydrates. *J. Comput. Chem.*, 16(18):1955–1970, 1997.
- [12] W.L. Jorgensen, J.D. Madura, and C.J. Swenson. Optimized Intermolecular Potential Functions for Liquid Hydrocarbons. *J. Am. Chem. Soc.*, (106):6638–6646, 1984.
- [13] A.D. MacKerell Jr., D. Bashford, M. Bellott, R. L. Dunbrack, Jr., J. D. Evanseck, M. J. Field, S. Fischer, J. Gao, H. Guo, S. Ha, D. Joseph-McCarthy, L. Kuchnir, K. Kuczera, F. T. K. Lau, C. Mattos, S. Michnick, T. Ngo, D. T. Nguyen, B. Prodhom, W. E. Reiher III, B. Roux, M. Schlenkrich, J. C. Smith, R. Stote, J. Straub, M. Watanabe, J. Wirkiewicz-Kuczera, D. Yin, and M. Karplus. All-Atom Empirical Potential for Molecular Modeling and Dynamics Studies of Proteins. *J. Phys. Chem. B*, (102):3586–3616, 1998.
- [14] H. Krivine. *Comprendre sans prévoir, prévoir sans comprendre*. Cassini, 2018.
- [15] L. Mandel and M. Pouzet. ReactiveML, A Reactive Extension to ML. In *ACM International conference on Principles and Practice of Declarative Programming (PPDP'05)*, Lisbon, Portugal, July 2005.
- [16] N. Metropolis, A. W. Rosenbluth, M. N. Rosenbluth, A. H. Teller, and E. Teller. Equation of State Calculations by Fast Computing Machines. *Journal of Chemical Physics*, 21:1087–1092, June 1953.
- [17] R.A. Miron and K.A. Fichthorn. Multiple-time Scale Accelerated Molecular Dynamics: Addressing the Small-barrier Problem. *Phys. Rev. Lett.*, (93):128301–128304, 2004.
- [18] Bernard Monasse and Frédéric Boussinot. Détermination des forces à partir d'un potentiel en dynamique moléculaire (note). Technical report, November 2013. <https://hal-mines-paristech.archives-ouvertes.fr/hal-00880202>.
- [19] Bernard Monasse and Frédéric Boussinot. Determination of Forces from a Potential in Molecular Dynamics. Technical report, 2014. arXiv:1401.1181.
- [20] B. Mukherjee, L. Delle Site, K. Kremer, and Ch. Peter. Derivation of Coarse Grained Models for Multiscale Simulation of Liquid Crystalline Phase Transitions. *J. Phys. Chem. B*, (116):8474–8484, 2012.
- [21] University of Groningen. GROMACS.

- [22] D. Reith, H. Meyer, and F. Muller-Plathe. CG-OPT: A Software Package for Automatic Force Field Design. *J. Comput. Phys. Commun.*, (148):299–313, 2002.
- [23] D. Reith, M. Putz, and F. Muller-Plathe. Deriving Effective Mesoscale Potentials from Atomistic Simulations. *J. Comput. Chem.*, (24):1624–1636, 2003.
- [24] K. Vanommeslaeghe, E. Hatcher, C. Acharya, S. Kundu, S. Zhong, J. Shim, E. Darian, O. Guvench, P. Lopes, I. Vorobyov, and A. D. MacKerell Jr. CHARMM General Force Field: A Force Field for Drug-like Molecules Compatible with the CHARMM All-atom Additive Biological Force Fields. *J. Comput. Chem.*, (31):671–690, 2010.
- [25] L. Verlet. Computer "Experiments" on Classical Fluids. I. Thermodynamical Properties of Lennard-Jones Molecules. *Phys. Rev.*, 159:98–103, Jul 1967.
- [26] A.F. Voter. A Method for Accelerating the Molecular Dynamics Simulation of Infrequent Events. *J. Chem. Phys.*, (106):4665–4677, 1997.